The Journal of Geology

Comparative analysis of the sedimentary cover units of the Jurassic Western Tethys ophiolites in the Northern Apennines and Western Alps (Italy): Processes of the formation of mass transport and chaotic deposits during seafloor spreading and subduction zone tectonics

--Manuscript Draft--

Manuscript Number:	81020R2
Full Title:	Comparative analysis of the sedimentary cover units of the Jurassic Western Tethys ophiolites in the Northern Apennines and Western Alps (Italy): Processes of the formation of mass transport and chaotic deposits during seafloor spreading and subduction zone tectonics
Article Type:	Major Article
Corresponding Author:	Andrea Festa University of Torino Torino, ITALY
Corresponding Author Secondary Information:	
Corresponding Author's Institution:	University of Torino
Corresponding Author's Secondary Institution:	
First Author:	Andrea Festa
First Author Secondary Information:	
Order of Authors:	Andrea Festa
	Francesca Meneghini
	Gianni Balestro
	Luca Pandolfi
	Paola Tartarotti
	Yildirim Dilek
	Michele Marroni
Order of Authors Secondary Information:	
Manuscript Region of Origin:	ITALY
Abstract:	The Jurassic ophiolites in the Northern Apennines and the Western Alps represent fossil mid–ocean ridge (MOR) oceanic lithosphere that formed in the Mesozoic Ligurian–Piedmont Ocean Basin (LPOB). Their sedimentary covers include chaotic rock units containing ophiolite–derived material. The processes of formation and the lithostratigraphic position of these chaotic units in the Western Alps remain a matter of debate, unlike their counterparts in the Northern Apennines. This is because of pervasive tectonic deformation and high-pressure metamorphism that affected their internal structure due to the collisional tectonics. A comparative analysis of these chaotic units in both mountain belts reveals the nature of processes involved in their formation. Chaotic deposits of gravitational origin occur both below and above the extrusive sequences in the ophiolites. They represent syn-extensional, hyper-concentrated deposits associated with the seafloor spreading evolution of the LPOB lithosphere during Middle and Late Jurassic time. MTDs occur as intercalations within turbiditic sequences above the ophiolites. They represent syn–contractional submarine slides that occurred on frontal accretionary prism slopes during the Late Cretaceous–Paleocene closure of the LPOB. The results of our comparative analysis imply that: (1) the structure–stratigraphy of the chaotic deposits and MTDs of the Northern Apennines can be used as a proxy to better identify their metamorphosed and highly deformed counterparts in the Western Alps; (2) sedimentological processes

	associated with slow–spreading MOR tectonics and with accretionary prism development in convergent margin tectonics contributed to the sediment budgets of the cover sequences; and, (3) magmatic, tectonic and sedimentological processes that occurred during the formation of the Jurassic oceanic lithosphere and its sedimentary cover in the LPOB were remarkably uniform and synchronous.

UNIVERSITA' DEGLI STUDI DI TORINO
DIPARTIMENTO DI SCIENZE DELLA TERRA
Via Valperga Caluso, 35 - 10125 TORINO (Italy)
Phone: +39-011-670.58.65

T
Torino, 24 May 2021

Dear Editor of *the Journal of Geology*,

We are submitting herein the revised version of our manuscript, entitled *"Comparative analysis of the sedimentary cover units of the Jurassic Western Tethys ophiolites in the Northern Apennines and Western Alps (Italy): Processes of the formation of mass transport and chaotic deposits during seafloor spreading and subduction zone tectonics"*, to be published in The Journal of Geology – SPECIAL ISSUE "Plate Tectonics anniversary" Edited by Dr. Yildirim Dilek. Please note that we have modified the title as requested by the Guest Editor.

At the outset, my co-authors and I would like to express our sincere thanks to the anonymous referee for the constructive and thorough reviews, from which we have benefited greatly in revising our manuscript.

As you will see in the **"Reply to comments"**, we have accepted all the pertinent comments and suggestions provided by the both the Guest Editor and the Reviewer and have modified the text accordingly. We believe that this revised version is now in much better shape both scientifically and organizationally due to our careful revisions following all the reviewer' comments and suggestions.

In the revised submission (**Festa et al_MARKED TEXT_J Geol_SI Plate Tectonics_R2.doc**) you will find all the changes and modifications highlighted in green for Reviewers #2 (i.e., example); the parts in the original text that have been removed in revision are marked in red color and crossed out (i.e., ~~example~~). A clean version of the revised submission is in the file "**Festa et al_REVISED TEXT_ J Geol_SI Plate Tectonics_R2.doc**".

We think that this revised manuscript well would make a significant contribution in and can have a wide appeal to a broad international readership of the JOURNAL OF GEOLOGY - **Special Issue on the "*Plate Tectonics anniversary*"**. We hope that you will agree.

We would like to confirm that this manuscript has not been published before nor it has been submitted elsewhere for consideration for publication. It is an original work, consisting of previously unreported / unpublished material, and original illustrations.

Seven (#7) color figures and one (#1) B&W table accompany the text.

Sincerely yours,

Dr Andrea Festa *(corresponding Author)*
Dipartimento di Scienze della Terra
Università di Torino
Via Valperga Caluso, 35
10125 – Torino (Italy)
Email: andrea.festa@unito.it

REVISED Manuscript (with changes marked)

Comparative analysis of ~~chaotic rock units in the Jurassic Western Tethys ophiolites from seafloor spreading to subduction (Northern Apennines and Western Alps)~~ the sedimentary cover units of the Jurassic Western Tethys ophiolites in the Northern Apennines and Western Alps (Italy): Processes of the formation of mass transport and chaotic deposits during seafloor spreading and subduction zone tectonics

Andrea Festa[1*], Francesca Meneghini[2], Gianni Balestro[1], Luca Pandolfi[2,3], Paola Tartarotti[4], Yildirim Dilek[5], Michele Marroni[2,3]

1. Dipartimento di Scienze della Terra, Università di Torino, Torino (Italy); ORCID #: AF, 0000-0001-5325-0263; GB, 0000-0001-5215-4659
2. Dipartimento di Scienze della Terra, Università di Pisa, Pisa (Italy); ORCID #: FM, 0000-0002-6809-6112; LP, 0000-0002-6129-647X; MM, 0000-0002-2947-3739
3. Istituto di Geoscienze e Georisorse, IGG-CNR, Pisa (Italy)
4. Dipartimento di Scienze della Terra, Università degli Studi di Milano, Milano (Italy); ORCID #: PT, 0000-0002-2236-2702
5. Department of Geology and Environmental Earth Science, Miami University, Oxford, (USA); ORCID#: YD, 0000-0003-2387-9575

***Corresponding author**:

Professor Andrea Festa
Street address: Via Valperga Caluso, 35
10125, Torino, Italy
E-mail address: andrea.festa@unito.it
Phone: +39-011-670.51.86

Submitted to: The Journal of Geology
Special Issue on the Plate Tectonics Anniversary
Re-revised version: 24 May 2021

ABSTRACT

The Jurassic ophiolites in the Northern Apennines and the Western Alps represent fossil mid–ocean ridge (MOR) oceanic lithosphere that formed in the Mesozoic Ligurian–Piedmont Ocean Basin (LPOB). Their sedimentary covers include chaotic rock units containing ophiolite–derived material. The processes of formation and the lithostratigraphic position of these chaotic units in the Western Alps remain a matter of debate, unlike their counterparts in the Northern Apennines. This is because of pervasive tectonic deformation and high-pressure metamorphism that affected their internal structure due to the collisional tectonics. A comparative analysis of these chaotic units in both mountain belts reveals the nature of processes involved in their formation. Chaotic deposits of gravitational origin occur both below and above the extrusive sequences in the ophiolites. They represent syn-extensional, hyper-concentrated deposits associated with the seafloor spreading evolution of the LPOB lithosphere during ~~the~~ Middle and Late Jurassic time. MTDs occur as intercalations within turbiditic sequences above the ophiolites. They represent syn–contractional submarine slides~~,~~ that occurred on frontal accretionary prism slopes during the Late Cretaceous–Paleocene closure of the LPOB. The results of our comparative analysis imply that: (1) the structure–stratigraphy of the chaotic deposits and MTDs of the Northern Apennines can be used as a proxy to better identify their metamorphosed and highly deformed counterparts in the Western Alps; (2) sedimentological processes associated with slow–spreading MOR tectonics and with accretionary prism development in convergent margin tectonics contributed to the sediment budgets of the cover sequences; and, (3) magmatic, tectonic and sedimentological processes ~~throughout~~ that occurred during the formation of the Jurassic oceanic lithosphere and its sedimentary cover in the LPOB were remarkably uniform and synchronous.

61

62 **Keywords**: Mesozoic Ligurian–Piedmont Ocean; submarine chaotic rock units; submarine
63 mass transport deposits; sedimentary cover of ophiolites; Western Alps; Internal Ligurian
64 Units – Northern Apennines.

65

INTRODUCTION

Chaotic rock units (i.e., tectonic, sedimentary and diapiric mélanges, broken formations and polygenetic mélanges, see Festa et al., 2019b)~~,~~ containing fragments of ~~the~~ an ophiolite ~~sequence,~~ represent the most significant component of the ocean-derived units preserved in Archean to Cenozoic collisional belts (e.g. Sample and Moore 1987; Orange 1990; Polat and Kerrich, 1999; Fitzherbert et al., 2005; Dilek, 2006; Yamamoto et al.2007; Federico et al., 2007; Festa et al., 2010, 2020c; Malatesta et al., 2012; Dilek et al., 2012; Balestro et al., 2015a, 2020; Ogawa et al., 2015; Ernst, 2016; Scarsi et al., 2018; Raymond, 2019; Roda et al., 2019; Wakabayashi, 2011, 2019; Hajná et al., 2019; Gao and Santosh, 2020; Kusky et al., 2020; Palin et al., 2020; Žak et al., 2020; Barbero et al., 2021). Understanding the formation and emplacement of these chaotic deposits in space and time is significant for better constraining the nature, tempo and order of the magmatic, tectonic and sedimentological processes, which operated during the formation of ancient oceanic lithosphere and its sedimentary cover. Related data and observations can provide ~~providing~~ additional constraints for ~~a refinition~~ redefining ~~of~~ the plate tectonic paradigm and developing a better understanding of the Earth systems.

In the Piedmont Zone of the Western Alps and in the Internal Ligurian Units of the Northern Apennines in Italy (Fig. 1), these types of chaotic rock units were derived from the deformation of the northern and southern parts of the Jurassic Ligurian-Piedmont oceanic rocks (Western Tethys), respectively (Marroni et al., 2017; Dilek and Furnes, 2019). In the Northern Apennines, the chaotic ~~units~~ deposits show a very low–grade metamorphic overprint, allowing documentation in detail of their preserved diagnostic sedimentological features and their lithostratigraphic position. In turn, this knowledge

allows interpretation of the chaotic rock masses as the products of different mass transport processes, which ~~that~~ occurred during the Middle-Late Jurassic seafloor spreading of the Ligurian-Piedmont Ocean Basin (LPOB) lithosphere and the Late Cretaceous – Paleocene tectonic convergence between Europe and Adria (e.g., Fierro and Terranova 1963; Elter 1975; Abbate et al., 1970, 1980; Cortesogno et al., 1987; Marroni and Pandolfi, 2001; Bortolotti and Principi, 2003; Principi et al., 2004; Lamarche et al., 2008; Festa et al., 2018; Meneghini et al., 2020).

Conversely, in the Western Alps, the chaotic rock units containing ophiolite–derived material were affected by pervasive subduction- and exhumation-related deformation and high–pressure metamorphism. ~~Their~~ As a result, primary sedimentological features in these rock units are partially obscured or obliterated, and lithostratigraphic position and evidence of tectonic versus sedimentary formational processes in their development, thus, remain matters of debate (see e.g., Balestro et al., 2015a, Tartarotti et al., 2017a; Roda et al., 2019 and references therein). This phenomenon complicates the detailed reconstruction of the syn-spreading to convergent stages of tectono-sedimentary evolution of the northern portion of the LPOB, as exposed in the Western Alps.

~~This paper aims to provide a comparative analysis and discuss the nature of processes involved in rock formation, using discussion and comparison of several notable examples of chaotic rocks units, containing ophiolite-derived material, from both~~ In this paper we define the original, oceanic sedimentary cover of the Jurassic ophiolites exposed in the Northern Apennines and the Western Alps (Italy), and document various chaotic rocks units preserved in these cover sequences. We compare and correlate both lithologically and chronologically these chaotic rock units and their stratigraphic positions in the Northern Apennines and the Western Alps (Fig. 1). We show that ~~the review of~~ the

well-known sedimentological-stratigraphical features of the chaotic deposits ~~of~~ in the Northern Apennines can be used as a proxy ~~to~~ that allows a better ~~define~~ definition of the tectonostratigraphy of their highly deformed and metamorphosed counterparts in the Western Alps. ~~We also show~~ Our results indicate that these types of chaotic rock units correlate well both chronologically and stratigraphically in the two orogenic belts. This indicates that the LPOB lithosphere underwent similar tectonic processes during the Jurassic seafloor spreading and Late Cretaceous – Early Paleocene closure phases of the ocean basin history throughout its entire length, providing additional constraints for a more detailed reconstruction of the Jurassic Western Tethys.

~~Chaotic rock units~~ Nomenclature and terminology of chaotic rock units

In this paper we use the term *chaotic rock unit* as general and descriptive, ~~and~~ but not genetic term, to describe different types of block-in-matrix rock assemblages. This term includes the entire range of chaotic rock ~~assemblage~~ mass occurrences in which mélanges and broken formations represent two end members (see Festa et al., 2019b for details). Hence, chaotic rock units may represent a rock ~~assemblage~~ mass that can be formed by: (1) ~~different processes (e.g.,~~ tectonic, sedimentary and/or diapiric~~)~~ processes; ~~or their superposition, by~~ (2) both stratal disruption and/or mixing processes, and (3) superposition of ~~that can consist of~~ exotic, native or mixed exotic - native blocks embedded in a matrix of various possible compositions. Chaotic rock units formed by sedimentary (gravitational) processes represent ancient submarine mass transport deposits (MTDs; see, e.g., Lucente and Pini, 2008; Ogata et al., 2012, 2020; Festa et al., 2016; Pini et al., 2020), commonly described as olistostromes (Flores, 1955; Elter and Trevisan, 1973; Pini, 1999) or sedimentary mélanges (e.g., Raymond, 1984; Bettelli and Panini, 1985, Bettelli et al., 2004;

Festa et al., 2016) in orogenic belts and exhumed subduction-accretion complexes. We use the terms "mass transport deposit (MTD)" and "chaotic deposit" to ~~indicate~~ denote two sedimentary (gravitational) chaotic rock unit~~s~~ types ~~differing each other in matrix types~~, which differ from each other in their matrix types. Chaotic deposits are characterized by a matrix- to clast-supported texture with a predominantly basic to ultrabasic sandy matrix, and more rarely by a hematitic to ~~carbonatic~~ carbonceous one matrix, ~~while~~ whereas MTDs ~~show~~ have a shaly matrix. Note also that some of the described examples of chaotic deposits and MTDs consist of single layers. This prevents us ~~to use~~ from using the terms sedimentary mélange and olistostrome, as these occurrences are not mappable at 1:25,000, as ~~requested~~ required by the definition of the mélange term ~~definition~~ (e.g., Berkland et al., 1972; Wood, 1974; Silver and Beutner, 1980; Raymond, 1984; Cowan, 1985; Festa et al., 2019b).

GEODYNAMIC HISTORY OF THE LIGURIAN – PIEDMONT OCEAN BASIN (LPOB)

The Ligurian – Piedmont Ocean Basin (LPOB), which evolved between Europe and Adria, was a restricted, Red Sea – type ocean basin in the Mesozoic paleogeography of the Western Tethys (Fig. 2a; see, e.g., Dilek and Furnes, 2019 and references therein). It was connected with the Central Atlantic Ocean Basins to the west via a NW–SE–oriented transform fault system (Fig. 2a; Dercourt et al., 2000; Stampfli and Borel, 2002; Stampfli et al., 2002; Golonka, 2007; Schettino and Turco, 2011; Berra and Angiolini, 2014; Hosseinpour et al., 2016 and Dilek and Furnes, 2019). The opening of the LPOB is

generally regarded as the result of ~~a~~ rift–drift and seafloor spreading ~~that occurred through different stages~~ during Middle Triassic through Middle Jurassic time (Marroni et al., 1998; Müntener and Hermann, 2001; Whitmarsh et al., 2001; Capitanio and Goes, 2006; Montanini et al., 2006; Marroni and Pandolfi, 2007; Piccardo et al., 2014; Festa et al., 2020a). Initial lithospheric stretching and distributed extension was followed by strain localization and hyper-extension, which led to continental rifting and seafloor spreading (Lavier and Manatschal 2006; Péron-Pinvidic and Manatschal 2009; Mohn et al., 2012; Ribes et al., 2019). The resulting conjugate margins were asymmetric in their structural architecture with the European margin showing a narrow ocean-continent transition zone (OCTZ) marked by high-angle normal faults and the Adria margin characterized by a wider OCTZ (Fig. 2a), along which the subcontinental mantle and the lower continental crust were exhumed (Marroni and Pandolfi 2007; Saccani et al., 2015).

The oceanic lithosphere of the LPOB was unlike a typical Penrose–type oceanic lithosphere with a complete crustal pseudostratigraphy (or ocean plate stratigraphy, *sensu* Kusky et al., 2013, Wakita, 2015) of a modern fast–spreading oceanic lithosphere (Anonymous, 1972; Dilek et al., 1998), ~~it~~ rather it resembled a Hess–type oceanic lithosphere (Dilek and Furnes, 2011) that commonly develops at slow– to ultra slow–spreading mid–ocean ridge settings (Pognante et al., 1986; Lemoine et al., 1987, Lagabrielle and Cannat, 1990, Treves and Harper, 1994; Cannat, 1996, Cannat et al., 1997, Michard et al. 1996; Magde et al., 2000, Rabain et al., 2001; Balestro et al., 2015b; Rampone e al., 2020). The available paleontological data from chert deposits in the Ligurian ophiolites (Bill et al., 2001; Principi et al., 2004), as well as the radiometric dating results (Li et al., 2013; Tribuzio et al., 2016), indicate that seafloor spreading within the LPOB lasted for ~25 m.y. from Bajocian to Tithonian time. The seafloor spreading phased

out and stopped at the beginning of the Early Cretaceous Epoch when the basin was about 600 to 700 km–wide (Abbate et al., 1980; Marroni and Pandolfi, 2007; Balestro et al., 2019). Throughout much of the Cretaceous Period the LPOB experienced deep-sea pelagic deposition without any tectonic or volcanic event interrupting this depositional record.

~~In the~~ During Campanian time, the mode of sedimentation changed abruptly with the onset of deep-sea clastic sedimentation, which involved the deposition of a vast amount of siliciclastic and carbonate turbidites, whose sediments were derived from the European margin (Marroni and Perilli, 1990; Marroni et al., 1992; Principi et al., 2004). The onset of this extensive turbidite deposition episode is considered to be the beginning of a contractional deformation phase in the evolutionary history of the LPOB that led to its closure in the Cenozoic Era. The early Campanian time of the turbidite deposition coincides with the age of high–pressure metamorphism in the internal sectors of Western Alps (see, e.g., Manzotti et al., 2014 and reference therein) and in Corsica (e.g., Lahondère and Guerrot, 1997).

The initial stages of basin closure were facilitated by an intraoceanic subduction event, which resulted in the development of a subduction–accretion system (Fig. 2b). The position of this intraoceanic subduction within the LPOB is still a matter of debate. Recent geodynamic models place this subduction–accretion system close to or within the OCTZ along the Adria continental margin, with subduction beginning, in the Late Cretaceous Epoch (Manzotti et al., 2014; Marroni et al., 2017; Barbero et al., 2020; Festa et al., 2020a).

The accretionary wedge experienced slope instability due to subduction of an oceanic crust characterized by seamounts and a rough topography, probably inherited from the spreading phase (Marroni and Pandolfi, 2001; Marroni et al., 2017; Meneghini et al., 2020). The instability of the slope resulted in large submarine slides recorded as debris

flows and slide deposits that were emplaced within or at the top of the trench turbidites (e.g., Pini, 1999; Festa et al., 2018; 2020b; Ogata et al., 2019; Meneghini et al., 2020 and references therein).

During the convergence, the LPOB lithosphere ~~disappeared~~ was subducted larely into the mantle or was locally accreted at the base or in front of an accretionary wedge (Fig. 2b). Thus, ~~in the Western Alps and in the Northern Apennines several segments of the LPOB, accreted at different depths, are found today as tectonic ophiolite units~~ several segments of the LPOB that were accreted at different depths are found today as tectonic thrust sheets of ophiolites in the Western Alps and the Northern Apennines. These units were affected by pervasive deformation associated with subduction-related metamorphism ranging from very low-grade to blueschist and eclogite facies (Goffè et al., 2003), similar to that typically described in many exhumed, sediment-dominated accretionary prisms (Ernst, 1970, 1971, 2015; Miyashiro, 1973; Raymond, 1973; More and Sample, 1986; Meneghini et al., 2009; Plunder et al., 2015). In the Northern Apennines the ophiolite units were subducted ~~at~~ to shallow levels (maximum of 25 km depth; Marroni et al., 2017), ~~while~~ whereas in the Western Alps ~~the suggested same units~~ they were subducted ~~at~~ to depths ranging from 30 km to 90 km (e.g. Handy et al., 2010; Roda et al., 2020 and reference therein) and were metamorphosed under ~~severe~~ peak P-T conditions during ~~the~~ latest Cretaceous(?) to middle Eocene time (e.g. Rosenbaum and Lister 2005; Zanoni et al., 2016; Rebay et al., 2018; Luoni et al., 2020 and references therein).

The deformation characteristics of these units indicate an accretion by coherent underplating during ~~an~~ east-dipping and low–rate subduction dominated by a high sediment budget. The deformation history and the related metamorphism testify not only to the accretion phases, but also to the exhumation history of these units (Polino et al. 1990;

Butler et al. 2013; Roda et al., 2020; Luoni et al., 2020). Ophiolite units detached from the subducting slab were ~~quickly exhumed, having been~~ uplifted to shallow crustal levels and rapidly exhumed before the early Oligocene. This is ~~as indicated~~ supported by the occurrence of continental conglomerates in the Tertiary Piedmont Basin (Fig. 1), ~~. The latter was~~ which represents a wide episutural basin ~~unconformably~~ overlying ~~at the top of~~ the metamorphosed ophiolites both in the Western Alps and in the Northern Apennines (Federico et al., 2015; Barbero et al., 2020; Festa et al., 2013, 2020b). During and after middle Eocene time, the Jurassic ophiolites underwent continental collision tectonics and deformation both in the Western Alps and the Northern Apennines and were involved in nappe and overthrust development and large–scale isoclinal and recumbent folding.

In summary, the LPOB developed during three main stages. The first stage involved continental rifting and seafloor spreading in Middle to Late Jurassic time (Fig. 2a). During the second stage, between the Berriasian and the Santonian ages, it experienced tectonic quiescence and extensive pelagic deposition. During the third stage, starting in the Campanian age, the LPOB underwent intraoceanic subduction, basin closure, and continental collision.

OPHIOLITE AND SEDIMENTARY COVER RECORD IN THE NORTHERN APENNINES

In the Internal Ligurian Units (Fig. 1), a series of tectonostratigraphic units occurs in thrust sheets. These thrust sheets extend from southern Tuscany to the city of Genova, in the north, where they are in contact with eclogitic oceanic rocks of the Voltri Group,

assigned to the Western Alps (Fig. 1). These tectonostratigraphic units show pervasive deformation structures that are spatially and temporally associated with a metamorphic overprint, decreasing in grade from the structurally lowermost units to those lying on top of the tectonic pile (Leoni et al. 1996; Ellero et al. 2001). The lowermost units (Cravasco-Voltaggio and Mt. Figogna Units) are affected by low-grade blueschist facies metamorphism, whereas the uppermost ones (Gottero, Bracco-Val Graveglia, Colli-Tavarone, Portello, Vermallo and Due Ponti units) display mineral phases and textures suggesting very low-grade metamorphic conditions, ranging from upper anchizone to epizone conditions (Leoni et al. 1996; Crispini and Capponi 2001; Ellero et al. 2001).

The Internal Ligurian Units, regardless of the degree of metamorphism or deformation, display a stratigraphic succession that reflects the inferred three stages of development of the LPOB. This succession includes a ~1–km–thick ophiolite sequence and a ~4–km–thick sedimentary cover, which ~~that~~ includes two lithologically and compositionally different parts with different geodynamic significance (Decandia and Elter, 1972, Abbate et al., 1980; Treves 1984; Marroni and Perilli 1990; Marroni et al. 1992; Abbate et al. 1994).

First Stage: Formation of the oceanic lithosphere and its oldest sedimentary cover

The Middle to Late Jurassic ophiolite sequence formed during the first stage in a slow- to ultraslow-spreading ridge environment, where magma supply was limited and tectonic (amagmatic) extension processes, producing high– to low–angle normal faults, were dominant (e.g., Lagabrielle and Cannat, 1990, Treves and Harper, 1994; Marroni and Pandolfi, 2007; Rampone et al., 2020). Tectonic extension in the absence of a steady–state magma supply resulted in the exhumation of upper mantle peridotites, which underwent

~~severe~~ wideaspread serpentinization, and in the formation of sags and structural highs, creating a rugged seafloor bathymetry (e.g., Principi et al., 2004; and reference therein).

Exhumed serpentinized peridotites were intruded by gabbroic stocks and plutons and were covered by volcanic and sedimentary rocks, composed of basaltic pillow-lavas and sills, radiolarian cherts and ophiolitic breccias. Basaltic lavas and sills have MORB-type geochemical signatures (e.g., Renna et al., 2018). Ophiolitic breccias represent chaotic deposits accumulated in half-grabens and tectonic sags developed in the hanging walls of normal faults (e.g., Elter 1975; Bortolotti and Principi, 2003; Principi et al., 2004). They are subdivided into several types according to their clast compositions, which reflect the source lithology and their lithostratigraphic position below or above the basaltic carapace of the ophiolite (Elter 1975; Cortesogno et al., 1987; Bortolotti and Principi, 2003; Principi et al., 2004).

Second Stage: Formation of deep-sea pelagic sedimentary cover

The ophiolite sequence is overlain by Callovian-Santonian deep-sea pelagic sedimentary rocks deposited during the second stage, which ~~The second stage~~ lasted nearly 80 m.y. The pelagic deposits include Middle Callovian to Early Berriasian cherts and fine-grained, carbonaceous turbidites that are composed of the Late Berriasian-Valanginian Calpionella Limestone and the Valanginian-Santonian Palombini Shale. All these deposits ~~are characterized by~~ were the products of a low ~~rate of~~ sedimentation rate in a deep–marine environment (Marroni and Perilli, 1990; Marroni et al., 2004).

Third Stage: Deposition of turbidites in a closing ocean basin

The deep–marine pelagic rocks are conformably overlain by a Lower Campanian–Lower Paleocene thick turbidite sequence, ~~whose~~ the deposition of which started contemporaneously with the onset of subduction within the LPOB. ~~This~~ The lower part of this sequence ~~includes~~ consists~~, at the bottom,~~ of carbonaceous and siliciclastic turbidites ~~of~~ (i.e., the Val Lavagna Shale Group, which ~~consists~~ includes ~~of~~ the lower Campanian Manganesiferi Shale, the lower to upper Campanian Monte Verzi Marl, and the lower Campanian to lower Maastrichtian Zonati Shale). These fine–grained ~~clastic~~ rocks ~~of the Val Lavagna Shale Group~~ reflect a high sedimentation rate within ~~the~~ a shrinking basin ~~that followed~~ following the onset of intra – basin subduction. They ~~Val Lavagna Shale Group~~ grade~~s~~ stratigraphically upward into the lower Maastrichtian to lower Paleocene sandstone (i.e., the Gottero Sandstone). Arenites in siliciclastic turbidites represent arkosic–subarkosic rocks, whose clast compositions are compatible with lithologies constituting the upper part of the rifted European margin. Hence, it is widely accepted that the provenance of the turbiditic sequence above the ophiolite was the passive continental margin of Europe (Valloni and Zuffa, 1984; Van de Kamp and Leake, 1995; Pandolfi, 1997; Marroni and Pandolfi, 2001). These turbiditic sequences (i.e., Zonati Shale and the Gottero Sandstone) were deposited in submarine fans adjacent to the European passive continental margin (Abbate and Sagri, 1982; Nielsen and Abbate, 1983; Fonnesu and Felletti, 2019). ~~The Zonati Shale and the Gottero Sandstone~~ The stratigraphically upper parts of ~~the~~ this submarine fan sequence contain ~~chaotic bodies~~ MTDs consisting of debris flow deposits, which include reworked clasts derived from an oceanic lithosphere and its sedimentary cover.

The youngest deposit of the Internal Ligurian Units ~~is the Lower Paleocene Bocco Shale (also known as the Colli Tavarone and Lavagnola Formations of Marroni et al.,~~

2017), consists of an MTD, represented by the Lower Paleocene Bocco Shale, also known as the Colli-Tavarone and Lavagnola Formations of Marroni et al., 2017). The Bocco Shale rests which lies unconformably on top of all the older formations, The Bocco Shale comprises and consists of thin-bedded turbidites, and slide and debris flow deposits. the Clasts and materials of these deposits which were derived from an oceanic lithosphere and its sedimentary cover, as is the case in the chaotic bodies found in the Zonati Shale and Gottero Sandstone (Marroni and Pandolfi, 2001; Marroni et al., 2017; Meneghini et al., 2020).

DIAGNOSTIC FEATURES AND DEPOSITIONAL MECHANISMS OF CHAOTIC DEPOSITS AND MTDs IN THE NORTHERN APENNINES

The sedimentary cover units of the Internal Ligurian ophiolites of in the Northern Apennines include two distinctive chaotic rock unit types of gravitational origin with specific age spans that corresponding to different phases in the evolutionary history of the LPOB. The oldest (Middle to Upper Jurassic) chaotic rock units developed during the seafloor spreading and hence the opening phase of the LPOB. We refer to these deposits as syn–extensional chaotic deposits in the rest of the paper. The youngest, Upper Cretaceous–Lower Paleocene chaotic rock units formed, on the other hand, during the convergence and closure phase of the LPOB. We refer to these deposits as syn–contractional mass–transport deposits (MTDs) in the rest of the paper. In both opening and closing phases, sedimentation accumulation of chaotic deposits and MTDs over a recently formed oceanic lithosphere can be considered to be was a tectonically induced depositional event.

353

354 **Syn–Extensional Chaotic Deposits**

355 The syn-extensional sedimentary chaotic rocks are well exposed in the Val
356 Graveglia and the Bracco Massif (see 11 and 12 of Fig. 1, also see Fig. 3), both of which
357 are located in the eastern Liguria region, between the cities of Genova and La Spezia ~~towns~~
358 ~~(Figs. 1 and 3)~~. ~~Clasts in~~ These chaotic deposits ~~reflect an entirely local source, and the~~
359 ~~rocks have been~~ are designated as the lower and upper ophiolitic breccias on the basis of
360 their stratigraphic position below or above the basaltic lava flows, respectively (Figs. 3A
361 and 3E; Principi et al., 2004); their clasts were sourced from an entirely local provenance.
362 These ophiolitic breccias represent one specific type of syn-extensional chaotic deposit.
363 The lower ophiolitic breccias rest directly on serpentinized peridotites or gabbros, and they
364 are overlain by basaltic flows or ~~directly by~~ cherts. The upper ophiolitic breccias occur
365 between the base of the basaltic lava flows and on top of the cherts. The ages of the lower
366 and upper breccias are poorly constrained ~~based on~~ due to the low resolution of radiolarian
367 assemblages in their matrix material. The available biostratigraphic data indicate an age of
368 the ophiolitic breccias and the associated basaltic flows spanning from Upper Bajocian to
369 Lower Callovian (Chiari et al., 2000, and reference therein).

370

371 ***Syn-extensional lower ophiolitic breccias.*** The lower ophiolitic breccias include the
372 Levanto, Framura, Casa Boeno and Monte Capra Breccias (Principi et al., 2004, and
373 references therein). The first three overlie the serpentinized peridotites, ~~while~~ whereas the
374 last breccia covers the gabbro. The lithological composition of these breccias reflects the
375 substrate on which they rest. The Levanto Breccia (ophicalcites *s.s.*) is a tectonic-
376 hydrothermal breccia, which ~~that~~ occurs above the serpentinized upper mantle rocks (Figs.

3E and 3F). ~~and is interpreted to~~ It marks a cataclastic shear zone composed of fragmented serpentinites crosscut by a network of veins, filled with sparry calcite, talc and locally by smaller serpentinite fragments. This cataclastic shear zone marks an oceanic detachment fault zone, which was exposed on the LPOB seafloor (Treves and Harper, 1994).

The overlying Framura Breccia consists mainly of reworked Levanto Breccia material (Abbate et al., 1980; Cortesogno et al., 1987), and is composed of a coarse-grained breccia containing mostly serpentinite and rare gabbro clasts in a hematitic matrix (Fig. 3G and H). ~~Similar to the Framura Breccia,~~ The Case Boeno Breccia (Cortesogno et al., 1987; Principi et al., 2004) is a monogenic breccia consisting of serpentinite clasts in a scarce, serpentinite–sand matrix. The Case Boeno Breccia locally includes large serpentinite blocks, up to several metres wide. As with the Framura Breccia, the Case Boeno Breccia also lies stratigraphically on top of the serpentinized peridotites. Overlying the gabbro intrusions, the Monte Capra Breccia represents a clast-supported polymictic breccia (Fig. 3B) with clasts of Fe-gabbro~~s~~, Fe-basalt~~s~~, plagiogranite~~s~~, and serpentinite~~s~~ in a scarce sandy matrix (Bortolotti and Principi, 2003; Principi et al., 2004). The existence of Fe-basalt and Fe-gabbro clasts is unique to the lower ophiolitic breccias.

Syn-extensional upper ophiolitic breccias. ~~These~~ The syn-extensional upper ophiolite breccias (Figs. 3A and 3E) include the Movea, Mt. Zenone, and Mt. Bianco Breccias (Principi et al., 2004, and references therein). The Movea Breccia is a polymictic breccia mainly containing clasts of foliated gabbro with minor amounts of pillow basalt, gabbro, and serpentinite clasts within a chloritized sandy matrix ~~–~~(Bortolotti and Principi, 2003; Principi et al., 2004). The Movea Breccia grades upward into the Mt. Zenone Breccia (Figs. 3C and 3F), which is a monomictic breccia showing only clasts of foliated gabbro in a

sandy matrix composed of gabbro fragments. In contrast, the Mt. Bianco Breccia consists of serpentinite and ophicalcite clasts within an abundant sparry calcite matrix (Bortolotti and Principi, 2003; Principi et al., 2004).

Both the syn-extensional lower and upper ophiolitic breccias are ~~all~~ characterized by comparable sedimentological features: they ~~are~~ all have a clast-supported texture~~s, and the clasts are~~ with angular or sub-angular clasts ~~in shape~~. The matrix has the same lithological composition as the main clast types. The maximum clast-size ranges from gravel to boulder. Beds are lenticular in shape, and their thicknesses range from 1 m up to 20 m. Bed bottoms display planar to erosive surfaces. The erosional nature of the basal contact is suggested by common bottom bedset scours and diffuse, amalgamated beds. A faint internal organization is locally present, and grading is roughly developed. Bed–cap, if not eroded, is characterized by a cm- to dm-~~size~~ thick, coarse-grained and laminated sandstone and siltstone beds composed of ophiolitic material. The downcurrent evolution of the~~se~~ turbidity current depositional events can produce poorly developed ophiolitic sandstones characterized by F5-F6 turbidite facies of Mutti (1992), capped by F9b siltstone beds. These beds are ~~often~~ commonly preserved in the lower part of the chert~~s~~ layers. The~~se~~ clastic sediments can be interpreted to have been formed either as hyperconcentrated flow-derived deposits (Costa, 1988) or, alternatively, as the downcurrent evolutionary products of cohesive debris flows that ~~transforming~~ trasformed into hyperconcentrated flows (F2 and F3 facies of Mutti, 1992).

Clasts of the lower ophiolitic breccias were mainly derived from reworking of the lower and upper crustal sections of the Jurassic oceanic lithosphere within the basin that had undergone ocean floor metamorphism. Stratigraphically higher up into the upper ophiolitic breccias, debris deposits derived from the upper oceanic crustal subunits and

even from oceanic siliceous sedimentary rocks become predominant. We summarize the thickness and other sedimentological features of these syn-extensional chaotic deposits in Figs. 3A and 3E.

Syn-Contractional Mass Transport Deposits (MTDs)

Syn-contractional MTDs, which are well exposed in the eastern Liguria region between the cities of Genova and La Spezia (see 9 and 10 of Fig. 1, also see Fig. 3), developed by submarine mass transport mechanisms and are subdivided on the basis of their spatial relationships with the turbiditic deposits (Figs. 4A, B). Some of ~~them~~ these MTDs occur as intercalations in the turbiditic deposits of the Val Lavagna Shale Group, whereas others overlie this lithostratigraphic unit and contain minor siliciclastic turbidites (Fig. 4C). All clastic materials for these turbiditic deposits were derived from the continental margin of Europe (Marroni and Pandolfi, 2001; Prinicipi et al., 2004; Marroni et al., 2017; Fonnesu and Felletti, 2019; Meneghini et al., 2020).

The MTDs intercalated within the turbiditic deposits of the Val Lavagna Shale Group consist of several mappable bodies of predominantly monomictic, pebbly-mudstones and, locally of varicolored mudflow-derived deposits. Their ages range from Lower Maastrichtian to Lower Paleocene. The predominantly monomictic pebbly-mudstones ~~consist~~ also include ~~of~~ gravel to boulder-sized clasts embedded in a muddy–silty matrix (Fig. 4D). The clast composition is dominated by calcilutites derived from the Palombini Shale, but clasts of fine-grained arenites also exist. The matrix is composed of arenitic to rudistic clasts of carbonate-free mudrock, mainly derived from hemipelagic shales (Fig. 4D). The thickness of beds ranges from a few centimeters to several meters (cf. Olistostroma di Passo della Forcella, Fierro and Terranova 1963). The bed shape is

lenticular, and erosional features are present at ~~their base~~ the bases of beds. The internal organization in the beds is faint to absent. The pebbly mudstone deposits represent cohesive debris flows (cf. olistostrome of Abbate et al., 1970 and F1and F2 facies of Mutti, 1992).

Varicolored shale beds also occur in the upper stratigraphic levels of the Gottero Sandstone (see Fig. 4). Their bed thicknesses ranges from a few meters to more than 20 meters. Bed shape in shale is lenticular and no erosional features are present at bed bases. These deposits were derived from mud flow processes probably related to submarine landslides originated from a steep slope~~,~~ draped by fine-grained sediments.

The MTDs overlying the turbiditic sequences are represented by the lower Paleocene Bocco Shale (Cf. Colli/Tavarone Formation, Giaiette Shale, Lavagnola Formation) (Figs. 4B, 4C, 4E-G). The Bocco Shale unconformably rests on the underlying formations of the Internal Ligurian Units, mainly the Palombini Shale and the Gottero Sandstone (Decandia and Elter, 1972; Marroni and Pandolfi, 2001; Marroni et al., 2017; Meneghini et al., 2020). Clasts within the Bocco Shale were derived from two main facies groups (Marroni and Pandolfi, 2001). The first group is composed of various rock blocks in a matrix of pebbly-mudstone, mudstone, clast-supported breccias, and very coarse- to coarse-grained turbidites. The second group consists of fine-grained, thinly bedded siliciclastic turbidite clasts. We summarize the thicknesses and stratigraphic features of these MTDs in Figure 4C.

Deposits containing the first facies group include MTDs that originated from reworking of an ophiolite sequence and its sedimentary cover (Lamarche et al. 2008; Festa et al. 2016). The block-in-matrix character is displayed by blocks of different sizes (ranging from 1 to 50 m) embedded in a shale–dominated matrix. Blocks are surrounded by syn-sedimentary deformation structures and by slide-block-derived, monomictic pebbly

mudstone and pebbly sandstone. Locally, blocks are missing from the beds and such interbeds are mud-flow-derived mudstone. Pebble-bearing beds range from pebbly mudstones to mud- to clast-supported conglomerates and/or breccias (pebbly mudstone, pebbly sandstone and orthoconglomerate), all interpreted as cohesive debris flow-derived deposits (sensu Mutti 1992). Blocks were derived entirely from reworked ophiolitic subunits (serpentinized peridotites, basaltic lavas, and rare gabbros) and from the Upper Jurassic–Lower Paleocene sedimentary cover of the ophiolite (chert~~s~~, Calpionella Limestone, Palombini Shale, Val Lavagna Shale, and Gottero Sandstone). The matrix ~~is composed of~~ also includes arenitic to ruditic clasts, originated from reworked hemipelagic pelites of the Palombini and Val Lavagna Shales.

Deposits ~~of~~ containing the first facies group are associated with dm- to m-thick beds of polymictic, clast-supported and poorly sorted conglomerates. These conglomerates, which show the same clast composition as the pebbly mudstones, represent the down-current evolution of cohesive debris flows into hyperconcentrated flows (F2 and F3 facies of Mutti 1992). Cohesive debris flow- and hyperconcentrated flow-derived deposits are associated with subordinate, coarse-grained high-density turbidity current deposits. These facies are locally associated with thin Bouma base-missing beds (F5 + F9 facies of Mutti 1992). Arenite framework composition analyses performed on three samples from F5 beds, collected from the Bocco Shale in the Gottero Sandstone indicate a litharenitic composition. This framework is characterized by fragments of basalt, serpentinite, chert and Calpionella-bearing limestone (Meneghini et al., 2020). Similarly, pebbles in F1, F2 and F3 beds show the same composition as recognized in the slide-blocks and arenites. These data and observations collectively point to a source area characterized by reworking

of ophiolites and related sedimentary cover within the Internal Ligurian tectonostratigraphy (Marroni and Pandolfi, 2001; Meneghini et al., 2020).

Clasts of the second facies group consist of thinly bedded turbidites and mudstones, the most common facies association recognized in the Bocco Shale. The thinly bedded turbidites ~~comprise~~ consists of alternations of fine- to medium-grained siliciclastic arenites with carbonate-free mudstones. Sand to shale ratio in this facies group is generally >1. Arenite beds show moderate lateral continuity. Stratigraphic and sedimentological features of ~~these~~ deposits of the second facies group point to low-density turbidity currents as the main depositional agent. Thick packages of thinly bedded turbidites were affected by widespread syn-sedimentary deformation due to slumping and submarine mass-wasting. These processes were responsible for the formation of meso-scale angular unconformities (more than 30°) among different packages of beds. The inferred processes and their manifestations suggest their development on a steep and unstable submarine slope. Thin–bedded turbidites grade into thick packages of varicolored carbonate-free mudstones, which are intensively bioturbated. These mudstones are also characterized by the presence of lenticular, thin beds of siltstones and fine–grained arenites. Bioturbation affected both the arenites and mudstones. The Bocco Shale likely originated from multiple submarine – slide events developed on an accretionary wedge slope (Figs. 4A, 4B), which was covered with thinly bedded turbidites near a lower–trench environment (Marroni and Pandolfi 2001; Meneghini et al., 2020).

OPHIOLITE AND SEDIMENTARY COVER RECORD IN THE WESTERN ALPS

Several examples of chaotic rock units composed of reworked ophiolitic material are preserved in the sedimentary cover of the Jurassic ophiolites (i.e., the Zermatt-Saas Zone, Monviso and Queyras Complexes) in the Piedmont Zone of the Western Alps (Elter, 1971; Tartarotti et al., 1998, 2017a; Dal Piaz et al., 2003; Balestro et al., 2015a; Corno et al., 2021). These ophiolites display strong deformation fabrics and variable, high to ultrahigh–pressure metamorphic overprints (i.e. eclogite- to blueschist-facies; Fig. 1). Prior to their emplacement and during their subduction, these ophiolites were stretched and sheared but not significantly dismembered, at least locally. They were further deformed during their exhumation, although they mostly remained as coherent slices of a metamorphosed oceanic lithosphere. This exhumation-related deformation produced NW- to W-vergent folding and shearing, coeval with greenschist-facies metamorphism of all ophiolitic subunits. ~~Earlier ophiolites and different rocks in their sedimentary cover were metamorphosed under high- and ultrahigh-pressure conditions, and then under greenschist facies conditions, before the continent-continent collision event (Alpine stage).~~

The Zermatt-Saas ophiolite (Fig. 1) is a large remnant of the Jurassic oceanic lithosphere, extending for ~~c.~~ about 60 km along-strike. It was metamorphosed under eclogite- and coesite-eclogite facies conditions as a result of its subduction (e.g., Groppo et al., 2009; Frezzotti et al., 2011; Luoni et al., 2018). The Zermatt-Saas ophiolite consists of serpentinized metaperidotites (Li et al., 2004; Rebay et al., 2012; Fontana et al., 2008) ~~, and~~ with Middle to Late Jurassic metagabbros ~~intrusions within~~ intruded into the ~~these~~ metaperidotites (Bearth, 1967; Rubatto et al., 1998; Zanoni et al., 2016). Peridotite host rocks and their gabbroic intrusive bodies were exhumed on the seafloor as a result of amagmatic extensional tectonics during the opening of the LPOB. Ophicalcite and ultramafic breccia deposits formed during this phase, directly overlying the exhumed

peridotite and gabbro bodies on the seafloor (Driesner, 1993; Tartarotti et al., 1998, 2021). The upper part of the Zermatt-Saas ophiolite includes discontinuous metabasaltic lava flows that locally show well preserved pillow structures (Bucher et al., 2005) and a thin metasedimentary cover made of Mn-rich chert, marble and calcschist (Dal Piaz and Ernst, 1978; Bearth and Schwander, 1981; Tartarotti et al., 2017b, 2021).

The Monviso ophiolite (Fig. 1), which is several–km–thick, extends for ~~c.~~ about 35 km from N to S. Similar to the Zermatt-Saas ophiolite, it was metamorphosed under eclogite facies conditions (Lombardo et al. 1978; Schwartz et al., 2000; Groppo and Castelli, 2010; Angiboust et al., 2012; Balestro et al., 2014, 2018). The Monviso ophiolite contains a major shear zone (i.e., Baracun Shear Zone of Festa et al., 2015) that separates massive serpentinite and metagabbro outcrops in its footwall from pillow metabasalts and metasedimentary rocks within its hanging wall. This shear zone has been interpreted as a fossil intraoceanic detachment fault with a Late Jurassic oceanic core complex developed in its footwall (Balestro et al., 2015b). Protoliths of the serpentinite are lherzolite and harzburgite, which were intruded by numerous stocks and dikes of Middle Jurassic gabbro (Rubatto and Hermann, 2003) and some Late Jurassic plagiogranite (Lombardo et al., 2002).

Metasedimentary rocks in the cover of the Monviso ophiolite make up two different sequences. The structurally and stratigraphically lower sequence rests below or is intercalated with metabasaltic lava flows~~, which~~ that display relict pillow lava structures and volcanic breccia textures. This lower sedimentary sequence includes calcschist interbedded with metasandstone and metabreccia units, whose clasts are gabbroic rocks (Balestro et al., 2011). The upper sedimentary sequence unconformably overlies serpentinite, metagabbro, metabasalt and ophiolitic metabreccias, and consists of thin

568 metaquartzite, ~~whitish~~ white marble and calcschist. These rocks in the upper sequence lack
569 any ophiolite-derived material (Balestro et al., 2019).

570 The Queyras ophiolite tectonically overlies the Monviso ophiolite along an E-
571 striking fault (Fig. 1). Its subunits display blueschist-facies metamorphic overprint (e.g.,
572 Vitale Brovarone et al., 2014), the degree of which decreases structurally up-section
573 throughout the ophiolite (Lagabrielle and Polino, 1988). Similar to the Monviso ophiolite,
574 the Queyras ophiolite also includes a fossil intraoceanic detachment fault with an oceanic
575 core complex in its footwall (Lagabrielle et al., 2015). The sedimentary cover ~~is~~ consists of
576 calcschist characterized by the occurrence of blocks of serpentinized metaperidotite,
577 metagabbro, metabasalt and mafic-ultramafic metabreccias (Tricart and Lemoine, 1991)
578 ranging in ~~size~~ thickness from a few metres to a few km ~~embedded in calcschist~~ (Schistes
579 Lustrés *Auct.*; Lemoine and Tricart, 1986; Tricart and Schwartz, 2006). Larger blocks
580 locally preserve a mantle-cover succession with mantle rocks ~~followed~~ overlain by
581 metachert, up to a few meters thick, ~~which contain~~ locally containing Middle Bathonian to
582 Late Oxfordian radiolarians (Cordey et al., 2012, and reference therein), and by several
583 meters ~~thick~~ of white marble, which has been correlated with the Calpionella limestone of
584 the Northern Apennines (Principi et al., 2004). The calcschist sequence includes a lower
585 member (Replatte Formation of Lemoine 1971), mainly consisting of carbonate-rich
586 calcschist, a middle member (Roche Noire Formation of Tricart, 1973) composed of black
587 micaschist, and an upper member (Gondran Flysch of Lemoine, 1971), ~~made~~ consisting of
588 alternating layers of calcschist and metasandstone. The sedimentological features of the
589 Gondran Flysch and the black shales at its base are correlative with the turbiditic deposits
590 of the Val Lavagna Group–Gottero Sandstone in the Internal Ligurian Units.
591

METAMORPHOSED CHAOTIC ROCK UNITS IN THE WESTERN ALPS

Notable examples of chaotic rock units with fragments of ophiolitic material occur in the metasedimentary covers of the Jurassic ophiolites in the Western Alps. These ophiolites and related metasedimentary covers were deformed during two main tectono-metamorphic phases (named D1 and D2), which are correlated to subduction and continental collision-related tectonics, respectively. The D1 developed an early foliation (S1) coeval with high-pressure metamorphism. The D2 was the main phase of folding and thrusting and developed a new foliation (S2) coeval with greenschist-facies metamorphic re-equilibration. Although these sedimentary cover units experienced alpine tectonic deformation and metamorphic recrystallization, they locally preserve lithostratigraphic and sedimentological features (Fig. 5B) that are well preserved in low-strain domains, where primary textures are deformed and overprinted by metamorphic foliation but not transposed and obscured (see also Balestro et al., 2015a; Tartarotti et al., 2017a for details). Here we discuss such rocks in the eclogite-facies (Zermatt-Saas and Monviso) and blueschist–facies (Queyras) cover rocks ~~(Queyras)~~ of the ophiolites and, we categorize them as syn-extensional chaotic deposits and syn-contractional MTDs of the Western Alps.

Syn–Extensional Chaotic Deposits

~~Following the above-described subdivision of the syn-extensional chaotic deposits of the Northern Apennines, we subdivide below their metamorphosed counterparts of the Western Alps.~~ Below, we subdivide and categorize the Western Alpine metamorphosed counterparts of the Northern Apennine syn-extensional chaotic deposits. The metabreccias

are divided into lower and upper ophiolitic metabreccias on the basis of their lithostratigraphic position below or above the base of basaltic lava flows, respectively.

Syn-extensional lower ophiolitic metabreccias. In both the eclogite-facies and blueschist-facies metaophiolites in the Western Alps, the structurally uppermost part of the exposed serpentinized metaperidotites contains a dense network of meters– to several tens of meters–thick carbonate–rich veins, forming metaophicarbonates (metaophicalcite *Auct.*, see OC1 of Lemoine et al., 1987) (e.g., Lagabrielle and Polino, 1985; Lemoine et al., 1987; Tricart and Lamoine, 1991; Driesner, 1993; Lagabrielle, 1994; Tartarotti et al., 1998, 2017a; Dal Piaz, 1999; Balestro et al., 2019, and reference therein). Similar to the Levanto Breccia in the Northern Apennines, the Western Alpine metaophicarbonates are characterized by a complex network of veins filled with carbonate minerals, antigorite, and/or talc (e.g., Lemoine et al., 1987; Tricart and Lemoine, 1991; Dresnier, 1993; Lafay et al., 2017; Tartarotti et al., 2017a). These veins surround dm- to m-sized, angular to rounded fragments of massive serpentinite. Complex crosscutting relationships between different generations of carbonate veins, the infilling and episodic growth of calcite fibers, and the pervasive replacement of serpentinite by carbonate minerals indicate repeated episodes of cracking–fracturing of peridotites and fluid–peridotite interactions during their development. These metaophicarbonate veins were the manifestations of both brittle failure and hydrothermal fluid circulation within the upper mantle peridotites, as these rocks were undergoing exhumation and extensional faulting in ~~the~~ Middle to Late Jurassic time.

As is the case in the Northern Apennines, the top of the metaophicarbonate unit in the Western Alps is extensively reworked, forming discontinuous layers of a clast-supported metabreccia. For example, in the Lake Miserin area (see 3 of Fig. 1, also see Figs. 3 ~~Figs. 1~~ and 5A ~~B~~) in the Zermatt-Saas ophiolite (see Tartarotti et al., 2017a, 2019),

the metaophicarbonate is overlain by a predominantly clast–supported metabreccia ("BrFm1" and "BrFm2" of Tartarotti et al., 2017a). Clasts are angular- to sub-angular in shape, made of serpentinite and metaophicarbonate, and range in size from cm to dm (Fig. ~~5B~~5C). The scarce matrix in this metabreccia consists of a coarse-grained metasandstone, ~~and is also made of~~ including serpentinite and metaophicarbonate derived sediments.

The bottom of this clast-supported metabreccia corresponds to an erosional surface, marked by a dm-thick layer of coarse- to medium-grained metasandstone composed of peridotite-derived sediments. The whole metabreccia unit shows a lenticular shape at a scale of hundreds of meters and a maximum thickness of about 15 m (Fig. 5A; see Tartarotti et al., 2017a for details). This metabreccia gradually passes upward into a chaotic rock unit ("sedimentary mélange" of Tartarotti et al., 2017a), which consists of serpentinite and ophicarbonate blocks in a carbonate (now marble) matrix (see the section on Syn-extensional upper ophiolitic metabreccias below). This marble is unconformably overlain by a post-extensional calcschist unit (Fig. 5A), which is devoid of any ophiolite-derived material. In terms of its stratigraphic–structural position above the ophiolite and its compositional makeup and sedimentological characteristics, this calcschist unit correlates with the Lower Cretaceous post-extensional deposits in the Northern Apennines (see Tartarotti et al., 2017a, 2019).

In the Mt. Avic ultramafic massif of the Zermatt-Saas ophiolite in the Western Alps (see 2 of Fig. 1, see Fontana et al., 2008, 2015; Panseri et al., 2008), prevalently monomictic clast-supported metabreccias with poorly sorted angular clasts of serpentinite are embedded in a carbonate matrix (Figs. 5A, ~~5E~~5F; see Tartarotti et al., 1998). Locally, mm– to cm–long mafic clasts derived from a gabbro source also occur, ~~thus~~ forming a

663 polymictic-type metabreccia. Structurally, these metabreccias generally occur on top of the
664 serpentinite and Mg-Al metagabbro units, and below a metabasaltic lava sequence.

665 In the Queyras ophiolite in the Western Alps, different types of poorly-sorted, clast-
666 supported metabreccia (i.e., the OC2 of Lemoine et al., 1987) range from monomictic–type
667 with cm–long, sub-angular clasts made only of serpentinite (e.g., Pic Cascavelier section,
668 see Tricart and Lemoine, 1983, 1991; Caby et al., 1987; Lemoine and Tricart, 1986) or
669 metagabbro (e.g., Crete Mouloun section, Le Mer et al., 1986), to polymictic–type
670 metabreccia (see 6, 7 and 8 of Figs. 1 and ~~5F~~5I, 5G) with clasts of both serpentinite and
671 metagabbro (see Le Mer et al., 1986; Lemoine et al., 1987; Balestro et al., 2019, and
672 reference therein). These metabreccias are laterally discontinuous in exposure and range
673 from a few cm to several tens of meters in thickness. Large blocks (olistoliths), up to tens
674 of meters wide, locally occur (Tricart and Lemoine, 1983) in a sandy matrix with grains of
675 mixed mafic rock and carbonate composition. The structural position of both monomictic
676 and polymictic metabreccias (Fig. ~~5F~~5I) is commonly above the exhumed serpentinite and
677 metagabbro and below the metabasaltic lava sequence (metapillow lavas and basaltic
678 metabreccias).

679 In the Monviso ophiolite in the Western Alps (see 5 of Fig. 1), a sedimentary
680 sequence, consisting of calcschist interbedded with mafic metasandstone and matrix-
681 supported metabreccia layers, onlaps a fossil detachment fault and its footwall units (Fig.
682 6A). The footwall of this detachment fault zone is made of serpentinized metaperidotites,
683 intruded by Mg-Al and Fe-Ti gabbro plutons and stocks. The mafic–ultramafic part of the
684 Monviso ophiolite has been interpreted as an exhumed oceanic core complex (OCC; see
685 Balestro et al., 2015a, 2019; Festa et al., 2015). The matrix-supported metabreccia includes
686 poorly sorted sub-angular to angular clasts of metagabbro (Figs. 6B-D) and laterally grades,

687 at a scale of tens of meters, into coarse-grained metasandstone of the same composition,
688 locally with a fining-upward texture (Fig. 6E). The thickness of these syn-extensional
689 metasedimentary rocks shows significant lateral variations, ranging from several
690 centimeters to about 70 meters, and generally tapers out toward an association of talcschist
691 and serpentine–schist~~,~~ containing blocks of highly sheared metagabbro. These intensely
692 foliated talcschist and serpentine–schist units correspond to an intra-oceanic detachment
693 fault zone (i.e., the Baracun Shear Zone of Festa et al., 2015). The shear zone is
694 unconformably overlain by post-extensional ~~whitish~~ white marble and carbonate-rich
695 calcschist (Fig. 6A), devoid of any ophiolite-derived material. The white marble and
696 calcschist correspond to the Upper Jurassic-Lower Cretaceous Calpionella Limestone and
697 the Early Cretaceous Palombini Shale of the Internal Ligurian Units in the Northern
698 Apennines, respectively (see Balestro et al., 2015a, 2019; Festa et al., 2015).
699
700 ***Syn-extensional upper ophiolitic metabreccias.*** The most notable examples of monomictic
701 basaltic metabreccia and polymictic-metabreccia, correlating lithologically and
702 stratigraphically with the upper ophiolitic breccias in the Northern Apennines, are best
703 preserved in the Queyras ophiolite (e.g., Caby et al., 1971, 1987; Tricart and Lemoine,
704 1983, 1991; Le Mer et al., 1986; Saby, 1986; Pinet et al., 1989). The metabreccias in the
705 Queyras ophiolite are stratigraphically situated between the base of the pillow metabasalt
706 sequence and the first post-extensional sedimentary units (i.e., metachert and white marble;
707 see Fig. ~~5F~~5I).
708 The monomictic metabreccia consists only of angular to sub-angular clasts, up to 30
709 cm – long, of metabasalt that are embedded within a sandy matrix composed of fragments
710 of metabasalt and/or metahyaloclastite (see, e.g., the Crete Mouloun and Pic Marcel

711 sections in Le Mer et al., 1986 and Tricart and Lemoine, 1983, respectively. See 6 and 7 of
712 Fig. 1). Although this monomictic metabreccia commonly overlies the metabasaltic pillow
713 lava sequence (e.g, Crete Mouloun), it locally occurs both at the base of (e.g., Pic Marcel)
714 and/or interfingered with these metabasaltic lava flows (e.g., Tricart and Lemoine, 1983).

715 Polymictic metabreccia with cm- to dm-long clasts of massive and variolitic
716 metabasaltic lavas, metagabbro, and quartzo-feldspathic rocks (plagiogranite) occur both at
717 the base (e.g., Pic Marcel, see Tricart and Lemoine, 1983) and at the top (e.g., Crete
718 Mouloun, see Le Mer et al., 1986) of the metamorphosed pillow ~~meta~~lava sequence. The
719 matrix of this metabreccia is sandstone, which is composed of fragments of the same
720 compositions as the clasts.

721 All these different types of metabreccias have a poorly sorted, clast-supported
722 texture with angular to sub-angular clasts. Stratigraphically upward, they grade into a
723 matrix-supported metabreccia and coarse-grained metasandstone with well – preserved
724 incipient layers of different compositions (see also Tricart and Lemoine, 1983). The
725 bottoms of these metabreccia layers are commonly lenticular and erosional.

726 The occurrence of metabreccias in a stratigraphic position comparable to the one of
727 the upper ophiolitic metabreccias of the Appennines is rare in the Monviso and Zermatt
728 Saas ophiolites in the Western Alps. There are, however, two examples of possible upper
729 ophiolitic metabreccias in the Zermatt-Saas ophiolite. The first one is part of the Garten
730 Formation (i.e., the Rifelberg-Garten mélange or Palon de Resey mélange; see Dal Piaz,
731 1965, 1992; 2004; Bearth, 1967; Dal Piaz and Ernst, 1978; Campari et al., 2004; Dal Piaz et
732 al., 2015; Gusmeo et al., 2018), which crops out discontinuously from the Cime Bianche
733 ridge to the highest Ayas Valley (see 1 of Fig. 1; see Dal Piaz, 1992; Dal Piaz et al., 2015
734 for details). The Garten Formation consists of a chaotic rock unit, meters– to tens of

meters–thick, with rounded to elongated clasts (cm to dm in size) of fine-grained metabasalt (metamorphosed to eclogite and glaucophanite), serpentinite and marble (Gusmeo et al., 2018), embedded in a matrix of alternating layers of micaschist and calcschist (Figs. 6F-H). This formation represents the superposition of different individual deposits, each a few decimeters to nearly one meter in thickness (Fig. 6F). The largest clasts occur in the lower part of the beds and "float" in a fully mixed and crudely graded matrix, made of calcschist (Figs. 6G, 6H). The stratigraphic position of this formation is at the base of metabasaltic lava flows with locally well – preserved pillow structures (Fig. 6I; see Dal Piaz, 1965, 2004). It is, however, important not to confuse the above-described chaotic deposit with the larger part of the Garten Formation that corresponds to a typical "broken formation" (*sensu* Hsü, 1968), resulting from layer-parallel tectonic extension of alternating micaschist and metabasite layers and boudinage formation.

In the Lake Miserin sedimentary cover sequence of the Zermatt-Saas ophiolite (Fig. 1), the lower ophiolitic metabreccia is overlain by a chaotic rock unit characterized by a block-in-matrix fabric with rounded to irregular – shaped blocks (dm- to a meter-wide) of massive to veined serpentinite and metaophicarbonate embedded in a white marble matrix (Figs. 5A, ~~5D~~5E). Blocks are randomly distributed within the matrix, except where elongated and deformed blocks are aligned with the regional tectonic foliation (Tartarotti et al., 2019). The matrix is commonly interbedded with cm- to dm-thick layers of metabreccia, with clasts ~~consisting of~~ angular to sub-angular clasts of serpentinite (Fig. ~~5D~~5E).

Syn-contractional mass–transport deposits (MTDs)

The identification of possible counterparts of the syn-contractional mass–transport deposits of the Northern Apennines in the metasedimentary cover of the ophiolites in the Western Alps is not easy. The gravity-induced MTDs, composed of material derived from both a continental margin and the ophiolites, are lacking in the Zermatt-Saas and Monviso ophiolites, but they occur in the Lago Nero Unit of the Queyras ophiolite (see 4 of Fig. 1). The Lago Nero Unit includes a thick metasedimentary sequence, starting at the bottom with a radiolarite member, topped by a limestone member and the Replatte Formation (Lemoine et al., 1970; Polino, 1984; Barfety et al., 1995; Burroni et al., 2003). The Replatte Formation contains alternating layers of thick calcschist and thin marble. It grades stratigraphically upwards into both a thin unit of grey to black schists and to the Gondran Flysch, composed of alternating layers of calcschist and metasandstone (Fig. ~~5F~~5I). The Gondran Flysch represents thinly bedded turbidites with minor occurrences of thick and coarse–grained, terrigenous metasandstone. Petrographic analysis of the terrigenous metasandstone indicates an arkosic composition, made predominantly of quartz, feldspar and minor lithic fragments. The metasedimentary cover sequence of the Lago Nero Unit stratigraphically is capped by the Rocher Renard Complex (Fig. ~~5F~~5I; Barfety et al., 1995; Burroni et al., 2003). The Rocher Renard Complex consists of homogeneous dark schists, locally containing metre- to decametre-size blocks~~,~~ composed mainly of limestone and chert, with local occurrences of metabasalt, metaophicalcite, serpentinite and metagabbro (Figs. ~~5F~~ 5H, 5I).

DISCUSSION: THE CHAOTIC DEPOSITS AND MTDs OF THE NORTHERN APENNINES AS A PROXY FOR METAMORPHOSED COUNTERPARTS IN THE WESTERN ALPS

Our detailed description of chaotic rock units and MTDs indicates that different ophiolite units in the Northern Apennines and ~~in~~ the Western Alps correlate well, both chronologically and stratigraphically (Table 1). These correlations suggest that the diagnostic features of the chaotic deposits and MTDs in the Internal Ligurian Units can be used as a proxy for better definition of the tectonostratigraphy of their highly deformed and metamorphosed counterparts in the Western Alps. The strong similarities between these chaotic deposits and MTDs within the epi–ophiolitic sequences in both ~~the~~ orogenic belts, allows reconstructing: (i) the pre-orogenic primary lithostratigraphy and sedimentological features of the Western Alpine occurrences, (ii) the processes and mechansims of Western Alpine rock formation and, (iii) the characteristics of the depositional or geodynamic settings of rock body origins. Our findings also indicate that the LPOB lithosphere underwent similar tectonic processes during the Jurassic seafloor spreading and Late Cretaceous – Early Paleocene closure phases of the ocean basin throughout its entire length (Fig. 7).

Processes of formation of chaotic deposits and MTDs in the Western Alps from seafloor spreading to subduction

Although they experienced severe tectonic deformation and metamorphic recrystallization, the described examples of chaotic rock units in the Western Alps locally preserve lithostratigraphic and sedimentological features (see also Balestro et al., 2015a;

804 Tartarotti et al., 2017a for details) that are comparable with those of the ~~poorly~~ little
805 metamorphosed Internal Ligurian Units in the Northern Apennines. The oldest syn-
806 extensional chaotic deposits (the lower ophiolitic metabreccias) of the Western Alps
807 preserve remnants of sedimentological features and internal organization that are diagnostic
808 of different products formed by the downcurrent transformation of cohesive flows through
809 progressive mixing with ambient fluids (F2 facies of Mutti, 1992). In different sections of
810 the Queyras (see Pic Cascavelier and Crete Mouloun) and Zermatt-Saas (see Lake Miserin
811 and Mt. Avic) ophiolites, the faint internal structure of the clast-supported breccia, such as
812 the lack of a well-defined grading, the scarcity of lamination, and the absence of any
813 pelagic interbeds, suggest rapid deposition through cohesive debris flows or
814 hyperconcentrated flows. In these processes, the larger clasts float in a mixed and crudely
815 graded matrix, which was probably composed of mud and mafic and/or ultramafic sand and
816 gravel, with largest clasts occurring in the lower part of the bed. In some cases, such as for
817 the lower ophiolitic metabreccia unit in the Monviso ophiolite, the occurrence of a poorly
818 sorted, coarse-grained sandstone, grading laterally into a coarse-grained sandstone with a
819 fining-upward texture, suggests that these deposits represent the products of downslope
820 transformation of a hyperconcentrated flow into a high-density and supercritical turbidity
821 current, and locally a low-density one, possibly corresponding to a gravity transformation
822 from F4-F5 to F7 facies of Mutti (1992).

823 The characteristics of the matrix-supported metabreccia and coarse-grained
824 metasandstone of the youngest syn-extensional upper ophiolitic metabreccias of Pic Marcel
825 and Crete Mouloun in the Queyras suggest that they represent the products of
826 hyperconcentrated flows. These products result from downslope transformation of
827 cohesive-flow (F2 and F3 facies of Mutti, 1992), which changes laterally and upward into

828 gravelly, high-to low-density turbidity currents (F4-F5 and F7 facies of Mutti, 1992). This
829 is similar to the examples interpreted for the Monviso ophiolite.

830 Our documented sedimentological features of part of the Garten Formation and of
831 the upper ophiolitic metabreccias of the Lake Miserin in the Zermatt-Saas ophiolites
832 confirm that they represent the products of submarine mass transport processes, as
833 suggested by Bearth (1963) and Dal Piaz (1965), and by Tartarotti et al (2017a, 2019),
834 respectively. We have observed that the sedimentary fabric elements of these metabreccias
835 are consistent with the deposition from either hyperconcentrated flows (F2 of Mutti et
836 al.,1992) or generally high–density turbidity currents (F4-F5 of Mutti et al., 1992) that
837 resulted from downslope transformation of closure flows through progressive mixing with
838 ambient fluids.

839 The sedimentological features of the syn-contractional MTD of the Lago Nero Unit
840 (i.e., the Rocher Renard Complex) in the Western Alps (i.e., prevailing shaly matrix and the
841 occurrence of angular blocks of ophiolitic material and sedimentary rocks) and its
842 stratigraphic position correlate well with the Bocco Shale in the Northern Apennines (Table
843 1; Burroni et al., 2003). Similarly, its sedimentological features fit well with those of the
844 product of multiple submarine cohesive debris flows evolving down-current to
845 hyperconcentrated turbidity deposits that were emplaced on an accretionary wedge slope.

846

847 **Comparison between chaotic deposits and MTDs in the Northern Apennines and the**
848 **Western Alps**

849 The documented similarities of the sedimentological features and internal
850 organization of the syn-extensional chaotic deposits in both the orogenic belts is consistent
851 with their formation through deposition of small volumes of poorly consolidated material

accumulated in the hanging walls of submarine normal faults and fault escarpments. These deposits formed above detachment faults and oceanic core complexes (Fig. 7A) during the Jurassic seafloor spreading (e.g., Tricart and Lemoine, 1983, 1991; Caby et al., 1987; Lemoine and Tricart, 1986; Dilek and Eddy, 1992; Tartarotti et al., 1998, 2017a; Principi et al., 2004; Lagabrielle, 2009; Balestro et al., 2015a, 2019 and reference therein). The occurrence of these deposits in two different specific tectonostratigraphic positions (below or above the basaltic pillow lava flows; Figs. 3, 5, 6) in both the Northern Apennines and the Western Alps, suggests that their formation occurred in two distinct events of extensional tectonics during a continuum of syn-spreading deformation. Moreover, the chaotic deposits in ~~both~~ the different sectors of the Jurassic LPOB (i.e., Western Alps and Northern Apennine) show the same features and the same lithological composition of clasts (Table 1), strongly indicating that the oceanic basin developed with the same features and in a similar basin floor architecture during its entire history and along its entire length (Fig. 7a). It is, however, necessary to use caution in the attempt to correlate the chaotic deposits related to syn-spreading extensional tectonics, and to discriminate between the lower and upper ophiolitic metabreccias in the metamorphosed Western Alps because, for example, their correlation is hampered when an incomplete oceanic crust stratigraphy exists, such as where extrusive rocks are missing, or when a diagnostic clast composition is not recognizable within gravitationally induced chaotic deposits.

Independent of the type of breccia (lower or upper), the composition of clasts depends on the nature of the source area and its location with respect to the site of deposition. In these cases, our findings show that the diagnostic sedimentological features of the non- to poorly metamorphosed syn-extensional ophiolitic breccias of the Northern Apennines may represent a proxy of comparison, providing useful constraints for the

interpretation of the metamorphosed Alpine breccias. For example, although basalt flows are not observed and basalt clasts are lacking, the upper ophiolitic metabreccias of the Lake Miserin (i.e., the "Sedimentary mélange" of Tartatotti et al., 2017a) are ~~quite~~ comparable with the syn-extensional upper ophiolitic Monte Bianco breccias of the Northern Apennines, whose stratigraphic position is well defined. They show ~~, in fact,~~ the same sedimentological features and composition of both clasts and the matrix (see Table 1). This correlation is further supported by field-evidence~~s~~, showing that the Lake Miserin upper breccia is deposited above the lower ophiolitic metabreccia of the same sequence and it is covered by mixed siliciclastic-carbonaceous sediments, corresponding to the Lower Cretaceous post-spreading deposits in the Northern Apennines (see Tartarotti et al., 2017a for details). Therefore, although caution is necessary in interpreting chaotic deposits in the highly deformed and metamorphosed Western Alpine units, the use of the Northern Apennines examples may represent a useful proxy for better interpretation of their metamorphosed counterparts, which were deposited during the Jurassic syn-spreading tectonics of the LPOB.

The syn-contractional MTDs with ophiolitic material~~, which~~ that are widespread in the Internal Ligurian Units of the Northern Apennines~~,~~ have been also identified in the Western Alps, as detected in the Lago Nero Unit of the Queyras ophiolite. In both ~~the~~ orogenic belts, the sedimentological features and internal organization of these deposits suggest they originated by several events of tectonic erosion at the front of the accretionary wedge (Fig. 7b), which developed in the Late Cretaceous in response to the development of an east-dipping subduction of the LPOB lithosphere close to or within the thinned Adria margin (Marroni et al., 2017 and reference therein). These events of frontal tectonic erosion were induced by ~~the~~ underthrusting of the seafloor morphological relief inherited from the

previous Jurassic syn-spreading tectonics (Fig. 7b; Marroni and Pandolfi, 2001; Burroni et al., 2003; Meneghini et al., 2020). The subduction of morphological relief commonly produces the uplift of the lower slope of the frontal wedge, its collapse and the subsequent downslope mobility of wide MTDs and their emplacement in the lower plate and/or in the trench (Fig. 7b; e.g., von Huene and Lallemand, 1990; von Huene et al., 2004; Kawamura et al., 2009; Remitti et al., 2011; Festa et al., 2018; Geersen et al., 2020; Meneghini et al., 2020; Ogata et al., 2020).

During the Late Cretaceous – Early Paleocene convergent stage of the LPOB, these ophiolitic MTDs, mainly consisting of pebbly mudstones and slides (Lamarche et al. 2008; Festa et al. 2016), interfingered with thin bedded, siliciclastic turbidites supplied by the European continental margin, as was the case in the Rocher Renard Complex in the Lago Nero Unit (Queyras ophiolite; see also Burroni et al., 2003) and the Bocco Shale in the Northern Apennines (see also Marroni and Pandolfi, 2001; Meneghini et al., 2020). Therefore, syn-contractional MTDs in both transects of the convergence system can be regarded as formed by similar processes widespread along the entire width of the oceanic basin. In the Western Alps, however, the occurrence of syn-contractional MTDs ~~seems to be~~ are restricted to the units subducted at moderate depths (i.e., those affected by blueschist-facies P-T metamorphic peak), ~~whereas~~ and they are not observed in the deeper eclogite-facies units. It is hard to discriminate whether the absence of these deposits in higher grade units is simply due to failure to recognize them in the field, if these deposits were not preserved, or they did not form at all ~~in those units~~. An explanation for the occurrence of syn-contractional MTDs only in the units accreted at shallow to moderate depths could be that frontal tectonic erosion was active in a restricted time span, probably in the Late Maastrichtian-Early Paleocene, when most of the eclogite facies units were

924 already underthrust at depth in the subduction zone. On the other hand, underplating at
925 shallow to moderate depths, especially in sediment-dominated systems, generally involves
926 preferential removal of the sedimentary cover from the upper part of an oceanic lithosphere
927 (Meneghini et al., 2009 and reference therein). This phenomenon occurs when the
928 downgoing plate reaches a depth consistent with the development of eclogite-facies
929 metamorphism (Moore and Sample, 1986). In this framework, the lack of syn-contractional
930 ophiolitic MTDs in the eclogite-facies units of the Western Alps could be also explained ~~as~~
931 ~~due to~~ by selective removal of these deposits during progressive subduction underthrusting.
932
933
934 **CONCLUDING REMARKS**
935
936 In this comparative analysis, we have examined the occurrence and the internal
937 structure of different types of chaotic rock units with ophiolitic material in the Internal
938 Ligurian Units of the Northern Apennines and in the Piedmont Zone of the Western Alps
939 that contain ophiolite-derived material. Our findings document that the internal structure-
940 stratigraphy and sedimentological characteristics of the chaotic deposits and MTDs ~~of~~ in
941 the Northern Apennines can be used as a proxy to identify the nature and processes of
942 formation of their highly deformed and metamorphosed counterparts in the Western Alps.
943 ~~The latters, which~~ The chaotic deposits and MTDs in the Western Alps are commonly
944 confused with tectonically ~~chaotic products~~ produced rocks assemblages and tectonic
945 mélanges. We have shown in this study that the MTDs in the Western Alps consist of two
946 different types of chaotic deposits of gravitational origin, formed by different submarine
947 mechanisms, and they occur in different tectonostratigraphic positions within the epi-

948 ophiolitic sedimentary cover. The oldest chaotic deposits occur both below and above the
949 extrusive sequences in the ophiolites, representing syn-extensional, hyper-concentrated
950 deposits associated with the seafloor spreading evolution of the LPOB lithosphere during
951 the Middle-Late Jurassic. The youngest chaotic deposits consist of MTDs, which occur as
952 intercalations within turbiditic sequences above the ophiolites, representing syn–
953 contractional submarine slides. The slides occurred on frontal accretionary prism slopes
954 during the Late Cretaceous–Paleocene closure of the LPOB.

955 This comparative study provides important clues ~~to~~ for the contextual framework of
956 the definition of magmatic, tectonic, and sedimentary processes, which ~~that~~ occurred
957 throughout the formation of the Jurassic oceanic lithosphere and its sedimentary cover in
958 the LPOB (Western Tethys), and during the subsequent Late Cretaceous – Paleocene
959 convergent margin tectonics. These processes were remarkably uniform and synchronous as
960 shown by the occurrence of comparable chaotic deposits and MTDs characterized by the
961 same features and the same lithological compositions of clasts. ~~The~~ Our data and
962 observations indicate that the LPOB developed with the same features and in a similar
963 basin floor architecture during its entire history and along its entire length.

964 The results and the geological implications of this comparative study ~~is~~ are not
965 limited ~~to~~ only to the Western ~~Alps~~ Alpine orogenic belt. The diagnostic features of the
966 different types of chaotic rock units described in this study can also help in distinguishing
967 among those similar units that extensively occur in many ~~Archean~~ Precambrian to Cenozoic
968 orogenic belts throughout the world, where the overprint of tectonic and metamorphic
969 processes obscured their primary features and the mode of formation. Their detailed
970 lithological, structural and chronological correlations ~~throughout the entire length of~~ along
971 and across the orogenic belts should provide~~s~~ additional constraints for ~~the~~ reconstruction

of the magmatic, tectonic and sedimentary evolution of ~~the~~ oceanic basins, and for the ~~in which they formed, and consequently for the~~ subsequent convergent tectonic evolution. Therfore, detailed, multidisciplinary studies of chaotic rock units ~~are insightful~~ are an integral part of systematic investigations of ~~for better understanding and constraining~~ the temporal evolution of different stages of orogenic buildup, from continental rifting and seafloor spreading to subduction, and crustal exhumation. ~~thus contributing to the improvement and refiniton of the plate tectonics paradigm.~~ Such studies and their results have contributed significantly to further refining the plate tectonics paradigm since the mid-1960s.

ACKNOWLEDGEMENTS

We extend our sincere thanks to the two anonymous reviewers for their constructive and thorough reviews, from which we have benefited greatly in revising our manuscript. The project was supported by the University of Pisa (PRA project and ATENEO grant), the University of Torino (Ricerca Lolcale ex 60% 2017-2020, grants to GB and AF), and by the Italian Ministry of University and Research ("Finanziamento annuale individuale delle attività base di ricerca 2017", grants to GB and AF). Grants to PT (PSR2018_DZANONI) were provided by the University of Milan. Y Dilek acknowledges the Miami University research funds for his fieldwork in the Western Alps. F. Meneghini and M. Marroni would like to dedicate this contribution to the beloving memory of Casey Moore, former supervisor of F. Meneghini, for his fundamental contribution to the understanding and definition of many aspects of plate tectonics concerning the dynamics of convergent margins, and the processes shaping the accretionary prisms.

REFERENCES CITED

Abbate, E., and Sagri, M. 1982. Le unità torbiditiche cretaciche dell'Appennino Settentrionale ed i margini continentali della Tetide. Mem. Soc. Geol. It. 24: 115-126.

Abbate, E., Bortolotti, V., and Passerini, P. 1970. Olistostromes and olistoliths. Sed. Geol. 4: 521-557.

Abbate, E., Bortolotti, V., Passerini, P., Principi, G. and Treves, B. 1994. Oceanisation processes and sedimentary evolution of the northern Apennine ophiolite suite: a discussion. Mem. Soc. Geol. It. 48: 117-136.

Abbate, E., Bortolotti V., and Principi, G. (1980), Apennine ophiolites: a peculiar oceanic crust. *In* G. Rocci ed. Special issue on Tethyan ophiolites, Western area. Ofioliti 5: 59-96.

Angiboust, S., Langdon, R., Agard, P., Waters, D., and Chopin, C. 2012. Eclogitization of the Monviso ophiolite (W. Alps) and implications on subduction dynamics. J. Metamorph. Geol. 30: 37-61.

Anonymous 1972. Penrose fi eld conference on ophiolites. Geotimes 17: 24-25

Balestro, G, Festa, A., Borghi, A., Castelli, D., Gattiglio, M. and Tartarotti, P. 2018. Role of Late Jurassic intra-oceanic structural inheritance in the Alpine tectonic evolution of the Monviso meta-ophiolite Complex (Western Alps). Geol. Mag. 155: 233-249.

Balestro, G., Festa, A., and Tartarotti, P. 2015a. Tectonic significance of different block-in matrix structures in exhumed converget plate margins: examples from oceanic

and continental HP rocks in Inner Western Alps (northwest Italy). Int. Geol. Rev. 57: 581-605.

Balestro, G., Festa, A., Dilek, Y. and Tartarotti, P. 2015b. Pre-Alpine extensional tectonics of a peridotite-localized oceanic core complex in the late Jurassic, high-pressure Monviso ophiolite (Western Alps). Episodes 38: 266-282.

Balestro, G., Festa, A., and Dilek, Y. 2019. Structural architecture of the Western Alpine Ophiolites, and the Jurassic seafloor spreading tectonics of the Alpine Tethys. J. Geol. Soc. 176: 913-930.

Balestro, G., Fioraso, G. and Lombardo, B. 2011. Geological map of the upper Pellice Valley (Italian Western Alps). J. Maps 2011: 634-654.

Balestro, G., Lombardo, B., Vaggelli, G., Borghi, A., Festa, A. and Gattiglio, M. 2014. Tectonostratigraphy of the northern Monviso meta-ophiolite complex (Western Alps). It. J. Geosci. 133: 409-426.

Balestro, G., Nosenzo, F., Cadoppi, P., Fioraso, G., Groppo, C. and Festa, A. 2020. Geology of the southern Dora-Maira Massif: insights from a sector with mixed ophiolitic and continental rocks (Valmala Tectonic Unit, Western Alps). J. Maps 16 (2): 736-744.

Barbero, E., Festa, A., Saccani, E., Catanzariti, R., and D'Onofrio, R. 2020. Redefinition of the Ligurian Units at the Alps-Apennines junction (NW Italy) and their role in the evolution of the Ligurian accretionary wedge: constraints from mélanges and broken formations. J. Geol. Soc. 177: 562-574.

Barbero, E., Pandolfi, L., Morteza, D., Dolati, A., Saccani, E., Catanzariti, R., Luciani, V., Chiari, M. and Marroni, M. 2021. The western Durkan Complex (Makran Accretionary Prism): A Late Cretaceous tectonically disrupted seamounts chain

and its role in controlling deformation style. Geosci. Front. 12 (3): 101106. https://doi.org/10.1016/j.gsf.2020.12.001

Barféty, J.C., Lemoine, M., De Graciansky, P.C., Tricart, P. and Mercier, D., 1995. Carte géologique de la France a 1/50000, Feuille 823 Briançon.

Bearth, P. 1963. Contribution à la subdivision tectonique et stratigraphique du cristallin de la nappe du Grand Saint-Bernard dans le Valais. Geol. Soc. Fr. Mem. H. 2: 407-418.

Bearth, P. 1967. Die Ophiolithe der Zone von Zermatt-Saas Fee. Beiträge zur Geologischen Karte der Schweiz, Neue Folge, 132: 1-130.

Bearth, P. and Schwander, H. 1981. The post-Triassic sediments of the ophiolite zone Zermatt-Saas Fee and the associated manganese mineralizations. Eclogae Geol. Helv. 74: 198-205.

Beltrando, M., Manatschal, G., Mohn, G., Dal Piaz, G.V., Vitale Brovarone, A. and Masini, E. 2014. Recognizing remnants of magma-poor rifted margins in high-pressure orogenic belts: The Alpine case study. Earth Sci. Rev. 131: 88–115.

Berkland, J.O., Raymond, L.A., Kramer, J.C., Moores, E.M., and O'Day, M. 1972. What is Franciscan? AAPG Bulletin 56: 2295–2302.

Berra, F. and L. Angiolini, 2014, The evolution of the Tethys region throughout the Phanerozoic: A brief tectonic reconstruction, In Marlow L., Kendall C. and Yose L. eds. Petroleum systems of the Tethyan region. Mem. Am. Assoc. Pet. Geol. 106: 1-27.

Bettelli, G. and Panini, F. 1985. Il mélange sedimentario della Val Tiepido (Appennino modenese) — composizione litologica, distribuzione areale e posizione stratigrafica. Atti Soc. Nat. Mat. Modena 115: 91–106.

1067 Bettelli, G., Conti, S., Panini, F., Vannucchi, P., Fioroni, C., Fregni, P., Bonacci, M.,
1068 Gibellini, R. and Mondani, C. 2004. The mapping of chaotic rocks in Abruzzo
1069 (Central Italy): comparison with selected examples from Northern Apennines,
1070 In Pasquarè, G., Venturini, C. and Groppelli, G., eds., Mapping Geology in
1071 Italy. APAT – SELCA, Firenze: 199–206.
1072 Bill, M., L. O'Dogherty, J. Guex, P.O. Baumgartner, and Masson, H. 2001. Radiolarite ages
1073 in Alpine-Mediterranean ophiolites: Constraints on the oceanic spreading and
1074 the Tethys-Atlantic connection. Geol. Soc. Am. Bull. 113: 129-143.
1075 Bortolotti, V., and Principi, G. 2003. The Bargonasco-Upper Val Graveglia ophiolitic
1076 succession, Northern Apennines, Italy. Ofioliti 28: 137-140.
1077 Bucher, K., Fazis, Y., De Capitani, C. and Grapes, R. 2005. Blueschists, eclogites, and
1078 decompression assemblages of the Zermatt-Saas ophiolite: high-pressure
1079 metamorphism of subducted Tethys lithosphere. Am. Mineral. 90: 821-835.
1080 Burroni, A., Levi, N., Marroni, M. and Pandolfi, L. 2003. Lithostratigraphy and structure of
1081 the Lago nero Unit (Chenaillet Massif, Western Alps): comparison with
1082 Internal Liguride Units of Northern Apennines. Ofioliti 28: 1-11.
1083 Butler, J. P., Beaumont, C., and Jamieson, R. A. 2013. The Alps 1: A working geodynamic
1084 model for burial and exhumation of (ultra) high-pressure rocks in Alpine-type
1085 orogens. Earth Planet. Sci. Lett. 377: 114-131.
1086 Caby, R., Dupuy, C., and Dostal, J. 1987. The very beginning of the Ligurian Tethys:
1087 Petrological and geochemical evidence from the oldest ultramafite-derived
1088 sediments in Queyras, Western Alps (France). Eclogae geol. Helv. 80: 223 240.
1089 Caby, R., Michard, A. and Tricart, P. 1971. Découverte d'une brèche polygénique à
1090 éléments de granitoïdes dans les ophiolites métamorphiques piemontaises

(schistes lustrés du Queyras, Alpes françaises). C.R. Acad. Sci. Paris 273: 999-1002.

Campari, E., Portera, F., Tartarotti, P., and Spalla, M.I. 2004. The Rifelberg-Garten unit in the eclogitic ophiolites of the Upper Valtournanche (Piedmont Zone, Northwestern Italian Alps). 32nd IGC, Florence, Italy, August 20-28, 2004, p. 294.

Cannat, M. 1996. How thick is the magmatic crust at slow spreading oceanic ridges? J. Geophys. Res. Solid Earth 101(B2): 2847-2857.

Cannat, M., Lagabrielle, Y., Bougault, H., Casey, J., de Coutures, N., Dmitriev, L., and Fouquet, Y. 1997. Ultramafic and gabbroic exposures at the Mid-Atlantic Ridge: Geological mapping in the 15 N region. Tectonophysics 279: 193-213.

Capitanio, F. A., and Goes, S. 2006. Mesozoic spreading kinematics: consequences for Cenozoic Central and Western Mediterranean subduction. Geophys. J. Int. 165: 804-816.

Chiari, M., Marcucci, M., and Principi, G. 2000. The age of the radiolarian cherts associated with the ophiolites in the Apennines (Italy) and Corsica (France): a revision. Ofioliti, 25: 141-146.

Cliff, R.A., Barnicoat, A.C. and Inger, S. 1998. Early Tertiary eclogite facies metamorphism in the Monviso Ophiolite. J. Metamorph. Geol. 16: 447-455.

Cordey, F., Tricart, P., Guillot, S., and Schwartz, S. 2012. Dating the Tethyan Ocean in the Western Alps with radiolarite pebbles from synorogenic Oligocene molasse basins (southeast France). Swiss J. Geosci. 105: 39-48.

1113 Corno, A., Mosca, P., Borghi, S., and Gattiglio, M. 2021. Geology of the Monte Banchetta
1114 – Punta Rognosa area (Troncea valley, Western Alps). J. Maps. 17 (2): 150-
1115 160.
1116 Cortesogno, L., Galbiati, B., and Principi, G. 1987. Note alla "Carta geologica delle ofioliti
1117 del Bracco" e ricostruzione della paleogeografia Giurassico-Cretacica. Ofioliti,
1118 12: 261-342.
1119 Costa, J.E., 1988. Rheologic, geomorphic, and sedimentologic differentiation of water
1120 floods, hyperconcentrated flows, and debris flows, *In* Baker, V. R., Kochel,
1121 R.C., and Patton, P.C. eds. Flood Geomorphology. Wiley, New York, pp. 113-
1122 122.
1123 Cowan, D.S. 1985. Structural styles in Mesozoic and Cenozoic mélanges in the western
1124 Cordillera of North America. Geol.l Soc. Am. Bull. 96: 451–462.
1125 Crispini, L., and Capponi, G. 2001, Tectonic evolution of the Voltri Group and Sestri
1126 Voltaggio Zone (southern limit of the NW Alps): a review. Ofioliti 26: 161-
1127 164.
1128 Dal Piaz, G.V. 1965. La formazione mesozoica dei calcescisti con pietre verdi fra la
1129 Valsesia e la Valtournanche ed i suoi rapporti con il ricoprimento Monte Rosa e
1130 con la Zona Sesia-Lanzo. Boll. Soc. Geol. It. 84: 67-104.
1131 Dal Piaz, G.V., 1992, Guida geologica: Le Alpi dal Monte Bianco al Lago Maggiore, Vol.
1132 3: BeMa Editrice, Milano, 311 pp.
1133 Dal Piaz, G.V. 1999. The Austroalpine–Piedmont nappe stack and the puzzle of Alpine
1134 Tethys. Mem. Sci. Geol. Padova 51: 155–176.
1135 Dal Piaz, G.V., 2004. From the European continental margin to the Mesozoic Tethyan
1136 ocean: a geological map of the upper Ayas valley (Western Alps). *In* Pasquarè,

1137 G. and Venturini, C. Eds. Mapping Geology in Italy. Mapping Geology in Italy.
1138 APAT – SELCA, Florence, pp. 265-272.
1139 Dal Piaz, G., Bistacchi, A., Gianotti, F., Monopoli, B., Passeri, L., Schiavo, A., et al. 2015.
1140 Carta Geologica d'Italia - Foglio 070 Monte Cervino. Servizio Geologico
1141 d'Italia, 219 pp.
1142 Dal Piaz, G.V., Bistacchi, A. and Massironi, M. 2003. Geological outline of the Alps.
1143 Episodes 26: 175-180.
1144 Dal Piaz, G.V., and Ernst, W.G. 1978. Areal geology and petrology of eclogites and
1145 associated metabasites of the Piemonte Ophiolite Nappe, Breuil-St. Jacques
1146 area, Italian Western Alps. Tectonophysics 51: 99-126.
1147 Decandia, F.A. and Elter, P. 1972. La zona ofiolitifera del Bracco nel settore compreso tra
1148 Levanto e la Val Graveglia (Appennino Ligure). Mem. Soc. Geol. It. 11: 503-
1149 530.
1150 Dercourt, J., Gaetani, M., Vrielynck, B., Barrier, E., Biju-Duval, B., Brunet, M.F., Cadet,
1151 J.P., Crasquin, S., and Sandulescu, M. 2000. Atlas PeriTethys,
1152 Palaeogeographical maps, 24 maps and explanatory notes I-XX.
1153 CCGM/CGMW, Paris, 1-269.
1154 Dilek, Y. 2006. Collision tectonics of the Eastern Mediterranean region: Causes and
1155 consequences. Geol. Soc. Am. Spe. Pap. 409: 1-13. doi: 10.1130/2006.2409(1).
1156 Dilek, Y., and Eddy, C.A. 1992. The Troodos (Cyprus) and Kizildag (S. Turkey) ophiolites
1157 as structural models for slow-spreading ridge segments. Journal of Geology,
1158 100, p. 305-322.
1159 Dilek, Y., Thy, P., Moores, E.M., and Ramsden, T.W. 1990. Tectonic evolution of the
1160 Troodos ophiolite within the Tethyan framework. Tectonics, 9, 811-823.

1161 Dilek, Y., Thy, P., Hacker, B. and Grundvig, S. 1999. Structure and petrology of Tauride
1162 ophiolites and mafic dike intrusions (Turkey): Implications for the Neo-Tethyan
1163 ocean. Bulletin of the Geological Society of America, 111(8), 1192-1216.
1164 Dilek, Y and Furnes, H., 2011. Ophiolite genesis and global tectonics: geochemical and
1165 tectonic fingerprinting of ancient oceanic lithosphere. Geological Society of
1166 America Bulletin, 123, 387-411, doi: 10.1130/B30446.1.
1167 Dilek, Y., Festa, A., Ogawa, Y., and Pini, G.A. 2012. Chaos and geodynamics: mélanges,
1168 mélange-forming processes and their significance in the geological record.
1169 Tectonophysics 568-569: 1-6.
1170 Dilek, Y., and Furnes, Y. 2014. Origins of ophiolites. Elements, 10, 93-100. doi:
1171 10.2013/gselements.10.2.93.
1172 Dilek, Y., and Furnes, H. 2019. Tethyan ophiolites and Tethyan seaways. J. Geol. Soc. 176:
1173 899-912.
1174 Driesner, T. 1993. Aspects of petrographical, structural and stable isotope geochemical
1175 evolution of ophicarbonate breccias from ocean floor to subduction and uplift;
1176 an example from Chatillon, Middle Aosta Valley, Italian Alps. Schweiz.
1177 Mineral. Petrogr. Mitt. 73: 69-84.
1178 Ellero, A., Leoni, L., Marroni, M., and Sartori, F. 2001. Internal Liguride Units from
1179 Central Liguria, Italy: new constraints to the tectonic setting from white mica
1180 and chlorite studies. Swiss Bull. Miner. Petrol. 81: 39-54.
1181 Elter, G. 1971. Schistes lustrés et ophiolites de la zone piémontaise entre Orco et Doire
1182 Baltée (Alpes Graies). Hypothèses sur l'origine des ophiolites. Géol, Alpine 47:
1183 147–169.
1184 Elter, P. 1975. L'ensemble ligure. Bull. Soc. Géol. Fr. 7: 984-997.

1185 Elter, P., Trevisan, L., 1973. Olistostromes in the tectonic evolution of the Northern
1186 Apennines, In De Jong, K.A. and Scholten, R., eds., Gravity and Tectonics.
1187 John Willey and Sons, New York: 175–188.
1188 Ernst,W.G. 1970. Tectonic contact between the Franciscan mélange and the Great Valley
1189 Sequence — crustal expression of a Late Mesozoic Benioff zone. J. Geophys.
1190 Res. 75: 886–901.
1191 Ernst, W.G. 1971. Metamorphic zonations on presumably subducted lithospheric plates
1192 from Japan, California and the Alps. Contrib. Mineral. Petrol. 34(1): 43-59.
1193 Ernst,W.G. 2015. Franciscan geologic history constrained by tectonic/olistostromal
1194 highgrademetamafic blocks in the iconic California Mesozoic-Cenozoic
1195 accretionary complex. Am. Mineral. 100: 6–13.
1196 Ernst, W.G. 2016. Franciscan mélanges: coherent blocks in a low-density, ductile matrix.
1197 Int. Geol. Rev. 58: 626-642.
1198 Federico, L., Crispini, L., Malatesta, C., Torchio, S., and Capponi, G. 2015. Geology of the
1199 Pontinvrea area (Ligurian Alps, Italy): structural setting of the contact between
1200 Montenotte and Voltri units. J. of Maps 11: 101 113.
1201 Federico, L., Crispini, L., Scambelluri, M., and Capponi, G. 2007. Ophiolite mélange zone
1202 records exhumation in a fossil subduction channel. Geology 35: 499-502.
1203 Festa, A., Balestro, G., Borghi, A., De Caroli, S., and Succo, A. 2020a. The role of
1204 structural inheritance in continental break-up and exhumation of Alpine
1205 Tethyan mantle (Canavese Zone, Western Alps). Geosci. Front. 11: 167-188.
1206 Festa, A., Balestro, G., Dilek, Y. and Tartarotti, P. 2015. A Jurassic oceanic core complex
1207 in the high-pressure Monviso ophiolite (western Alps, NW Italy). Lithosphere
1208 7: 646-652.

1209 Festa, A., Cavagna, S., Barbero, E., Catanzariti, R., and Pini, G.A. 2020b. Mid-Eocene
1210 giant slope failure (sedimentary mélanges) in the Ligurian accretionary wedge
1211 (NW Italy) and relationships with tectonics, global climate changes and the
1212 dissociation of gas hydrates. J. Geol. Soc., 177: 575-586.
1213 Festa, A., Dilek, Y., Codegone, G., Cavagna, S., Pini, G.A., 2013. Structural anatomy of
1214 the Ligurian accretionary wedge (Monferrato, NW Italy), and evolution of
1215 superposed mélanges. Geol. Soc. Am. Bull. 125:1580-1598.
1216 Festa, A., Dilek, Y., Mittempergher, S., Ogata, K., Pini, G.A. and Remitti, F. 2018. Does
1217 subduction of mass transport deposits (MTDs) control seismic behavior of
1218 shallow-level megathrusts at convergent margins? Gondwana Res. 60: 186-193.
1219 Festa, A., Ogata, K., Pini, G. A., Dilek, Y., and Alonso, J. L. 2016. Origin and significance
1220 of olistostromes in the evolution of orogenic belts: A global synthesis.
1221 Gondwana Res., 39: 180-203.
1222 Festa, A., Ogata, K., and Pini, G.A. 2019a. Mélanges: 100th anniversary of the inception of
1223 the term and concept. Gondwana Res. 39: 1-6.
1224 Festa, A., Ogata, K., Pini, G.A. 2020c. Polygenetic mélanges: a glimpse on tectonic,
1225 sedimentary and diapiric recycling in convergent margins. J. Geol. Soc. 177:
1226 551-561.
1227 Festa, A., Ogata, K., Pini, G. A., Dilek, Y., and Alonso, J. L. 2016. Origin and significance
1228 of olistostromes in the evolution of orogenic belts: A global synthesis.
1229 Gondwana Res. 39: 180-203.
1230 Festa, A., Pini, G. A., Ogata, K., and Dilek, Y. 2019b. Diagnostic features and field-criteria
1231 in recognition of tectonic, sedimentary and diapiric mélanges in orogenic belts
1232 and exhumed subduction-accretion complexes. Gondwana Res. 74: 7-30.

1233 Festa, A., Pini, G.A., Dilek, Y., and Codegone, G. 2010. Mélanges and mélange-forming
1234 processes: a historical overview and new concepts. Int. Geol. Rev. 52: 1040-
1235 1105.
1236 Fierro, G., and Terranova, R. 1963. Microfacies fossilifere e sequenze litologiche nelle
1237 "Arenarie superiori" dei monti Ramaceto e Zatta. Att. Ist. Geol., Univ. Genova:
1238 1: 473-510.
1239 Fitzherbert, J. A., Clarke, G. L., and Powell, R. 2005. Preferential retrogression of high-P
1240 metasediments and the preservation of blueschist to eclogite facies metabasite
1241 during exhumation, Diahot terrane, NE New Caledonia. Lithos 83: 67-96.
1242 Flores, G. 1955. Les résultats des études pour les recherches pétroliféres en Sicile:
1243 Discussion. Proceedings of the 4th World Petroleum Congress. Casa Editrice
1244 Carlo Colombo, Rome: 121–122 (Section 1/A/2).
1245 Fonnesu, M., and Felletti, F. 2019. Facies and architecture of a sand-rich turbidite system in
1246 an evolving collisional-trench basin: a case history from the upper Cretaceous-
1247 Palaeocene Gottero system (NW Apennines). Riv. It. Pal. Strat. 125(2): 449-
1248 487.
1249 Fontana, E., Panseri, M., and Tartarotti, P. 2008. Oceanic relict textures in the Mount Avic
1250 serpentinites, Western Alps. Ofioliti 33: 105-118.
1251 Fontana, E., Tartarotti, P., Panseri, M., and Buscemi, S. 2015. Geological map of the Mount
1252 Avic massif (Western Alps Ophiolites). J. Maps 11(1): 126-135.
1253 Frezzotti, M.L., Selverstone, J., Sharp, Z.D., and Compagnoni, R. 2011. Carbonate
1254 dissolution during subduction revealed by diamond-bearing rocks from the
1255 Alps. Nature Geoscience 4: 703-706.

1256 Gao, P., and Santosh, M. 2020. Mesoarchean accretionary mélange and tectonic erosion in
1257 the Archean Dharwar Craton, southern India: Plate tectonics in the early Earth.
1258 Gonwana Res. 85: 291-305.
1259 Geersen, J., Festa, A., and Remitti, F. 2020. Structural constraints on the subduction of
1260 mass transport deposits in convergent margins. *In* Subaqueous mass movements
1261 and their consequences: advances in process understanding monitoring and
1262 hazard assesments (Georgiopoulou, A. et al., eds). Geol. Soc. London Spec.
1263 Publ. 500: 115-128. https://doi.org/10.1144/SP500-2019-174
1264 Goffé, B., Bousquet, R., Henry, P., and Le Pichon, X. 2003. Effect of the chemical
1265 composition of the crust on the metamorphic evolution of orogenic wedges. J.
1266 Metamorph. Geol. 21:123-141.
1267 Golonka, J. 2007. Late Triassic and Early Jurassic palaeogeography of the world. Palaeog.,
1268 Palaeoclimatol., Palaeoecol. 244: 297-307.
1269 Groppo, C. and Castelli, D. 2010. Prograde P-T evolution of a lawsonite eclogite from the
1270 Monviso Meta-ophiolite (Western Alps): Dehydration and redox reactions
1271 during subduction of oceanic Fe-Ti-oxide gabbro. J. Petrol. 51, 2489-2514.
1272 Groppo, C., Beltrando, M., and Compagnoni, R. 2009. The P-Tpath of the ultra-high
1273 pressure Lago Di Cignana and adjoining high-pressure meta-ophiolitic units:
1274 insights into the evolution of the subducting Tethyan slab. J. Metamorph. Geol.
1275 27: 207-231.
1276 Gusmeo, T., Spalla, M.I., Tartarotti, P., Zanoni, D., and Gosso, G. 2018. Structural-
1277 geological survey of an eclogitized chaotic complex: the Riffelberg-Garten Unit
1278 in the Breuil dell (Zermatt-Saas Zone, Italian Wester Alps). SGI-SIMP
1279 Meeting, 12-14 September 2018, Catania (Italy), Abstract book: 219.

1280 Hajná J., Žák, J., Ackerman, L., Svojtka, M., and Pašava, J., 2019. A giant late Precambrian
1281 chert-bearing olistostrome discovered in the Bohemian Massif: A record of
1282 Ocean Plate Stratigraphy (OPS) disrupted by mass-wasting along an outer
1283 trench slope. Gondwana Res. 74: 173-188.
1284 Handy, M., Schmid, S., Bousquet, R., Kissling E., and Bernoulli, D. 2010. Reconciling
1285 plate-tectonic reconstructions of Alpine Tethys with the geological-geophysical
1286 record of spreading and subduction in the Alps. Earth Sci. Rev. 102: 121-158.
1287 Hosseinpour, M., Williams, S., Seton, M., Barnett-Moore, N., and Müller, R. D. 2016.
1288 Tectonic evolution of Western Tethys from Jurassic to present day: coupling
1289 geological and geophysical data with seismic tomography models. Int. Geol.
1290 Rev. 58: 1616-1645.
1291 Hsü, K.J. 1968. Principles of mélanges and their bearing on the Franciscan-Knoxville
1292 Paradox. Geol. Soc. Am. Bull. 79: 1063-1074.
1293 Kawamura, K., Ogawa, Y., Anma, R., Yokoyama, S., Kawakami, S., Dilek, Y., Moore, G.F.,
1294 Hirano, S., Yamaguchi, A., Sasaki, T., YK05-08-Leg 2, YK06-02 Shipboard
1295 Scientific Parties. Geol. Soc. Am. Bull. 121 (11-12): 1629-1646.
1296 Kusky, T.M., Windley, B.F., Safonova, I., Wakita, K., Wakabayashi, J., Polat, A., and
1297 Santosh, M. 2013. Recognition of ocean plate stratigraphy in accretionary
1298 orogens through Earth history: A record of 3.8 billion years of sea floor
1299 spreading, subduction, and accretion. Gondwana Res. 24: 501–547.
1300 Kusky, T., Wang, J., Wang, L., Huang, B., Ning, W., Fu, D., Peng, H., Deng, H., Polat, A.,
1301 Zhong, Y., and Shi, G. 2020. Mélanges through time: Life cycle of the world's
1302 largest Archean mélange compared with Mesozoic and Paleozoic subduction-
1303 accretion-collision mélanges. Earth-Science Rev. 209: 103303.

1304 Lafay, R., Baumgartner, L., Schwartz, S., Picazo, S., Montes-Hernandez, G. and
1305 Vennemann, T. 2017. Petrologic and stable isotopic studies of a fossil
1306 hydrothermal system in ultramafic environment (Chenaillet ophicalcites,
1307 Western Alps, France): processes of carbonate cementation. Lithos 294-295:
1308 319-338.
1309 Lagabrielle, Y. 1994. Ophiolites of the Western Alps and the nature of the Tethyan oceanic
1310 lithosphere. Ofioliti 19: 413-434.
1311 Lagabrielle, Y. 2009. Mantle exhumation and lithospheric spreading: An historical
1312 perspective from investigations in the oceans and in the Alps-Apennines
1313 ophiolites. Ital. J. Geosci. 128: 279-293.
1314 Lagabrielle, Y., Vitale Brovarone, A. and Ildefonse, B. 2015. Fossil oceanic core
1315 complexes recognized in the blueschist metaophiolites of Western Alps and
1316 Corsica. Earth Sci. Rev. 141: 1-26.
1317 Lagabrielle, Y. and Polino, R. 1985. Origine volcano-détritique de certaines prasinites des
1318 Schistes lustrés du Queyras (France): arguments texturaux et géochimiques.
1319 Bull. Soc. Geol. Fr. 4: 461-471.
1320 Lagabrielle, Y. and Polino, R. 1988. Un schéma structural du domaine des Schistes lustrés
1321 ophiolitifères au nord-ouest du massif du Mont Viso (Alpes sud-occidentales) et
1322 ses implications. C. R. Acad. Sci. 306: 921-928.
1323 Lagabrielle, Y., and Cannat, M. 1990. Alpine Jurassic ophiolites resemble the modern
1324 central Atlantic basement. Geology 18: 319-322.
1325 Lahondère, D., and Guerrot, C. 1997. Datation Sm-Nd du métamorphisme éclogitique en
1326 Corse alpine: un argument pour l'existence au Crétacé supérieur d'une zone de
1327 subduction active localisée sous le bloc corso-sarde. Géol. France 3: 3-11.

1328 Lamarche, G., Joanne, C. and Collot, J.-Y. 2008. Successive, large mass transport deposits
1329 in the south Kermadec fore-arc basin, New Zealand: The Matakaoa Submarine
1330 Instability Complex. Geochem., Geophys., Geosyst. 9: Q04001,
1331 https://doi.org/10.1029/2007GC001843.
1332 Lavier, L. L., and Manatschal, G. 2006. A mechanism to thin the continental lithosphere at
1333 magma-poor margins. Nature 440: 324-328.
1334 Le Mer, O., Lagabrielle, Y., and Polino, R. 1986. Une série sédimentaire détritique liée aux
1335 Ophiolites piémontaises: analyses lithostratigraphiques, texturales et
1336 géochimiques dans le massif de la Crête de Mouloun (Haut-Queyras, Alpes
1337 sud-occidentales, France). Géol. Alpine 62: 63-86.
1338 Lemoine, M. 1971. Données nouvelles sur la série du Gondran près Briançon (Alpes
1339 Cottiennes). Réflexions sur les problèmes stratigraphique et paléogéographique
1340 de la zone piémontaise. Géol. Alp. 47: 181-201.
1341 Lemoine, M., Steen, D., and Vuagnat, M., 1970. Sur le probléme stratigraphique des
1342 ophiolites piémontaises et des róches sédimentaires associées: Observations
1343 dans le massif de Chabrière en Haute-Ubaye (Basses-Alpes, France). C. R. des
1344 Séances, S.P.H.N., Genevé, 5: 44-59.
1345 Lemoine, M. and Tricart, P. 1986. Les Schistes lustrés piémontais des Alpes Occidentales:
1346 Approche stratigraphique, structural et sédimentologique. Eclogae Geol. Helv.
1347 79: 271-294.
1348 Lemoine, M., Tricart, P., and Boillot, G. 1987. Ultramafic and gabbroic ocean floor of the
1349 Ligurian Tethys (Alps, Corsica, Apennines): In search of a genetic model.
1350 Geology 15: 622-625.

1351 Leoni, L., Marroni, M., Sartori, F., and Tamponi, M. 1996, The grade of metamorphism in
1352 the metapelites of the Internal Ligurid Units Northern Apennines, Italy. Eur. J.
1353 Min. 8: 35-50.
1354 Li, X. H., Faure, M., Lin, W. and Manatschal, G. 2013. New isotopic constraints on age and
1355 magma genesis of an embryonic oceanic crust: The Chenaillet Ophiolite in the
1356 Western Alps. Lithos 160: 283-291.
1357 Li, X.P., Rahn, M. and Bucher, K., 2004. Serpentinites of the Zermatt-Saas ophiolite
1358 complex and their texture evolution. J. Metamorph. Geol. 22: 159-177.
1359 Lombardo, B., Nervo, R., Compagnoni, R., Messiga, B., Kienast, J., Mevel, C., Fiora, L.,
1360 Piccardo, G. and Lanza, R. 1978. Osservazioni preliminari sulle ofioliti
1361 metamorfiche del Monviso (Alpi Occidentali). Rend. Soc. It. Min. Petr. 34:
1362 253-305.
1363 Lombardo, B., Rubatto, D. and Castelli, D. 2002. Ion microprobe U-Pb dating of zircon
1364 from a Monviso metaplagiogranite: Implications for the evolution of the
1365 Piedmont-Liguria Tethys in the Western Alps. Ofioliti 27: 109-117.
1366 Lucente, C. C., and Pini, G. A. 2008. Basin- wide mass- wasting complexes as markers of
1367 the Oligo- Miocene foredeep- accretionary wedge evolution in the Northern
1368 Apennines, Italy. Basin Res. 20: 49–71.
1369 Luoni, P., Rebay, G., Roda, M., Zanoni, D., and Spalla, M.I. 2020. Tectono-metamorphic
1370 evolution of UHP Zermatt-Saas serpentinites: a tool for vertical
1371 palaeogeographic restoration. Int. Geol. Rev. (first online). Doi:
1372 10.1080/00206814.2020.1758967.

1373 Luoni, P., Rebay, G., Spalla, M.I., and Zanoni, D. 2018. UHP Ti-chondrodite in the
1374 Zermatt-Saas serpentinite: Constraints on a new tectonic scenario. Am. Mineral
1375 103(6): 1002-1005.
1376 Magde, L. S., Barclay, A. H., Toomey, D. R., Detrick, R. S., and Collins, J. A. 2000.
1377 Crustal magma plumbing within a segment of the Mid-Atlantic Ridge, 35 N.
1378 Earth Planet. Sci. Lett. 175: 55-67.
1379 Malatesta, C., Crispini, L., Federico, L., Capponi, G., and Scambelluri, M. 2012. The
1380 exhumation of high pressure ophiolites (Voltri Massif, Western Alps): insights
1381 fromstructural and petrologic data on metagabbro bodies. Tectonophysics 568-
1382 569: 102-123.
1383 Manatschal, G., Sauter, D., Karpoff, A.M., Masini, E., Mohn, G. and Lagabrielle, Y. 2011.
1384 The Chenaillet Ophiolite in the French/Italian Alps: an ancient analogue for an
1385 Oceanic Core Complex? Lithos 124, 169-184.
1386 Manzotti, P., Ballevre, M., Zucali, M., Robyr, M., and Engi, M. 2014. The
1387 tectonometamorphic evolution of the Sesia-Dent Blanche nappes (internal
1388 Western Alps): review and synthesis. Swiss J. Geosci. 107: 309-336.
1389 Marroni, M., Meneghini, F., and Pandolfi, L. 2004. From accretion to exhumation in a
1390 fossil accretionary wedge: a case history from Gottero Unit (Northern
1391 Apennines, Italy). Geod. Acta 17: 41-53.
1392 Marroni M., Meneghini F., and Pandolfi, L. 2017. A revised subduction inception model to
1393 explain the Late Cretaceous, double vergent orogen in the pre-collisional
1394 Western Tethys: evidence from the Northern Apennines. Tectonics 36: 2227–
1395 2249.

1396 Marroni, M., and Pandolfi, L. 2001. Debris flow and slide deposits at the top of the Internal
1397 Liguride ophiolitic sequence, Northern Apennines, Italy: A record of frontal
1398 tectonic erosion in a fossil accretionary wedge. Isl. Arc 10: 9-21.
1399 Marroni, M., and Pandolfi, L. 2007. The architecture of the Jurassic Ligure-Piemontese
1400 oceanic basin: tentative reconstruction along the Northern Apennines - Alpine
1401 Corsica transect. Int. J. Earth Sci. 96: 1059-1078.
1402 Marroni, M. and Perilli, N. 1990. The age of the ophiolite sedimentary cover from the Mt.
1403 Gottero Unit (Internal Liguride Units, Northern Apennines): new data from
1404 calcareous nannofossils. Ofioliti 15: 232-251.
1405 Marroni, M., Molli, G., Montanini, A., and Tribuzio, R. 1998. The association of
1406 continental crust rocks with ophiolites (northern Apennines, Italy): Implications
1407 for the continent-ocean transition. Tectonophysics 292: 43-66.
1408 Marroni, M., Monechi, S., Perilli, N., Principi, G., and Treves, B. 1992. Late Cretaceous
1409 flysch deposits in the Northern Apennines, Italy: age of inception of orogenesis-
1410 controlled sedimentation. Cretaceous Res. 13: 487-504.
1411 Meneghini, F., Marroni, M., Moore, J.C., Pandolfi, L., and Rowe, C.D. 2009, The process
1412 of underplating in the geologic record: structural diversity between the
1413 Franciscan Complex California, the Kodiak Complex Alaska and the Internal
1414 Ligurian Units Italy. Geol. J. 44: 126-152.
1415 Meneghini, F., Pandolfi, L., and Marroni, M. 2020. Recycling of heterogeneous material in
1416 the subduction factory: evidence from the sedimentary mélange of the Internal
1417 Ligurian Units, Italy. J. Geol. Soc. 177: 587-599.
1418 Michard, A., Chalouan, A., Feinberg, H., Goffé, B., and Montigny, R. 2002. How does the
1419 Alpine belt end between Spain and Morocco? Bull. Soc. Geol. Fr. 173(1): 3–15.

1420 Michard, A., Goffe, B., Chopin, C. and Henry, C. 1996. Did the Western Alps develop
1421 through an Oman-type stage? The geotectonic setting of high-pressure
1422 metamorphism in two contrasting Tethyan transects. Eclogae Geol. Helv. 89:
1423 43-80.
1424 Miyashiro, A., 1973, Metamorphism and Metamorphic Belts: Halsted Press, JohnWiley &
1425 Sons, New York: 492p.
1426 Mohn, G., Manatschal, G., Beltrando, M., Masini, E., and Kusznir, N. 2012. Necking of
1427 continental crust in magma-poor rifted margins: Evidence from the fossil
1428 Alpine Tethys margins. Tectonics 31: doi:10.1029/2011TC002961
1429 Montanini, A., Tribuzio, R., and Anczkiewicz, R. 2006. Exhumation history of a garnet
1430 pyroxenite-bearing mantle section from a continent-ocean transition (Northern
1431 Apennine ophiolites, Italy). J. Petrol. 47: 1943-1971.
1432 Moore, J.C. and Sample, J. 1986. Mechanism of accretion at sediment-dominated
1433 subduction zones: consequences for the stratigraphic record and accretionary
1434 prism hydrogeology. Mem. Soc. Geol. It. 31: 107–118.
1435 Müntener, O., and Hermann, J. 2001. The role of lower crust and continental upper mantle
1436 during formation of non-volcanic passive margins: evidence from the Alps, *In*
1437 Al Hosani, K., Roure, F., Ellison, R., Stephen Lokier, S., eds. Lithosphere
1438 Dynamics and Sedimentary Basins: The Arabian Plate and Analogues. Geol.
1439 Soc. London Spec. Publ. 187(1): 267 288.
1440 Mutti, E. 1992. Turbidite sandstones. AGIP-Istituto di Geologia, Università di Parma, San
1441 Donato Milanese, 275 pp.

1442 Nielsen, T. H., and Abbate, E. 1983. Submarine-fan facies associations of the Upper
1443 Cretaceous and Paleocene Gottero sandstone, Ligurian Apennines Italy. Geo-
1444 Mar. Lett. 3: 193-197.
1445 Ogata, K., Festa, A., Pini, G. A., Pogačnik, Ž., and Lucente, C. C. 2019. Substrate
1446 deformation and incorporation in sedimentary mélanges (olistostromes):
1447 Examples from the northern Apennines (Italy) and northwestern Dinarides
1448 (Slovenia). Gondwana Res. 74: 101-125
1449 Ogata, K., Festa, A., Pini, G.A., and Alonso, J.L., 2020. Submarine landslide deposits in
1450 orogenic belts: olistostromes and sedimentary mélanges. *In* Ogata, K., Festa,
1451 A., and Pini, G.A. Eds. Submarine Landslides: subaqueous mass transport
1452 deposits from outcrop to seismic profiles. Geophysical Monograph 247, First
1453 Edition, American Geophysical Union, John Wiley and Sons Inc., USA, p. 3-
1454 26.
1455 Ogata, K., Tinterri, R., Pini, G. A., and Mutti, E. 2012. Mass transport- related stratal
1456 disruption within sedimentary melanges: Examples from the northern
1457 Apennines (Italy) and south- central Pyrenees (Spain). Tectonophysics 568–
1458 569: 185–199.
1459 Ogawa, Y., Mori, R., Tsunogae, T., Dilek, Y., and Harris, R. 2015. New interpretation of
1460 the Franciscan mélange at San Simeon coast, California: tectonic intrusion into
1461 an accretionary prism. Int. Geol. Rev. 57: 824-842.
1462 Orange, D.L. 1990. Criteria helpful in recognizing shear-zone and diapiric mélanges:
1463 examplesfrom the Hoh accretionary complex, Olympic Peninsula, Washington.
1464 Geol. Soc. Am. Bull. 102: 935-951.

1465 Palin, R.M., Santosh, M., Cao, W., Li, S-S., Hernandez-Uribe, D., and Parsons, A. 2020.
1466 Secular change and the onset of plate tectonics on Earth. Eart-Science Rev. 207:
1467 103172.
1468 Pandolfi, L. 1997. Stratigrafia ed evoluzione strutturale delle successioni torbiditiche
1469 cretacee della Liguria orientale (Appennino Settentrionale). PhD Thesis,
1470 Università di Pisa.
1471 Panseri, M., Fontana, E., and Taratrotti, P., 2008. Evolution of rodingitic dykes:
1472 metasomatism and metamorphism in the Mount Avic serpentinites (Alpine
1473 ophiolites, southern Aosta Valley). Ofioliti 33(2): 165-185.
1474 Péron-Pinvidic, G., and Manatschal, G. 2009. The final rifting evolution at deep magma-
1475 poor passive margins from Iberia-Newfoundland: a new point of view. Int. J.
1476 Earth Sci. 98: 1581-1597.
1477 Piccardo, G.B., Padovano, M., and Guarnieri, L. 2014. The Ligurian Tethys: mantle
1478 processes and geodynamics. Earth Sci. Rev. 138: 409–434.
1479 Pinet, N., Lagabrielle, Y. and Whitechurch, H. 1989. Le complexe du Pic des Lauzes (Haut
1480 Queyras, Alpes Occidentales, France): structures alpines et océaniques dans un
1481 massif ophiolitique de type liguro-piémontais. Bull. Soc. Geol. Fr. 2: 317-326.
1482 Pini, G. A. (1999). Tectonosomes and olistostromes in the Argille Scagliose of the
1483 Northern Apennines, Italy (Vol. 335). Geol. Soc. Am. Spec. Pap. 338: 73 pp.
1484 Pini, G.A., Ogata, K., Camerlenghi, A., Festa, A., Lucente, C.C., and Codegone, G. 2012.
1485 Sedimentary mélanges and fossil mass-transport complexes: a key for better
1486 understanding submarine mass movements?, In Yamada, Y. et al., eds.,
1487 Submarine Mass Movements and Their ConsequencesAdvances in Natural and

Technological Hazards Research 31. Springer Science+Business Media B.V.: 585–594

Pini, G. A., Venturi, S., Lucente, C. C., and Ogata, K. 2020. Mass transport complexes of the Marnoso- arenacea foredeep turbidites system, Northern Apennine of Italy: A twenty- year after reappraisal, In Ogata K., Festa A., and Pini G.A., eds., Submarine landslides: Subaqueous mass transport deposits from outcrops to seismic profiles: 117–137. Hoboken, NJ/Washington, WC: Wiley/American Geophysical Union.

Plunder, A., Agard, P., Chopin, C., Pourteau, A., and Okay, A. I. 2015. Accretion, underplating and exhumation along a subduction interface: from subduction initiation to continental subduction (Tavşanlı zone, W. Turkey). Lithos 226: 233-254.

Pognante, U., Perotto, A., Salino, C., and Toscani, L. 1986. The ophiolitic peridotites of the Western Alps: record of the evolution of a small oceanic type basin in the Mesozoic Tethys. Tsch. Min. Petr. Mitt. 35: 47-65.

Polat, A., and Kerrich, R. 1999. Formation of an Archean tectonic mélange in the Schreiber-Hemlo greenstone belt, Superior Province, Canada: Implications for Archean subduction-accretion process. Tectonics 18 (5): 733-755.

Polino, R., 1984. Les series oceaniques du haut val de Suse (Alpes Cottiennes): analyse des couvertures sedimentaires. Ofioliti, 9: 547-554.

Polino, R., Dal Piaz, G.V., Gosso, G. 1990. Tectonic erosion at the Adria margin and accretionaryprocesses for the Cretaceous orogeny of the Alps. Mém. Soc. Géol. Fr. 156: 345-367.

1511 Principi, G., Bortolotti, V., Chiari, M., Cortesogno, L., Gaggero, L., Marcucci, M., Saccani,
1512 E. and Treves, B. 2004. The pre-orogenic volcano-sedimentary covers of the
1513 western Tethys oceanic basin: a review. Ofioliti 29:177-212.
1514 Rabain, A., Cannat, M., Escartín, J., Pouliquen, G., Deplus, C., and Rommevaux Jestin, C.
1515 2001. Focused volcanism and growth of a slow spreading segment (Mid-
1516 Atlantic Ridge, 35 N). Earth Planet. Sci. Lett. 185: 211-224.
1517 Rampone, E., Borghini, G., and Basch, V. 2020. Melt migration and melt-rock reaction in
1518 the Alpine-Apennine peridotites: Insights on mantle dynamics in extending
1519 lithosphere. Geosci. Front. 11: 151-166.
1520 Raymond, L.A., 1973, Tesla-Ortigalita fault, Coast Range thrust fault, and Franciscan
1521 metamorphism, northeastern Diablo Range, California. Geol. Soc. Am. Bull.
1522 84: 3547–3562.
1523 Raymond, L.A. 1984. Classification of melanges, In Raymond, L.A., ed., Melanges: Their
1524 Nature, Origin and Significance. Boulder, Colorado Geological Society of
1525 America Special Papers 198: 7–20.
1526 Raymond, L.A. 2019, Perspectives on the roles of melanges in subduction accretionary
1527 complexes: A review. Gondwana Res. 74: 68-89.
1528 Rebay, G., Zanoni, D., Langone, A., Luoni, P., Tiepolo, M., and Spalla, M. I. 2018. Dating
1529 of ultramafic rocks from the Western Alps ophiolites discloses Late Cretaceous
1530 subduction ages in the Zermatt-Saas Zone. Geol. Mag. 155: 298-315.
1531 Rebay, G.; Spalla, M.I.; and Zanoni, D. 2012. Interaction of deformation and
1532 metamorphism during subduction and exhumation of hydrated oceanic mantle:
1533 Insights from the Western Alps. J. Metamorph. Geol. 30: 687-702.

1534 Remitti, F., Vannucchi, P., Bettelli, G., Fantoni, L., Panini, F., and Vescovi, P. 2011.
1535 Tectonic and sedimentary evolution of the frontal part of an ancient subduction
1536 complex at the transition from accretion to erosion: the case of the Ligurian
1537 wedge of the northern Apennines, Italy. Geol. Soc. Am. Bull, 123: 51–70.
1538 Renna, M.R., Tribuzio, R., Sanfilippo, A. and Thirlwall, M. 2018. Role of melting process
1539 and melt-rock reaction in the formation of Jurassic MORB-type basalts (Alpine
1540 ophiolites). Contr. Min. Petr. 173: 31.
1541 Ribes, C., Ghienne, J. F., Manatschal, G., Decarlis, A., Karner, G. D., Figueredo, P. H., and
1542 Johnson, C. A. 2019. Long-lived mega fault-scarps and related breccias at distal
1543 rifted margins: Insights from present-day and fossil analogues. J. Geol. Soc.
1544 176: 801-816.
1545 Roda, M., Regorda, A., Spalla, M.I., and Marotta, A.M. 2019, What drives Alpine Tethys
1546 opening? Clues from the review of geological data and model predictions: Geol.
1547 J. 54: 2646-2664.
1548 Roda, M., Zucali, M., Regorda, A., and Spalla, M. I. 2020. Formation and evolution of a
1549 subduction-related mélange: The example of the Rocca Canavese Thrust Sheets
1550 (Western Alps). Geol. Soc. Am. Bull. 132: 884-896.
1551 Rosenbaum G., and Lister, G. S. 2005. The Western Alps from the Jurassic to Oligocene:
1552 spatio-temporal constraints and evolutionary reconstructions. Earth Sci. Rev.,
1553 69(3-4): 281-306.
1554 Rubatto, D., Gebauer, D. and Fanning, M. 1998. Jurassic formation and Eocene subduction
1555 of the Zermatt-Saas-Fee ophiolites: Implications for the geodynamic evolution
1556 of the Central and Western Alps. Contr. Min. Petr. 132: 269-287.

1557 Rubatto, D. and Hermann, J. 2003. Zircon formation during fluid circulation in eclogites
1558 (Monviso, Western Alps): implications for Zr and Hf budget in subduction
1559 zones. Geochim. Cosmochim. Acta 67 (12): 2173-2187.
1560 Saby, P. 1986. La lithosphère océanique de la Tethys ligure: etude du magmatisme et des
1561 mineralisations associées dans les ophiolites du Queyras (zone piémontaise des
1562 Alpes occidentales). PHD Thesis. Universite Scientique et Medicale de
1563 Grenoble, 222 pp.
1564 Saccani, E., Dilek, Y., Marroni, M., and Pandolfi, L. 2015. Continental margin ophiolites of
1565 Neotethys: remnants of ancient Ocean-Continent Transition Zone (OCTZ)
1566 Lithosphere and their geochemistry, mantle sources and melt evolution patterns.
1567 Episodes 38: 230-249.
1568 Sample, J.C., and Moore, J.C. 1987. Structural style and kinematics of an uderplated slate
1569 belt, Kodiak and adjacent islands, Alaska. Geol. Soc. Am. Bull. 99: 7-20.
1570 Scarsi, M., Malatesta, C. and Fornasero, S. 2018. Lawsonite-bering eclogite from a tectonic
1571 mélange in the Ligurian Alps: new constraints for the subduction plate-interface
1572 evolution. Geol. Mag. 155: 280-297.
1573 Schettino, A., and Turco, E. 2011. Tectonic history of the western Tethys since the Late
1574 Triassic. Geol. Soc. Am. Bull. 123: 89-105.
1575 Schwartz, S., Lardeaux, J., Guillot, S. and Tricart, P. 2000. Diversité du métamorphisme
1576 éclogitique dans le massif ophiolitique du Monviso (Alpes occidentales, Italie).
1577 Geod. Acta 13: 169-88.
1578 Silver, E.A. and Beutner, E.C. 1980. Melanges. Geology 8: 32–34.
1579 Skora, S., Mahlen, N.J., Johnson, C.M., Baumgartner, L.P., Lapen, T.J., Beard, B.L., and
1580 Szilvagyi, E.T. 2015. Evidence for protracted prograde metamorphism followed

1581 by rapid exhumation of the Zermatt-Saas Fee ophiolite. J. Metamorph. Geol.
1582 33: 711-734
1583 Stampfli, G. M., and Borel, G. D. 2002. A plate tectonic model for the Paleozoic and
1584 Mesozoic constrained by dynamic plate boundaries and restored synthetic
1585 oceanic isochrons. Earth Planet. Sci. Lett. 196: 17-33.
1586 Stampfli, G. M., Borel, G. D., Marchant, R., and Mosar, J. 2002. Western Alps geological
1587 constraints on western Tethyan reconstructions. J. Virt. Expl. 8: 77.
1588 Stampfli, G. M., and Kozur, H. W. 2006. Europe from the Variscan to the Alpine cycles.
1589 Geol. Soc. London Mem. 32: 57-82.
1590 Tartarotti, P., Festa, A., Benciolini, L. and Balestro, G. 2017a. Record of Jurassic mass
1591 transport processes through the orogenic cycle: Understanding chaotic rock
1592 units in the high pressure Zermatt-Saas ophiolite (Western Alps). Lithosphere
1593 9: 399-407.
1594 Tartarotti, P., Guerini, S., Rotondo, F., Festa, A., Balestro, G., Bebout, G.E., Cannaò, E.,
1595 Epstein, S., and Scambelluri, M. 2019. Superposed Sedimentary and Tectonic
1596 Block-In-Matrix Fabrics in a Subducted Serpentinite Mélange (High-Pressure
1597 Zermatt Saas Ophiolite, Western Alps). Geosciences 9: 358.
1598 Tartarotti, P., Benciolini, L., and Monopoli, B. 1998. Brecce serpentinitiche nel massiccio
1599 ultrabasico del Monte Avic (Falda Ofiolitica Piemontese): possibili evidenze di
1600 erosione sottomarina. Atti Tic. Sc. Terra 7: 73-86.
1601 Tartarotti, P., Martin, S., Festa, A., and Balestro, G. 2021. Metasediments covering
1602 ophiolites in the HP internal belt of the Western Alps: Review of tectono-
1603 stratigraphic successions and constraints for the Alpine evolution. Minerals 11:
1604 411, http://doi.org/10.3390/min11040411.

1605 Tartarotti, P., Martin, S., Monopoli, B., Benciolini, L., Schiavo, A., Campana, R., and
1606 Vigni, I. 2017b. Geology of the Saint-Marcel valle metaophiolites
1607 (Northwestern Alps, Italy). J. Maps 13(2): 707-717.
1608 Treves, B. 1984. Orogenic belts as accretionary prisms: The example of the northern
1609 Apennines. Ofioliti 9: 577-618.
1610 Treves, B.A., and Harper, G.D. 1994. Exposure of serpentinites on the ocean floor:
1611 sequence of faulting and hydrofracturing in the Northern Apennines
1612 ophicalcites. Ofioliti 19: 435-466.
1613 Tribuzio, R., Garzetti, F., Corfu, F., Tiepolo, M., and Renna, M. R. 2016. U-Pb zircon
1614 geochronology of the Ligurian ophiolites (Northern Apennine, Italy):
1615 Implications for continental breakup to slow seafloor spreading.
1616 Tectonophysics 666: 220-243.
1617 Tricart, P. 1973. Les Schistes lustrés du Haut-Cristillan; analyse tectonique d'un secteur
1618 externe du domaine piémontais (Alpes cottiennes, France). Thesis 3 cycle,
1619 Strasbourg, 193 p.
1620 Tricart, P., and Lemoine, M. 1983. Serpentinite oceanic bottom in South Queyras ophiolites
1621 (French Western Alps): record of the incipient oceanic opening of the mesozoic
1622 ligurian Tethys. Eclogae. Geol. Helv. 76: 611-629.
1623 Tricart, P. and Lemoine, M. 1991. The Queyras ophiolite west of Monte Viso (Western
1624 Alps): indicator of a peculiar ocean floor in the Mesozoic Tethys. J. Geod. 13:
1625 163-181.
1626 Tricart, P., and Schwartz, S. 2006. A north-south section across the Queyras Schistes
1627 lustrés (Piedmont zone, western Alps): Syn-collision refolding of a subduction
1628 wedge. Eclogae Geol. Helv. 99: 429-442.

1629 Valloni, R., and Zuffa, G.G. 1984. Provenance changes for arenaceous formations of the
1630 Northern Apennines (Italy). Geol. Soc. Am. Bull. 95: 1035-1039.
1631 Van de Kamp, P.C. and Leake, B.E. 1995. Petrology and geochemistry of siliciclastic rocks
1632 of mixed feldspatic and ophiolitic provenance in the Northern Apennines, Italy.
1633 Chem. Geol. 122: 1-20.
1634 Vitale Brovarone, A., Picatto, M., Beyssac, O., Lagabrielle, Y., and Castelli, D., 2014. The
1635 blueschist-eclogite transition in the Alpine chain: P-T paths and the role of
1636 slow-spreading extensional structures in the evolution of HP-LT mountain
1637 belts. Tectonophysics 615-616: 96-121.
1638 von Huene, R., and Lallemand, S. 1990. Tectonic erosion along the Japan and Peru
1639 convergent margin. Geol. Soc. Am. Bull. 102: 704–720.
1640 von Huene, R., Ranero, C.R., and Vannucchi, P. 2004. Generic model of subduction
1641 erosion. Geology 32: 913–916.
1642 Wakabayashi, J. 2011. Mélanges of the Franciscan Complex, California: diverse structural
1643 settings, evidence for sedimentary mixing, and their connection to subduction
1644 processes: in Wakabayashi, J., and Dilek, Y. eds. Mélanges: Processes of
1645 Formation and Societal Significance, Geological Society of America Special
1646 Paper 480: 117–141.
1647 Wakabayashi, J. 2019. Sedimentary compared to tectonically-deformed serpentinites and
1648 tectonic serpentinite mélanges at outcrop to petrographic scales: Unambiguous
1649 and disrupted examples from California. Gondwana Res. 74: 51-67.
1650 Wakita, K. 2015. OPS mélange: a new term for mélanges of convergent margins of the
1651 world. Int. Geol. Rev. 57 (5–8): 529–539.

1652 Whitmarsh, R. B., Manatschal, G., and Minshull, T. A. 2001. Evolution of magma-poor
1653 continental margins from rifting to seafloor spreading. Nature 413: 150-154.
1654 Wood, D.S. 1974. Ophiolites, mélanges, blue schists, and ignimbrites: early Caledonian
1655 subduction inWales? In Dott, R.H., and Shaver, R.H., eds., Modern and Ancient
1656 Geosynclinal Sedimentation. SEPM Special Publications 19: 334–343.
1657 Yamamoto, Y., Ogawa, Y., Uchino, T., Muraoka, S., and Chiba, T. 2007, Large-scale
1658 chaotically mixed sedimentary body within the Late Pliocene to Pleistocene
1659 Chikura Group, Central Japan. Island Arc 16: 505-507.
1660 Žák, J., Svojtka, M., Hajná J., and Ackerman, L. 2020. Detrital zircon geochronology and
1661 processes in accretionary wedges. Earth-Science Rev. 207: 103214.
1662 Zanoni, D., Rebay, G. and Spalla, M. I. 2016. Ocean floor and subduction record in the
1663 Zermatt-Saas rodingites, Valtournanche, Western Alps. Journal Metamorphic
1664 Geology 34: 941-961.

FIGURE AND TABLE CAPTIONS

Figure 1. ~~Structural sketch map of the Western Alps and northwestern Northern Apennine (modified from Balestro et al., 2015) with locations of examples described in the text.~~ Tectonic map of the Western Alps and the Northern Apennines (**A**), showing the distribution of different lithospheric plates and ocean basins that were involved in the evolution of the orogenic belts in this region (modified from Balestro et al., 2015). Locations of the major chaotic rock units and MTDs discussed in the text are also shown in red circles and numbers. (**B**) Index map, showing the Alps and the Apennines in their Mediterranean context.

Figure 2. Paleogeographic reconstruction of the Western Tethyan realm (Ligurian-Piedmont Ocean Basin) in the (**A**) Middle Jurassic (modified from Sampfli and Kozur, 2006; Schettino and Turco, 2011) and (**B**) late Maastrichtian (modified from Michard et al., 2002; Sampfli and Kozur, 2006; Schettino and Turco, 2011; Marroni et al., 2017; Festa et al., 2020).

Figure 3. Stratigraphic columnar sections and outcrop photos showing the ~~stratigraphic position~~ sedimentary and structural features of the syn-extensional, lower and upper ophiolitic breccias of the Internal Ligurian Units in the Graveglia (**A**) and Bracco (**E**) sections (Northern Apennines) ~~and related field occurrences~~. (**B**) Polymictic clasts composed of ~~(~~Fe-gabbros~~,~~ Fe-basalts~~,~~ plagiogranites~~,~~ and serpentinites~~)~~ in a scarce sandy matrix of the Monte Capra Breccia (lower ophiolitic breccia). Hammer for scale; (**C**) close-

up view of subrounded ~~shaped~~ clasts of Mg-gabbros in the Monte Zenone Breccia (upper ophiolitic breccias) and their stratigraphic relationships (**D**) with Radiolarian cherts. Hammer for scale; (**F**) close-up view of the ophicalcite texture of the Levanto Breccia.; (**G**) close-up view of the Framura Breccia (lower ophiolitic breccia) showing serpentinite clasts in a serpentinite-derived matrix. Coin for scale; (**H**) panoramic view ~~showing~~ displaying the relationships between the lower ophiolitic breccia (Levanto Breccia) and massive basalts. The stratigraphic relationships are highlighted by ophiolitic sandstones.

Figure 4. Inferred tectonic settings for the emplacement of the syn-contractional MTDs in the Northern Apennines: ~~General~~ (**A**) General; ~~and~~ (**B**) In detail.~~ed (B)~~ (**C**) Representative stratigraphic columnar sections (with scale) ~~tectonic setting proposed for the emplacement of the syn-contractional MTDs of the Northern Apennine, and representative stratigraphic columns (C)~~. **(D)** Close-up view ~~(D)~~ of the cohesive debris flows ~~from~~ in the Val Lavagna Shale Group (i.e., "Olistostroma del Passo della Forcella"), showing angular to subangular clasts of calcilutites embedded in a muddy-silty matrix. Coin for scale; (**E**) stratigraphic contact (white arrows) between the Bocco Shale (BS) and the Val Lavagna Shale (VLS) in the Portello Unit. Coin for scale; (**F**) Panoramic, and (**G**) Detail view ~~(F) and detail (G)~~ of the Bocco Shale (early Paleocene), showing angular to subangular clasts of calcilutite in muddy-silty, foliated matrix. Hammer for scale.

Figure 5. (**A**) Representative stratigraphic sections, depicting the distribution of the lower and upper syn-extensional ophiolitic metabreccias within the Zermatt-Saas ophiolites in the sector between the Lake Miserin (modified from Tartarotti et al., 2017) and Mt. Avic. (**B**) Field evidence of the superposition of two tectono-metamorphic stages (D1 and D2) of the

Alpine deformation onto the eclogite-facies ophiolite metabreccias of the Lake Miserin (Zermatt-Saas ophiolites). Note that the orientation of irregularly shaped clasts, centimeter in size, marks the relict of S1 foliation (dashed yellow line) which is deformed by D2 folds (dashed white lines indicate S2 foliation and D2 fold axial plane; see Tartarotti et al., 2017a for details). (~~B~~**C**) Field occurrence of lower ophiolite metabreccias (Zermatt-Saas ophiolites) in the Lake Miserin area ~~lower ophiolite metabreccias (Zermatt-Saas ophiolites)~~, showing alternating layers of different sized clast-supported metabreccias made of angular clasts of serpentinized metaperidotite and metaophicarbonate. Field book for scale; (~~C~~**D** and ~~D~~**E**) Different close-up views of the Lake Miserin Sedimentary mélange (syn-extensional upper ophiolitic metabreccias; Zermatt-Saas ophiolites), showing angular to sub-rounded clasts of serpentinized metaperidotite in a carbonate-rich (marble) matrix. Dashed white line indicates the S2 foliation. Pencil for scale; (~~E~~**F**) Close-up view of the Mt. Avic lower ophiolitic metabreccias (Zermatt-Saas ophiolites), showing angular shaped clasts of serpentinized metaperidotite and metaophicarbonate in a mixed carbonate-ultramafic metasandstone matrix. ~~(F) Stratigraphic columnar section of the Queyras ophiolite (modified from Balestro et al., 2019), depicting the stratigraphic position of the lower and upper syn-extensional ophiolitic metabreccias, and syn-contractional MTDs.~~ (**G**) Close-up view of the polymictic syn-extensional upper ophiolitic metabreccias (blueschist facies) of the Queyras ophiolite, showing angular clasts of serpentinized metaperidotite and metagabbros in a calcschist matrix; (**H**) Close-up view of the syn-contractional MTDs of the Rocher Renard Complex (lower Paleocene?), showing rounded clasts of serpentinized metaperidotite and marble in a metapelite matrix. ~~Photo~~Camera cap for scale; (~~F~~**I**) Stratigraphic columnar section of the Queyras ophiolite (modified from Balestro et al.,

2019), depicting the stratigraphic position of the lower and upper syn-extensional ophiolitic metabreccias, and syn-contractional MTDs.

Figure 6. (**A**) Stratigraphic columnar section of the Monviso ophiolite (modified from Balestro et al., 2019), depicting the lateral and vertical relations between the syn-extensional chaotic deposits, the exhumed ~~ophiolite~~ upper mantle rocks and the sedimentary succession. (**B**, **C** and **D**) ~~Different~~ Various close-up views of angular to irregular shaped clasts of gabbro in a coarse-grained matrix of mafic-metasandstone (lower syn-extensional ophiolitic metabreccias), and line drawing (**E**) of the overturned mantle-cover succession cropping out at Colle del Baracun (Monviso ophiolite); ~~showing~~ notice the stratigraphic position of mafic metabreccias and metasandstones within the calcschist ~~succession~~ sequence (modified from Balestro et al., 2015a) (**F**) Panoramic view of the Garten Formation (syn-extensional upper ophiolitic metabreccias) to the East of Cime Bianche (Aosta Valley), showing intercalations of hyperconcentrated deposits (dashed white lines), decimeters to one meters thick, in a calcschist matrix. Dashed black line indicates the S2 foliation. Backpack for scale. (**G** and **H**) Close-up views of the internal arrangement of the Garten Formation, showing rounded to elongated shaped clasts of metabasalt in a coarse-grained calcschist matrix. (**I**) Interpreted stratigraphic sections, depicting the distribution of the syn-extensional upper ophiolitic metabreccias of the Garten Formation in the Zermatt-Saas ophiolite sequence of the Cime Bianche sector.

Table 1. Comparison among syn-extensional lower and upper ophiolitic breccias and syn-contractional MTDs of the Internal Ligurian Units of Northern Apennines and Western Alps.

Figure 7. Interpretative block diagrams depicting the geodynamic and tectono-stratigraphic depositional setting for syn-extensional, lower and upper ophiolitic breccias and syn-contractional MTDs during: **(A)** The Middle-Late Jurassic seafloor spreading, and ~~(A) and~~ **(B)** Late Cretaceous – Paleocene convergence ~~(B)~~ tectonic stages of the evolution of the Western Tethyan realm (Ligurian – Piemont Ocean Basin), respectively.

REVISED Manuscript (with no changes marked)

Comparative analysis of the sedimentary cover units of the Jurassic Western Tethys ophiolites in the Northern Apennines and Western Alps (Italy): Processes of the formation of mass transport and chaotic deposits during seafloor spreading and subduction zone tectonics

Andrea Festa[1*], Francesca Meneghini[2], Gianni Balestro[1], Luca Pandolfi[2,3], Paola Tartarotti[4], Yildirim Dilek[5], Michele Marroni[2,3]

1. Dipartimento di Scienze della Terra, Università di Torino, Torino (Italy); ORCID #: AF, 0000-0001-5325-0263; GB, 0000-0001-5215-4659
2. Dipartimento di Scienze della Terra, Università di Pisa, Pisa (Italy); ORCID #: FM, 0000-0002-6809-6112; LP, 0000-0002-6129-647X; MM, 0000-0002-2947-3739
3. Istituto di Geoscienze e Georisorse, IGG-CNR, Pisa (Italy)
4. Dipartimento di Scienze della Terra, Università degli Studi di Milano, Milano (Italy); ORCID #: PT, 0000-0002-2236-2702
5. Department of Geology and Environmental Earth Science, Miami University, Oxford, (USA); ORCID#: YD, 0000-0003-2387-9575

***Corresponding author**:

Professor Andrea Festa
Street address: Via Valperga Caluso, 35
10125, Torino, Italy
E-mail address: andrea.festa@unito.it
Phone: +39-011-670.51.86

Submitted to: The Journal of Geology
Special Issue on the Plate Tectonics Anniversary
Re-revised version: 24 May 2021

ABSTRACT

The Jurassic ophiolites in the Northern Apennines and the Western Alps represent fossil mid–ocean ridge (MOR) oceanic lithosphere that formed in the Mesozoic Ligurian–Piedmont Ocean Basin (LPOB). Their sedimentary covers include chaotic rock units containing ophiolite–derived material. The processes of formation and the lithostratigraphic position of these chaotic units in the Western Alps remain a matter of debate, unlike their counterparts in the Northern Apennines. This is because of pervasive tectonic deformation and high-pressure metamorphism that affected their internal structure due to the collisional tectonics. A comparative analysis of these chaotic units in both mountain belts reveals the nature of processes involved in their formation. Chaotic deposits of gravitational origin occur both below and above the extrusive sequences in the ophiolites. They represent syn-extensional, hyper-concentrated deposits associated with the seafloor spreading evolution of the LPOB lithosphere during Middle and Late Jurassic time. MTDs occur as intercalations within turbiditic sequences above the ophiolites. They represent syn–contractional submarine slides that occurred on frontal accretionary prism slopes during the Late Cretaceous–Paleocene closure of the LPOB. The results of our comparative analysis imply that: (1) the structure–stratigraphy of the chaotic deposits and MTDs of the Northern Apennines can be used as a proxy to better identify their metamorphosed and highly deformed counterparts in the Western Alps; (2) sedimentological processes associated with slow–spreading MOR tectonics and with accretionary prism development in convergent margin tectonics contributed to the sediment budgets of the cover sequences; and, (3) magmatic, tectonic and sedimentological processes that occurred during the formation of the Jurassic oceanic lithosphere and its sedimentary cover in the LPOB were remarkably uniform and synchronous.

61

62 **Keywords**: Mesozoic Ligurian–Piedmont Ocean; submarine chaotic rock units; submarine
63 mass transport deposits; sedimentary cover of ophiolites; Western Alps; Internal Ligurian
64 Units – Northern Apennines.

65

INTRODUCTION

Chaotic rock units (i.e., tectonic, sedimentary and diapiric mélanges, broken formations and polygenetic mélanges, see Festa et al., 2019b) containing fragments of an ophiolite represent the most significant component of the ocean-derived units preserved in Archean to Cenozoic collisional belts (e.g. Sample and Moore 1987; Orange 1990; Polat and Kerrich, 1999; Fitzherbert et al., 2005; Dilek, 2006; Yamamoto et al.2007; Federico et al., 2007; Festa et al., 2010, 2020c; Malatesta et al., 2012; Dilek et al., 2012; Balestro et al., 2015a, 2020; Ogawa et al., 2015; Ernst, 2016; Scarsi et al., 2018; Raymond, 2019; Roda et al., 2019; Wakabayashi, 2011; Hajná et al., 2019; Gao and Santosh, 2020; Palin et al., 2020; Žak et al., 2020; Barbero et al., 2021). Understanding the formation and emplacement of these chaotic deposits in space and time is significant for better constraining the nature, tempo and order of the magmatic, tectonic and sedimentological processes, which operated during the formation of ancient oceanic lithosphere and its sedimentary cover. Related data and observations can provide additional constraints for redefining the plate tectonic paradigm and fro developing a better understanding of the Earth systems.

In the Piedmont Zone of the Western Alps and in the Internal Ligurian Units of the Northern Apennines in Italy (Fig. 1), these types of chaotic rock units were derived from the deformation of the northern and southern parts of the Jurassic Ligurian-Piedmont oceanic rocks (Western Tethys), respectively (Marroni et al., 2017; Dilek and Furnes, 2019). In the Northern Apennines, the chaotic rock deposits show a very low–grade metamorphic overprint, allowing documentation in detail of their preserved diagnostic sedimentological features and their lithostratigraphic position. In turn, this knowledge allows interpretation of the chaotic rock masses as the products of different mass transport processes, which occurred

during the Middle-Late Jurassic seafloor spreading of the Ligurian-Piedmont Ocean Basin (LPOB) lithosphere and the Late Cretaceous – Paleocene tectonic convergence between Europe and Adria (e.g., Fierro and Terranova 1963; Elter 1975; Abbate et al., 1970, 1980; Cortesogno et al., 1987; Marroni and Pandolfi, 2001; Bortolotti and Principi, 2003; Principi et al., 2004; Lamarche et al., 2008; Festa et al., 2018; Meneghini et al., 2020).

Conversely, in the Western Alps, the chaotic rock units containing ophiolite–derived material were affected by pervasive subduction- and exhumation-related deformation and high–pressure metamorphism. As a result, primary sedimentological features in these rock units are partially obscured or obliterated; lithostratigraphic position and evidence of tectonic versus sedimentary formational processes in their development, thus, remain matters of debate (see e.g., Balestro et al., 2015a, Tartarotti et al., 2017a; Roda et al., 2019 and references therein). This phenomenon complicates the detailed reconstruction of the syn-spreading to convergent stages of tectono-sedimentary evolution of the northern portion of the LPOB, as exposed in the Western Alps.

In this paper we define the original, oceanic sedimentary cover of the Jurassic ophiolites exposed in the Northern Apennines and the Western Alps (Italy), and document various chaotic rocks units preserved in these cover sequences. We compare and correlate both lithologically and chronologically these chaotic rock units and their stratigraphic positions in the Northern Apennines and the Western Alps (Fig. 1). We show that the well-known sedimentological-stratigraphical features of the chaotic deposits in the Northern Apennines can be used as a proxy allowing us to refine the tectonostratigraphy of their highly deformed and metamorphosed counterparts in the Western Alps. Our results indicate that the LPOB lithosphere underwent similar tectonic processes during the Jurassic seafloor

113 spreading and Late Cretaceous–Early Paleocene closure phases of the ocean basin history
114 throughout its entire length.
115
116 **Nomenclature and terminology of chaotic rock units**
117 In this paper we use the term *chaotic rock unit* as a general and descriptive, but not a
118 genetic term, to describe different types of block-in-matrix rock assemblages. This term
119 includes the entire range of chaotic rock mass occurrences, in which mélanges and broken
120 formations represent two end members (see Festa et al., 2019b for details). Hence, chaotic
121 rock units may represent a rock mass that can be formed by: (1) tectonic, sedimentary and/or
122 diapiric processes; (2) both stratal disruption and/or mixing processes, and (3) superposition
123 of exotic, native or mixed exotic – native blocks embedded in a matrix of various possible
124 compositions. Chaotic rock units formed by sedimentary (gravitational) processes represent
125 ancient submarine mass transport deposits (MTDs; see, e.g., Lucente and Pini, 2008; Ogata
126 et al., 2012, 2020; Festa et al., 2016; Pini et al., 2020), commonly described as olistostromes
127 (Flores, 1955; Elter and Trevisan, 1973; Pini, 1999) or sedimentary mélanges (e.g.,
128 Raymond, 1984; Bettelli and Panini, 1985, Bettelli et al., 2004; Festa et al., 2016) in orogenic
129 belts and exhumed subduction – accretion complexes. We use the terms "mass transport
130 deposit (MTD)" and "chaotic deposit" to denote two sedimentary (gravitational) chaotic rock
131 unit types, which differ from each other in their matrix types. Chaotic deposits are
132 characterized by a matrix- to clast-supported texture with a predominantly basic to ultrabasic
133 sandy matrix, and more rarely by a hematitic to carbonaceous matrix, whereas MTDs have
134 a shaly matrix. Note also that some of the described examples of chaotic deposits and MTDs
135 consist of single layers. This prevents us from using the terms sedimentary mélange and
136 olistostrome, as these occurrences are not mappable at 1:25,000, as required by the definition

of the mélange term (e.g., Berkland et al., 1972; Wood, 1974; Silver and Beutner, 1980; Raymond, 1984; Cowan, 1985; Festa et al., 2019b).

GEODYNAMIC HISTORY OF THE LIGURIAN – PIEDMONT OCEAN BASIN (LPOB)

The Ligurian – Piedmont Ocean Basin (LPOB), which evolved between Europe and Adria, was a restricted, Red Sea – type ocean basin in the Mesozoic paleogeography of the Western Tethys (Fig. 2a; see, e.g., Dilek and Furnes, 2019 and references therein). It was connected with the Central Atlantic Ocean Basins to the west via a NW–SE–oriented transform fault system (Fig. 2a; Dercourt et al., 2000; Stampfli and Borel, 2002; Stampfli et al., 2002; Golonka, 2007; Schettino and Turco, 2011; Berra and Angiolini, 2014; Hosseinpour et al., 2016 and Dilek and Furnes, 2019). The opening of the LPOB is generally regarded as the result of rift–drift and seafloor spreading during Middle Triassic through Middle Jurassic time (Marroni et al., 1998; Müntener and Hermann, 2001; Whitmarsh et al., 2001; Capitanio and Goes, 2006; Montanini et al., 2006; Marroni and Pandolfi, 2007; Piccardo et al., 2014; Festa et al., 2020a). Initial lithospheric stretching and distributed extension was followed by strain localization and hyper-extension, which led to continental rifting and seafloor spreading (Lavier and Manatschal 2006; Péron-Pinvidic and Manatschal 2009; Mohn et al., 2012; Ribes et al., 2019). The resulting conjugate margins were asymmetric in their structural architecture with the European margin showing a narrow ocean-continent transition zone (OCTZ) marked by high-angle normal faults and the Adria margin characterized by a wider OCTZ (Fig. 2a), along which the subcontinental mantle and the lower continental crust were exhumed (Marroni and Pandolfi 2007; Saccani et al., 2015).

The oceanic lithosphere of the LPOB was unlike a typical Penrose–type oceanic lithosphere with a complete crustal pseudostratigraphy (or ocean plate stratigraphy, *sensu* Wakita, 2015) of a modern fast–spreading oceanic lithosphere (Anonymous, 1972; Dilek et al., 1998), rather it resembled a Hess–type oceanic lithosphere (Dilek and Furnes, 2011) that commonly develops at slow– to ultra slow–spreading mid–ocean ridge settings (Pognante et al., 1986; Lemoine et al., 1987, Lagabrielle and Cannat, 1990, Treves and Harper, 1994; Cannat, 1996, Cannat et al., 1997, Michard et al. 1996; Magde et al., 2000, Rabain et al., 2001; Balestro et al., 2015b; Rampone e al., 2020). The available paleontological data from chert deposits in the Ligurian ophiolites (Bill et al., 2001; Principi et al., 2004), as well as the radiometric dating results (Li et al., 2013; Tribuzio et al., 2016), indicate that seafloor spreading within the LPOB lasted for ~25 m.y. from Bajocian to Tithonian time. The seafloor spreading phased out and stopped at the beginning of the Early Cretaceous Epoch when the basin was about 600 to 700 km–wide (Abbate et al., 1980; Marroni and Pandolfi, 2007; Balestro et al., 2019). Throughout much of the Cretaceous Period the LPOB experienced deep-sea pelagic deposition without any tectonic or volcanic event interrupting this depositional record.

During Campanian time, the mode of sedimentation changed abruptly with the onset of deep-sea clastic sedimentation, which involved the deposition of a vast amount of siliciclastic and carbonate turbidites, whose sediments were derived from the European margin (Marroni and Perilli, 1990; Marroni et al., 1992; Principi et al., 2004). The onset of this extensive turbidite deposition episode is considered to be the beginning of a contractional deformation phase in the evolutionary history of the LPOB that led to its closure in the Cenozoic Era. The early Campanian time of the turbidite deposition coincides with the age of high–pressure metamorphism in the internal sectors of Western Alps (see,

185 e.g., Manzotti et al., 2014 and reference therein) and in Corsica (e.g., Lahondère and Guerrot,
186 1997).

187 The initial stages of basin closure were facilitated by an intraoceanic subduction
188 event, which resulted in the development of a subduction–accretion system (Fig. 2b). The
189 position of this intraoceanic subduction within the LPOB is still a matter of debate. Recent
190 geodynamic models place this subduction–accretion system close to or within the OCTZ
191 along the Adria continental margin, with subduction beginning, in the Late Cretaceous
192 Epoch (Manzotti et al., 2014; Marroni et al., 2017; Barbero et al., 2020; Festa et al., 2020a).

193 The accretionary wedge experienced slope instability due to subduction of an oceanic
194 crust characterized by seamounts and a rough topography, probably inherited from the
195 spreading phase (Marroni and Pandolfi, 2001; Marroni et al., 2017; Meneghini et al., 2020).
196 The slope instability resulted in large submarine slides recorded as debris flows and slide
197 deposits that were emplaced within or at the top of the trench turbidites (e.g., Pini, 1999;
198 Festa et al., 2018; 2020b; Ogata et al., 2019; Meneghini et al., 2020 and references therein).

199 During the convergence, the LPOB lithosphere was subducted largely into the mantle
200 or was locally accreted at the base or in front of an accretionary wedge (Fig. 2b). Thus,
201 several segments of the LPOB that were accreted at different depths are found today as
202 tectonic thrust sheets of ophiolites in the Western Alps and the Northern Apennines. These
203 units were affected by pervasive deformation associated with subduction-related
204 metamorphism ranging from very low-grade to blueschist and eclogite facies (Goffè et al.,
205 2003), similar to that typically described in many exhumed, sediment-dominated
206 accretionary prisms (Ernst, 1970, 1971, 2015; Miyashiro, 1973; Raymond, 1973; More and
207 Sample, 1986; Meneghini et al., 2009; Plunder et al., 2015). In the Northern Apennines the
208 ophiolite units were subducted to shallow levels (maximum of 25 km depth; Marroni et al.,

2017), whereas in the Western Alps they were subducted to depths ranging from 30 km to 90 km (e.g. Handy et al., 2010; Roda et al., 2020 and reference therein) and were metamorphosed under peak P-T conditions during latest Cretaceous(?) to middle Eocene time (e.g. Rosenbaum and Lister 2005; Zanoni et al., 2016; Rebay et al., 2018; Luoni et al., 2020 and references therein).

The deformation characteristics of these units indicate an accretion by coherent underplating during east–dipping and low–rate subduction dominated by a high sediment budget. The deformation history and the related metamorphism testify not only to the accretion phases, but also to the exhumation history of these units (Polino et al. 1990; Butler et al. 2013; Roda et al., 2020; Luoni et al., 2020). Ophiolite units detached from the subducting slab were uplifted to shallow crustal levels and rapidly exhumed before the early Oligocene. This inference is supported by the occurrence of continental conglomerates in the Tertiary Piedmont Basin (Fig. 1), which represents a wide episutural basin overlying the metamorphosed ophiolites both in the Western Alps and in the Northern Apennines (Federico et al., 2015; Barbero et al., 2020; Festa et al., 2013, 2020b). During and after middle Eocene time, the Jurassic ophiolites underwent continental collision tectonics and deformation both in the Western Alps and the Northern Apennines and were involved in nappe and overthrust development and large–scale isoclinal and recumbent folding.

In summary, the LPOB developed during three main stages. The first stage involved continental rifting and seafloor spreading in Middle to Late Jurassic time (Fig. 2a). During the second stage, between the Berriasian and the Santonian ages, it experienced tectonic quiescence and extensive pelagic deposition. During the third stage, starting in the Campanian age, the LPOB underwent intraoceanic subduction, basin closure, and continental collision.

OPHIOLITE AND SEDIMENTARY COVER RECORD IN THE NORTHERN APENNINES

In the Internal Ligurian Units (Fig. 1), a series of tectonostratigraphic units occurs in thrust sheets. These thrust sheets extend from southern Tuscany to the city of Genova, in the north, where they are in contact with eclogitic oceanic rocks of the Voltri Group, assigned to the Western Alps (Fig. 1). These tectonostratigraphic units show pervasive deformation structures that are spatially and temporally associated with a metamorphic overprint, decreasing in grade from the structurally lowermost units to those lying on top of the tectonic pile (Leoni et al. 1996; Ellero et al. 2001). The lowermost units (Cravasco-Voltaggio and Mt. Figogna Units) are affected by low-grade blueschist facies metamorphism, whereas the uppermost ones (Gottero, Bracco-Val Graveglia, Colli-Tavarone, Portello, Vermallo and Due Ponti units) display mineral phases and textures suggesting very low-grade metamorphic conditions, ranging from upper anchizone to epizone conditions (Leoni et al. 1996; Crispini and Capponi 2001; Ellero et al. 2001).

The Internal Ligurian Units, regardless of the degree of metamorphism or deformation, display a stratigraphic succession that reflects the inferred three stages of development of the LPOB. This succession includes a ~1–km–thick ophiolite sequence and a ~4–km–thick sedimentary cover, which includes two lithologically and compositionally different parts with different geodynamic significance (Decandia and Elter, 1972, Abbate et al., 1980; Treves 1984; Marroni and Perilli 1990; Marroni et al. 1992; Abbate et al. 1994).

First Stage: Formation of the oceanic lithosphere and its oldest sedimentary cover

The Middle to Late Jurassic ophiolite sequence formed during the first stage in a slow- to ultraslow-spreading ridge environment, where magma supply was limited and tectonic (amagmatic) extension processes, producing high– to low–angle normal faults, were dominant (e.g., Lagabrielle and Cannat, 1990, Treves and Harper, 1994; Marroni and Pandolfi, 2007; Rampone et al., 2020). Tectonic extension in the absence of a steady–state magma supply resulted in the exhumation of upper mantle peridotites, which underwent widespread serpentinization, and in the formation of sags and structural highs, creating a rugged seafloor bathymetry (e.g., Principi et al., 2004; and reference therein).

Exhumed serpentinized peridotites were intruded by gabbroic stocks and plutons and were covered by volcanic and sedimentary rocks, composed of basaltic pillow-lavas and sills, radiolarian cherts and ophiolitic breccias. Basaltic lavas and sills have MORB-type geochemical signatures (e.g., Renna et al., 2018). Ophiolitic breccias represent chaotic deposits accumulated in half-grabens and tectonic sags developed in the hanging walls of normal faults (e.g., Elter 1975; Bortolotti and Principi, 2003; Principi et al., 2004). They are subdivided into several types according to their clast compositions, which reflect the source lithology and their lithostratigraphic position below or above the basaltic carapace of the ophiolite (Elter 1975; Cortesogno et al., 1987; Bortolotti and Principi, 2003; Principi et al., 2004).

Second Stage: Formation of deep-sea pelagic sedimentary cover

The ophiolite sequence is overlain by Callovian-Santonian deep-sea pelagic sedimentary rocks deposited during the second stage, which lasted nearly 80 m.y. The pelagic deposits include Middle Callovian to Early Berriasian cherts and fine-grained, carbonaceous turbidites that are composed of the Late Berriasian-Valanginian Calpionella

Limestone and the Valanginian-Santonian Palombini Shale. All these deposits were the products of a low sedimentation rate in a deep–marine environment (Marroni and Perilli, 1990; Marroni et al., 2004).

Third Stage: Deposition of turbidites in a closing ocean basin

The deep–marine pelagic rocks are conformably overlain by a Lower Campanian–Lower Paleocene, thick turbidite sequence, the deposition of which started contemporaneously with the onset of subduction within the LPOB. The lower part of this sequence consists of carbonaceous and siliciclastic turbidites (i.e., the Val Lavagna Shale Group, which includes the lower Campanian Manganesiferi Shale, the lower to upper Campanian Monte Verzi Marl, and the lower Campanian to lower Maastrichtian Zonati Shale). These fine–grained rocks reflect a high sedimentation rate within a shrinking basin following the onset of intra–basin subduction. They grade stratigraphically upwards into the lower Maastrichtian to lower Paleocene sandstone (i.e., the Gottero Sandstone). Arenites in siliciclastic turbidites represent arkosic–subarkosic rocks, whose clast compositions are compatible with lithologies constituting the upper part of the rifted European margin. Hence, it is widely accepted that the provenance of the turbiditic sequence above the ophiolite was the passive continental margin of Europe (Valloni and Zuffa, 1984; Van de Kamp and Leake, 1995; Pandolfi, 1997; Marroni and Pandolfi, 2001). These turbiditic sequences (i.e., Zonati Shale and the Gottero Sandstone) were deposited in submarine fans adjacent to the European passive continental margin (Abbate and Sagri, 1982; Nielsen and Abbate, 1983; Fonnesu and Felletti, 2019). The stratigraphically upper parts of this submarine fan sequence contain MTDs consisting of debris flow deposits, which include reworked clasts derived from an oceanic lithosphere and its sedimentary cover.

The youngest deposit of the Internal Ligurian Units consists of an MTD, represented by the Lower Paleocene Bocco Shale, also known as the Colli-Tavarone and Lavagnola Formations (Marroni et al., 2017). The Bocco Shale rests unconformably on top of all the older formations and consists of thin-bedded turbidites, and slide and debris flow deposits. Clasts and materials of these deposits were derived from an oceanic lithosphere and its sedimentary cover (Marroni and Pandolfi, 2001; Marroni et al., 2017; Meneghini et al., 2020).

DIAGNOSTIC FEATURES AND DEPOSITIONAL MECHANISMS OF CHAOTIC DEPOSITS AND MTDs IN THE NORTHERN APENNINES

The sedimentary cover units of the Internal Ligurian ophiolites in the Northern Apennines include two distinctive chaotic rock unit types of gravitational origin with specific age spans corresponding to different phases in the evolutionary history of the LPOB. The oldest (Middle to Upper Jurassic) chaotic rock units developed during the seafloor spreading and hence the opening phase of the LPOB. We refer to these deposits as syn–extensional chaotic deposits in the rest of the paper. The youngest, Upper Cretaceous–Lower Paleocene chaotic rock units formed during the convergence and closure phase of the LPOB. We refer to these deposits as syn–contractional mass–transport deposits (MTDs) in the rest of the paper. In both the opening and the closing phases, accumulation of chaotic deposits and MTDs over a recently formed oceanic lithosphere was a tectonically induced depositional event.

Syn–Extensional Chaotic Deposits

The syn-extensional sedimentary chaotic rocks are well exposed in the Val Graveglia and the Bracco Massif (see 11 and 12 of Fig. 1, also see Fig. 3), both of which are located in the eastern Liguria region, between the cities of Genova and La Spezia. These chaotic deposits are designated as the lower and upper ophiolitic breccias on the basis of their stratigraphic position below or above the basaltic lava flows, respectively (Figs. 3A and 3E; Principi et al., 2004); their clasts were sourced from an entirely local provenance. These ophiolitic breccias represent one specific type of a syn-extensional chaotic deposit. The lower ophiolitic breccias rest directly on serpentinized peridotites or gabbros, and they are overlain by basaltic flows or cherts. The upper ophiolitic breccias occur between the base of the basaltic lava flows and on top of the cherts. The ages of the lower and upper breccias are poorly constrained due to the low resolution of radiolarian assemblages in their matrix material. The available biostratigraphic data indicate an age of the ophiolitic breccias and the associated basaltic flows spanning from Upper Bajocian to Lower Callovian (Chiari et al., 2000, and reference therein).

Syn-extensional lower ophiolitic breccias. The lower ophiolitic breccias include the Levanto, Framura, Casa Boeno and Monte Capra Breccias (Principi et al., 2004, and references therein). The first three overlie the serpentinized peridotites, whereas the last breccia covers the gabbro. The lithological composition of these breccias reflects the substrate on which they rest. The Levanto Breccia (ophicalcites *s.s.*) is a tectonic-hydrothermal breccia, which occurs above the serpentinized upper mantle rocks (Figs. 3E and 3F). It marks a cataclastic shear zone composed of fragmented serpentinites crosscut by a network of veins, filled with sparry calcite, talc and locally by smaller serpentinite

fragments. This cataclastic shear zone marks an oceanic detachment fault zone, which was exposed on the LPOB seafloor (Treves and Harper, 1994).

The overlying Framura Breccia consists mainly of reworked Levanto Breccia material (Abbate et al., 1980; Cortesogno et al., 1987), and is composed of a coarse-grained breccia containing mostly serpentinite and rare gabbro clasts in a hematitic matrix (Fig. 3G and H). The Case Boeno Breccia (Cortesogno et al., 1987; Principi et al., 2004) is a monogenic breccia consisting of serpentinite clasts in a scarce, serpentinite–sand matrix. The Case Boeno Breccia locally includes large serpentinite blocks, up to several metres wide. As with the Framura Breccia, the Case Boeno Breccia also lies stratigraphically on top of the serpentinized peridotites. Overlying the gabbro intrusions, the Monte Capra Breccia represents a clast-supported polymictic breccia (Fig. 3B) with clasts of Fe-gabbro, Fe-basalt, plagiogranite, and serpentinite in a scarce sandy matrix (Bortolotti and Principi, 2003; Principi et al., 2004). The existence of Fe-basalt and Fe-gabbro clasts is unique to the lower ophiolitic breccias.

Syn-extensional upper ophiolitic breccias. The syn-extensional upper ophiolite breccias (Figs. 3A and 3E) include the Movea, Mt. Zenone, and Mt. Bianco Breccias (Principi et al., 2004, and references therein). The Movea Breccia is a polymictic breccia mainly containing clasts of foliated gabbro with minor amounts of pillow basalt, gabbro, and serpentinite clasts within a chloritized sandy matrix (Bortolotti and Principi, 2003; Principi et al., 2004). The Movea Breccia grades upward into the Mt. Zenone Breccia (Figs. 3C and 3F), which is a monomictic breccia showing only clasts of foliated gabbro in a sandy matrix composed of gabbro fragments. In contrast, the Mt. Bianco Breccia consists of serpentinite and ophicalcite

clasts within an abundant sparry calcite matrix (Bortolotti and Principi, 2003; Principi et al., 2004).

Both the syn-extensional lower and upper ophiolitic breccias are characterized by comparable sedimentological features: they all have a clast-supported texture with angular or sub-angular clasts. The matrix has the same lithological composition as the main clast types. The maximum clast-size ranges from gravel to boulder. Beds are lenticular in shape, and their thicknesses range from 1 m up to 20 m. Bed bottoms display planar to erosive surfaces. The erosional nature of the basal contact is suggested by common bottom bedset scours and diffuse, amalgamated beds. A faint internal organization is locally present, and grading is roughly developed. Bed–cap, if not eroded, is characterized by a cm- to dm-thick, coarse-grained and laminated sandstone and siltstone beds composed of ophiolitic material. The downcurrent evolution of the turbidity current depositional events can produce poorly developed ophiolitic sandstones characterized by F5-F6 turbidite facies of Mutti (1992), capped by F9b siltstone beds. These beds are commonly preserved in the lower part of the chert layers. The clastic sediments can be interpreted to have been formed either as hyperconcentrated flow-derived deposits (Costa, 1988) or, alternatively, as the downcurrent evolutionary products of cohesive debris flows that trasformed into hyperconcentrated flows (F2 and F3 facies of Mutti, 1992).

Clasts of the lower ophiolitic breccias were mainly derived from reworking of the lower and upper crustal sections of the Jurassic oceanic lithosphere within the basin that had undergone ocean floor metamorphism. Stratigraphically higher up into the upper ophiolitic breccias, debris deposits derived from the upper oceanic crustal subunits and even from oceanic siliceous sedimentary rocks become predominant. We summarize the thickness and other sedimentological features of these syn-extensional chaotic deposits in Figs. 3A and 3E.

399

400 **Syn-Contractional Mass Transport Deposits (MTDs)**

401 Syn-contractional MTDs, which are well exposed in the eastern Liguria region
402 between the cities of Genova and La Spezia (see 9 and 10 of Fig. 1, also see Fig. 3),
403 developed by submarine mass transport mechanisms and are subdivided on the basis of their
404 spatial relationships with the turbiditic deposits (Figs. 4A, B). Some of these MTDs occur as
405 intercalations in the turbiditic deposits of the Val Lavagna Shale Group, whereas others
406 overlie this lithostratigraphic unit and contain minor siliciclastic turbidites (Fig. 4C). All
407 clastic materials for these turbiditic deposits were derived from the continental margin of
408 Europe (Marroni and Pandolfi, 2001; Prinicipi et al., 2004; Marroni et al., 2017; Fonnesu
409 and Felletti, 2019; Meneghini et al., 2020).

410 The MTDs intercalated within the turbiditic deposits of the Val Lavagna Shale Group
411 consist of several mappable bodies of predominantly monomictic, pebbly-mudstones and,
412 locally of varicolored mudflow-derived deposits. Their ages range from Lower
413 Maastrichtian to Lower Paleocene. The predominantly monomictic pebbly-mudstones also
414 include gravel to boulder-sized clasts embedded in a muddy–silty matrix (Fig. 4D). The clast
415 composition is dominated by calcilutites derived from the Palombini Shale, but clasts of fine-
416 grained arenites also exist. The matrix is composed of arenitic to rudistic clasts of carbonate-
417 free mudrock, mainly derived from hemipelagic shales (Fig. 4D). The thickness of beds
418 ranges from a few centimeters to several meters (cf. Olistostroma di Passo della Forcella,
419 Fierro and Terranova 1963). The bed shape is lenticular, and erosional features are present
420 at the bases of beds. The internal organization in the beds is faint to absent. The pebbly
421 mudstone deposits represent cohesive debris flows (cf. olistostrome of Abbate et al., 1970
422 and F1and F2 facies of Mutti, 1992).

Varicolored shale beds also occur in the upper stratigraphic levels of the Gottero Sandstone (see Fig. 4). Their bed thickness ranges from a few meters to more than 20 meters. Bed shape in shale is lenticular and no erosional features are present at bed bases. These deposits were derived from mud flow processes probably related to submarine landslides originated from a steep slope draped by fine-grained sediments.

The MTDs overlying the turbiditic sequences are represented by the lower Paleocene Bocco Shale (Cf. Colli/Tavarone Formation, Giaiette Shale, Lavagnola Formation) (Figs. 4B, 4C, 4E-G). The Bocco Shale unconformably rests on the underlying formations of the Internal Ligurian Units, mainly the Palombini Shale and the Gottero Sandstone (Decandia and Elter, 1972; Marroni and Pandolfi, 2001; Marroni et al., 2017; Meneghini et al., 2020). Clasts within the Bocco Shale were derived from two main facies groups (Marroni and Pandolfi, 2001). The first group is composed of various rock blocks in a matrix of pebbly-mudstone, mudstone, clast-supported breccias, and very coarse- to coarse-grained turbidites. The second group consists of fine-grained, thinly bedded siliciclastic turbidite clasts. We summarize the thicknesses and stratigraphic features of these MTDs in Figure 4C.

Deposits containing the first facies group include MTDs that originated from reworking of an ophiolite sequence and its sedimentary cover (Lamarche et al. 2008; Festa et al. 2016). The block-in-matrix character is displayed by blocks of different sizes (ranging from 1 to 50 m) embedded in a shale–dominated matrix. Blocks are surrounded by syn-sedimentary deformation structures and by slide-block-derived, monomictic pebbly mudstone and pebbly sandstone. Locally, blocks are missing from the beds and such interbeds are mud-flow-derived mudstone. Pebble-bearing beds range from pebbly mudstones to mud- to clast-supported conglomerates and/or breccias (pebbly mudstone, pebbly sandstone and orthoconglomerate), all interpreted as cohesive debris flow-derived

447 deposits (sensu Mutti 1992). Blocks were derived entirely from reworked ophiolitic subunits
448 (serpentinized peridotites, basaltic lavas, and rare gabbros) and from the Upper Jurassic–
449 Lower Paleocene sedimentary cover of the ophiolite (chert, Calpionella Limestone,
450 Palombini Shale, Val Lavagna Shale, and Gottero Sandstone). The matrix also includes
451 arenitic to ruditic clasts, originated from reworked hemipelagic pelites of the Palombini and
452 Val Lavagna Shales.

453 Deposits containing the first facies group are associated with dm- to m-thick beds of
454 polymictic, clast-supported and poorly sorted conglomerates. These conglomerates, which
455 show the same clast composition as the pebbly mudstones, represent the down-current
456 evolution of cohesive debris flows into hyperconcentrated flows (F2 and F3 facies of Mutti
457 1992). Cohesive debris flow- and hyperconcentrated flow-derived deposits are associated
458 with subordinate, coarse-grained high-density turbidity current deposits. These facies are
459 locally associated with thin Bouma base-missing beds (F5 + F9 facies of Mutti 1992).
460 Arenite framework composition analyses performed on three samples from F5 beds,
461 collected from the Bocco Shale in the Gottero Sandstone indicate a litharenitic composition.
462 This framework is characterized by fragments of basalt, serpentinite, chert and Calpionella-
463 bearing limestone (Meneghini et al., 2020). Similarly, pebbles in F1, F2 and F3 beds show
464 the same composition as recognized in the slide-blocks and arenites. These data and
465 observations collectively point to a source area characterized by reworking of ophiolites and
466 related sedimentary cover within the Internal Ligurian tectonostratigraphy (Marroni and
467 Pandolfi, 2001; Meneghini et al., 2020).

468 Clasts of the second facies group consist of thinly bedded turbidites and mudstones,
469 the most common facies association recognized in the Bocco Shale. The thinly bedded
470 turbidites consists of alternations of fine- to medium-grained siliciclastic arenites with

carbonate-free mudstones. Sand to shale ratio in this facies group is generally >1. Arenite beds show moderate lateral continuity. Stratigraphic and sedimentological features of deposits of the second facies group point to low-density turbidity currents as the main depositional agent. Thick packages of thinly bedded turbidites were affected by widespread syn-sedimentary deformation due to slumping and submarine mass-wasting. These processes were responsible for the formation of meso-scale angular unconformities (more than 30°) among different packages of beds. The inferred processes and their manifestations suggest their development on a steep and unstable submarine slope. Thin–bedded turbidites grade into thick packages of varicolored carbonate-free mudstones, which are intensively bioturbated. These mudstones are also characterized by the presence of lenticular, thin beds of siltstones and fine–grained arenites. Bioturbation affected both the arenites and mudstones. The Bocco Shale likely originated from multiple submarine – slide events developed on an accretionary wedge slope (Figs. 4A, 4B), which was covered with thinly bedded turbidites near a lower–trench environment (Marroni and Pandolfi 2001; Meneghini et al., 2020).

OPHIOLITE AND SEDIMENTARY COVER RECORD IN THE WESTERN ALPS

Several examples of chaotic rock units composed of reworked ophiolitic material are preserved in the sedimentary cover of the Jurassic ophiolites (i.e., the Zermatt-Saas Zone, Monviso and Queyras Complexes) in the Piedmont Zone of the Western Alps (Elter, 1971; Tartarotti et al., 1998, 2017a; Dal Piaz et al., 2003; Balestro et al., 2015a; Corno et al., 2021). These ophiolites display strong deformation fabrics and variable, high to ultrahigh–pressure metamorphic overprints (i.e., eclogite- to blueschist-facies; Fig. 1). Prior to their

emplacement and during their subduction, these ophiolites were stretched and sheared but not significantly dismembered, at least locally. They were further deformed during their exhumation, although they mostly remained as coherent slices of a metamorphosed oceanic lithosphere. This exhumation-related deformation produced NW- to W-vergent folding and shearing, coeval with greenschist-facies metamorphism of all ophiolitic subunits.

The Zermatt-Saas ophiolite (Fig. 1) is a large remnant of the Jurassic oceanic lithosphere, extending for about 60 km along-strike. It was metamorphosed under eclogite- and coesite-eclogite facies conditions as a result of its subduction (e.g., Groppo et al., 2009; Frezzotti et al., 2011; Luoni et al., 2018). The Zermatt-Saas ophiolite consists of serpentinized metaperidotites (Li et al., 2004; Rebay et al., 2012; Fontana et al., 2008) with Middle to Late Jurassic metagabbros intruded into the metaperidotites (Bearth, 1967; Rubatto et al., 1998; Zanoni et al., 2016). Peridotite host rocks and their gabbroic intrusive bodies were exhumed on the seafloor as a result of amagmatic extensional tectonics during the opening of the LPOB. Ophicalcite and ultramafic breccia deposits formed during this phase, directly overlying the exhumed peridotite and gabbro bodies on the seafloor (Driesner, 1993; Tartarotti et al., 1998, 2021). The upper part of the Zermatt-Saas ophiolite includes discontinuous metabasaltic lava flows that locally show well preserved pillow structures (Bucher et al., 2005) and a thin metasedimentary cover made of Mn-rich chert, marble and calcschist (Dal Piaz and Ernst, 1978; Bearth and Schwander, 1981; Tartarotti et al., 2017b, 2021).

The Monviso ophiolite (Fig. 1), which is several–km–thick, extends for about 35 km from N to S, and tectonically overlies the Dora-Maira continental margin unit (Groppo et al., 2019; Balestro et al., 2020). Similar to the Zermatt-Saas ophiolite, it was metamorphosed under eclogite facies conditions (Lombardo et al. 1978; Schwartz et al., 2000; Groppo and

519 Castelli, 2010; Angiboust et al., 2012; Balestro et al., 2014, 2018). The Monviso ophiolite
520 contains a major shear zone (i.e., Baracun Shear Zone of Festa et al., 2015) that separates
521 massive serpentinite and metagabbro outcrops in its footwall from pillow metabasalts and
522 metasedimentary rocks within its hanging wall. This shear zone has been interpreted as a
523 fossil intraoceanic detachment fault with a Late Jurassic oceanic core complex developed in
524 its footwall (Balestro et al., 2015b). Protoliths of the serpentinite are lherzolite and
525 harzburgite, which were intruded by numerous stocks and dikes of Middle Jurassic gabbro
526 (Rubatto and Hermann, 2003) and some Late Jurassic plagiogranite (Lombardo et al., 2002).
527 Metasedimentary rocks in the cover of the Monviso ophiolite make up two different
528 sequences. The structurally and stratigraphically lower sequence rests below or is
529 intercalated with metabasaltic lava flows that display relict pillow lava structures and
530 volcanic breccia textures. This lower sedimentary sequence includes calcschist interbedded
531 with metasandstone and metabreccia units, whose clasts are gabbroic rocks (Balestro et al.,
532 2011). The upper sedimentary sequence unconformably overlies serpentinite, metagabbro,
533 metabasalt and ophiolitic metabreccias, and consists of thin metaquartzite, white marble and
534 calcschist. These rocks in the upper sequence lack any ophiolite-derived material (Balestro
535 et al., 2019).
536 The Queyras ophiolite tectonically overlies the Monviso ophiolite along an N-
537 striking fault (Fig. 1). Its subunits display blueschist-facies metamorphic overprint (e.g.,
538 Vitale Brovarone et al., 2014), the degree of which decreases structurally up-section
539 throughout the ophiolite (Lagabrielle and Polino, 1988). Similar to the Monviso ophiolite,
540 the Queyras ophiolite also includes a fossil intraoceanic detachment fault with an oceanic
541 core complex in its footwall (Lagabrielle et al., 2015). The sedimentary cover consists of
542 calcschist characterized by the occurrence of blocks of serpentinized metaperidotite,

543 metagabbro, metabasalt and mafic-ultramafic metabreccias (Tricart and Lemoine, 1991)
544 ranging in thickness from a few metres to a few km (Schistes Lustrés *Auct*.; Lemoine and
545 Tricart, 1986; Tricart and Schwartz, 2006). Larger blocks locally preserve a mantle-cover
546 succession with mantle rocks overlain by metachert, up to a few meters thick, locally
547 containing Middle Bathonian to Late Oxfordian radiolarians (Cordey et al., 2012, and
548 reference therein), and by several meters of white marble, which has been correlated with
549 the Calpionella limestone of the Northern Apennines (Principi et al., 2004). The calcschist
550 sequence includes a lower member (Replatte Formation of Lemoine 1971), mainly
551 consisting of carbonate-rich calcschist, a middle member (Roche Noire Formation of Tricart,
552 1973) composed of black micaschist, and an upper member (Gondran Flysch of Lemoine,
553 1971), consisting of alternating layers of calcschist and metasandstone. The
554 sedimentological features of the Gondran Flysch and the black shales at its base are
555 correlative with the turbiditic deposits of the Val Lavagna Group–Gottero Sandstone in the
556 Internal Ligurian Units.
557
558 **METAMORPHOSED CHAOTIC ROCK UNITS IN THE WESTERN ALPS**
559
560 Notable examples of chaotic rock units with fragments of ophiolitic material occur
561 in the metasedimentary covers of the Jurassic ophiolites in the Western Alps. These
562 ophiolites and related metasedimentary covers were deformed during two main tectono-
563 metamorphic phases (named D1 and D2), which are correlated to subduction and continental
564 collision-related tectonics, respectively. The D1 developed an early foliation (S1) coeval
565 with high-pressure metamorphism. The D2 was the main phase of folding and thrusting and
566 developed a new foliation (S2) coeval with greenschist-facies metamorphic re-equilibration.

Although these sedimentary cover units experienced alpine tectonic deformation and metamorphic recrystallization, they locally preserve lithostratigraphic and sedimentological features (Fig. 5B) that are well preserved in low – strain domains, where primary textures are deformed and overprinted by metamorphic foliation but not transposed and obscured (see also Balestro et al., 2015a; Tartarotti et al., 2017a for details). Here we discuss such rocks in the eclogite-facies (Zermatt-Saas and Monviso) and blueschist–facies (Queyras) cover rocks of the ophiolites and, we categorize them as syn-extensional chaotic deposits and syn-contractional MTDs of the Western Alps.

Syn–Extensional Chaotic Deposits

Below, we subdivide and categorize the Western Alpine metamorphosed counterparts of the Northern Apennine syn-extensional chaotic deposits. The metabreccias are divided into lower and upper ophiolitic metabreccias on the basis of their lithostratigraphic position below or above the base of basaltic lava flows, respectively.

Syn-extensional lower ophiolitic metabreccias. In both the eclogite-facies and blueschist-facies metaophiolites in the Western Alps, the structurally uppermost part of the exposed serpentinized metaperidotites contains a dense network of meters– to several tens of meters–thick carbonate–rich veins, forming metaophicarbonates (metaophicalcite *Auct.*, see OC1 of Lemoine et al., 1987) (e.g., Lagabrielle and Polino, 1985; Lemoine et al., 1987; Tricart and Lamoine, 1991; Driesner, 1993; Lagabrielle, 1994; Tartarotti et al., 1998, 2017a; Dal Piaz, 1999; Balestro et al., 2019, and reference therein). Similar to the Levanto Breccia in the Northern Apennines, the Western Alpine metaophicarbonates are characterized by a complex network of veins filled with carbonate minerals, antigorite, and/or talc (e.g.,

591 Lemoine et al., 1987; Tricart and Lemoine, 1991; Dresnier, 1993; Lafay et al., 2017;
592 Tartarotti et al., 2017a). These veins surround dm- to m-sized, angular to rounded fragments
593 of massive serpentinite. Complex crosscutting relationships between different generations of
594 carbonate veins, the infilling and episodic growth of calcite fibers, and the pervasive
595 replacement of serpentinite by carbonate minerals indicate repeated episodes of cracking–
596 fracturing of peridotites and fluid–peridotite interactions during their development. These
597 metaophicarbonate veins were the manifestations of both brittle failure and hydrothermal
598 fluid circulation within the upper mantle peridotites, as these rocks were undergoing
599 exhumation and extensional faulting in Middle to Late Jurassic time.

600 As is the case in the Northern Apennines, the top of the metaophicarbonate unit in
601 the Western Alps is extensively reworked, forming discontinuous layers of a clast-supported
602 metabreccia. For example, in the Lake Miserin area (see 3 of Fig. 1, also see Figs. 3 and 5A)
603 in the Zermatt-Saas ophiolite (see Tartarotti et al., 2017a, 2019), the metaophicarbonate is
604 overlain by a predominantly clast–supported metabreccia ("BrFm1" and "BrFm2" of
605 Tartarotti et al., 2017a). Clasts are angular- to sub-angular in shape, made of serpentinite and
606 metaophicarbonate, and range in size from cm to dm (Fig. 5C). The scarce matrix in this
607 metabreccia consists of a coarse-grained metasandstone, including serpentinite and
608 metaophicarbonate derived sediments.

609 The bottom of this clast-supported metabreccia corresponds to an erosional surface,
610 marked by a dm-thick layer of coarse- to medium-grained metasandstone composed of
611 peridotite-derived sediments. The whole metabreccia unit shows a lenticular shape at a scale
612 of hundreds of meters and a maximum thickness of about 15 m (Fig. 5A; see Tartarotti et al.,
613 2017a for details). This metabreccia gradually passes upward into a chaotic rock unit
614 ("sedimentary mélange" of Tartarotti et al., 2017a), which consists of serpentinite and

615 ophicarbonate blocks in a carbonate (now marble) matrix (see the section on Syn-extensional
616 upper ophiolitic metabreccias below). This marble is unconformably overlain by a post-
617 extensional calcschist unit (Fig. 5A), which is devoid of any ophiolite-derived material. In
618 terms of its stratigraphic–structural position above the ophiolite and its compositional
619 makeup and sedimentological characteristics, this calcschist unit correlates with the Lower
620 Cretaceous post-extensional deposits in the Northern Apennines (see Tartarotti et al., 2017a,
621 2019).

622 In the Mt. Avic ultramafic massif of the Zermatt-Saas ophiolite in the Western Alps
623 (see 2 of Fig. 1, see Fontana et al., 2008, 2015; Panseri et al., 2008), prevalently monomictic
624 clast-supported metabreccias with poorly sorted angular clasts of serpentinite are embedded
625 in a carbonate matrix (Figs. 5A, 5F; see Tartarotti et al., 1998). Locally, mm– to cm–long
626 mafic clasts derived from a gabbro source also occur, forming a polymictic-type
627 metabreccia. Structurally, these metabreccias generally occur on top of the serpentinite and
628 Mg-Al metagabbro units, and below a metabasaltic lava sequence.

629 In the Queyras ophiolite in the Western Alps, different types of poorly-sorted, clast-
630 supported metabreccia (i.e., the OC2 of Lemoine et al., 1987) range from monomictic–type
631 with cm–long, sub-angular clasts made only of serpentinite (e.g., Pic Cascavelier section,
632 see Tricart and Lemoine, 1983, 1991; Caby et al., 1987; Lemoine and Tricart, 1986) or
633 metagabbro (e.g., Crete Mouloun section, Le Mer et al., 1986), to polymictic–type
634 metabreccia (see 6, 7 and 8 of Figs. 1 and 5I, 5G) with clasts of both serpentinite and
635 metagabbro (see Le Mer et al., 1986; Lemoine et al., 1987; Balestro et al., 2019, and
636 reference therein). These metabreccias are laterally discontinuous in exposure and range
637 from a few cm to several tens of meters in thickness. Large blocks (olistoliths), up to tens of
638 meters wide, locally occur (Tricart and Lemoine, 1983) in a sandy matrix with grains of

639 mixed mafic rock and carbonate composition. The structural position of both monomictic
640 and polymictic metabreccias (Fig. 5I) is commonly above the exhumed serpentinite and
641 metagabbro and below the metabasaltic lava sequence (metapillow lavas and basaltic
642 metabreccias).

643 In the Monviso ophiolite in the Western Alps (see 5 of Fig. 1), a sedimentary
644 sequence, consisting of calcschist interbedded with mafic metasandstone and matrix-
645 supported metabreccia layers, onlaps a fossil detachment fault and its footwall units (Fig.
646 6A). The footwall of this detachment fault zone is made of serpentinized metaperidotites,
647 intruded by Mg-Al and Fe-Ti gabbro plutons and stocks. The mafic–ultramafic part of the
648 Monviso ophiolite has been interpreted as an exhumed oceanic core complex (OCC; see
649 Balestro et al., 2015a, 2019; Festa et al., 2015). The matrix-supported metabreccia includes
650 poorly sorted sub-angular to angular clasts of metagabbro (Figs. 6B-D) and laterally grades,
651 at a scale of tens of meters, into coarse-grained metasandstone of the same composition,
652 locally with a fining-upward texture (Fig. 6E). The thickness of these syn-extensional
653 metasedimentary rocks shows significant lateral variations, ranging from several centimeters
654 to about 70 meters, and generally tapers out toward an association of talcschist and
655 serpentine–schist containing blocks of highly sheared metagabbro. These intensely foliated
656 talcschist and serpentine–schist units correspond to an intra-oceanic detachment fault zone
657 (i.e., the Baracun Shear Zone of Festa et al., 2015). The shear zone is unconformably overlain
658 by post-extensional white marble and carbonate-rich calcschist (Fig. 6A), devoid of any
659 ophiolite-derived material. The white marble and calcschist correspond to the Upper
660 Jurassic-Lower Cretaceous Calpionella Limestone and the Early Cretaceous Palombini
661 Shale of the Internal Ligurian Units in the Northern Apennines, respectively (see Balestro et
662 al., 2015a, 2019; Festa et al., 2015).

Syn-extensional upper ophiolitic metabreccias. The most notable examples of monomictic basaltic metabreccia and polymictic-metabreccia, correlating lithologically and stratigraphically with the upper ophiolitic breccias in the Northern Apennines, are best preserved in the Queyras ophiolite (e.g., Caby et al., 1971, 1987; Tricart and Lemoine, 1983, 1991; Le Mer et al., 1986; Saby, 1986; Pinet et al., 1989). The metabreccias in the Queyras ophiolite are stratigraphically situated between the base of the pillow metabasalt sequence and the first post-extensional sedimentary units (i.e., metachert and white marble; see Fig. 5I).

The monomictic metabreccia consists only of angular to sub-angular clasts, up to 30 cm–long, of metabasalt that are embedded within a sandy matrix composed of fragments of metabasalt and/or metahyaloclastite (see, e.g., the Crete Mouloun and Pic Marcel sections in Le Mer et al., 1986 and Tricart and Lemoine, 1983, respectively. See 6 and 7 of Fig. 1). Although this monomictic metabreccia commonly overlies the metabasaltic pillow lava sequence (e.g, Crete Mouloun), it locally occurs both at the base of (e.g., Pic Marcel) and/or interfingered with these metabasaltic lava flows (e.g., Tricart and Lemoine, 1983).

Polymictic metabreccia with cm- to dm-long clasts of massive and variolitic metabasaltic lavas, metagabbro, and quartzo-feldspathic rocks (plagiogranite) occur both at the base (e.g., Pic Marcel, see Tricart and Lemoine, 1983) and at the top (e.g., Crete Mouloun, see Le Mer et al., 1986) of the metamorphosed pillow lava sequence. The matrix of this metabreccia is sandstone, which is composed of fragments of the same compositions as the clasts.

All these different types of metabreccias have a poorly sorted, clast-supported texture with angular to sub-angular clasts. Stratigraphically upward, they grade into a matrix-

687 supported metabreccia and coarse-grained metasandstone with well–preserved incipient
688 layers of different compositions (see also Tricart and Lemoine, 1983). The bottoms of these
689 metabreccia layers are commonly lenticular and erosional.

690 The occurrence of metabreccias in a stratigraphic position comparable to the one of
691 the upper ophiolitic metabreccias of the Appennines is rare in the Monviso and Zermatt Saas
692 ophiolites in the Western Alps. There are, however, two examples of possible upper
693 ophiolitic metabreccias in the Zermatt-Saas ophiolite. The first one is part of the Garten
694 Formation (i.e., the Rifelberg-Garten mélange or Palon de Resey mélange; see Dal Piaz,
695 1965, 1992; 2004; Bearth, 1967; Dal Piaz and Ernst, 1978; Campari et al., 2004; Dal Piaz et
696 al., 2015; Gusmeo et al., 2018), which crops out discontinuously from the Cime Bianche
697 ridge to the highest Ayas Valley (see 1 of Fig. 1; see Dal Piaz, 1992; Dal Piaz et al., 2015
698 for details). The Garten Formation consists of a chaotic rock unit, meters– to tens of meters–
699 thick, with rounded to elongated clasts (cm to dm in size) of fine-grained metabasalt
700 (metamorphosed to eclogite and glaucophanite), serpentinite and marble (Gusmeo et al.,
701 2018), embedded in a matrix of alternating layers of micaschist and calcschist (Figs. 6F-H).
702 This formation represents the superposition of different individual deposits, each a few
703 decimeters to nearly one meter in thickness (Fig. 6F). The largest clasts occur in the lower
704 part of the beds and "float" in a fully mixed and crudely graded matrix, made of calcschist
705 (Figs. 6G, 6H). The stratigraphic position of this formation is at the base of metabasaltic lava
706 flows with locally well – preserved pillow structures (Fig. 6I; see Dal Piaz, 1965, 2004). It
707 is, however, important not to confuse the above-described chaotic deposit with the larger
708 part of the Garten Formation that corresponds to a typical "broken formation" (*sensu* Hsü,
709 1968), resulting from layer-parallel tectonic extension of alternating micaschist and
710 metabasite layers and boudinage formation.

In the Lake Miserin sedimentary cover sequence of the Zermatt-Saas ophiolite (Fig. 1), the lower ophiolitic metabreccia is overlain by a chaotic rock unit characterized by a block-in-matrix fabric with rounded to irregular–shaped blocks (dm- to a meter-wide) of massive to veined serpentinite and metaophicarbonate embedded in a white marble matrix (Figs. 5A, 5E). Blocks are randomly distributed within the matrix, except where elongated and deformed blocks are aligned with the regional tectonic foliation (Tartarotti et al., 2019). The matrix is commonly interbedded with cm- to dm-thick layers of metabreccia, with clasts angular to sub-angular clasts of serpentinite (Fig. 5E).

Syn-contractional mass–transport deposits (MTDs)

The identification of possible counterparts of the syn-contractional mass–transport deposits of the Northern Apennines in the metasedimentary cover of the ophiolites in the Western Alps is not easy. The gravity-induced MTDs, composed of material derived from both a continental margin and the ophiolites, are lacking in the Zermatt-Saas and Monviso ophiolites, but they occur in the Lago Nero Unit of the Queyras ophiolite (see 4 of Fig. 1). The Lago Nero Unit includes a thick metasedimentary sequence, starting at the bottom with a radiolarite member, topped by a limestone member and the Replatte Formation (Lemoine et al., 1970; Polino, 1984; Barfety et al., 1995; Burroni et al., 2003). The Replatte Formation contains alternating layers of thick calcschist and thin marble. It grades stratigraphically upwards into both a thin unit of grey to black schists and to the Gondran Flysch, composed of alternating layers of calcschist and metasandstone (Fig. 5I). The Gondran Flysch represents thinly bedded turbidites with minor occurrences of thick and coarse–grained, terrigenous metasandstone. Petrographic analysis of the terrigenous metasandstone indicates an arkosic composition, made predominantly of quartz, feldspar and minor lithic fragments.

735 The metasedimentary cover sequence of the Lago Nero Unit stratigraphically is capped by
736 the Rocher Renard Complex (Fig. 5I; Barfety et al., 1995; Burroni et al., 2003). The Rocher
737 Renard Complex consists of homogeneous dark schists, locally containing metre- to
738 decametre-size blocks composed mainly of limestone and chert, with local occurrences of
739 metabasalt, metaophicalcite, serpentinite and metagabbro (Figs. 5H, 5I).
740
741 **DISCUSSION: THE CHAOTIC DEPOSITS AND MTDs OF THE NORTHERN**
742 **APENNINES AS A PROXY FOR METAMORPHOSED COUNTERPARTS IN THE**
743 **WESTERN ALPS**
744
745 Our detailed description of chaotic rock units and MTDs indicates that different
746 ophiolite units in the Northern Apennines and the Western Alps correlate well, both
747 chronologically and stratigraphically (Table 1). These correlations suggest that the
748 diagnostic features of the chaotic deposits and MTDs in the Internal Ligurian Units can be
749 used as a proxy for better definition of the tectonostratigraphy of their highly deformed and
750 metamorphosed counterparts in the Western Alps. The strong similarities between these
751 chaotic deposits and MTDs within the epi–ophiolitic sequences in both orogenic belts, allows
752 reconstructing: (i) the pre-orogenic primary lithostratigraphy and sedimentological features
753 of the Western Alpine occurrences, (ii) the processes and mechansims of Western Alpine
754 rock formation and, (iii) the characteristics of the depositional or geodynamic settings of
755 rock body origins. Our findings also indicate that the LPOB lithosphere underwent similar
756 tectonic processes during the Jurassic seafloor spreading and Late Cretaceous – Early
757 Paleocene closure phases of the ocean basin throughout its entire length (Fig. 7).
758

Processes of formation of chaotic deposits and MTDs in the Western Alps from seafloor spreading to subduction

Although they experienced severe tectonic deformation and metamorphic recrystallization, the described examples of chaotic rock units in the Western Alps locally preserve lithostratigraphic and sedimentological features (see also Balestro et al., 2015a; Tartarotti et al., 2017a for details) that are comparable with those of the little metamorphosed Internal Ligurian Units in the Northern Apennines. The oldest syn-extensional chaotic deposits (the lower ophiolitic metabreccias) of the Western Alps preserve remnants of sedimentological features and internal organization that are diagnostic of different products formed by the downcurrent transformation of cohesive flows through progressive mixing with ambient fluids (F2 facies of Mutti, 1992). In different sections of the Queyras (see Pic Cascavelier and Crete Mouloun) and Zermatt-Saas (see Lake Miserin and Mt. Avic) ophiolites, the faint internal structure of the clast-supported breccia, such as the lack of a well-defined grading, the scarcity of lamination, and the absence of any pelagic interbeds, suggest rapid deposition through cohesive debris flows or hyperconcentrated flows. In these processes, the larger clasts float in a mixed and crudely graded matrix, which was probably composed of mud and mafic and/or ultramafic sand and gravel, with largest clasts occurring in the lower part of the bed. In some cases, such as for the lower ophiolitic metabreccia unit in the Monviso ophiolite, the occurrence of a poorly sorted, coarse-grained sandstone, grading laterally into a coarse-grained sandstone with a fining-upward texture, suggests that these deposits represent the products of downslope transformation of a hyperconcentrated flow into a high-density and supercritical turbidity current, and locally a low-density one, possibly corresponding to a gravity transformation from F4-F5 to F7 facies of Mutti (1992).

782 The characteristics of the matrix-supported metabreccia and coarse-grained
783 metasandstone of the youngest syn-extensional upper ophiolitic metabreccias of Pic Marcel
784 and Crete Mouloun in the Queyras suggest that they represent the products of
785 hyperconcentrated flows. These products result from downslope transformation of cohesive-
786 flow (F2 and F3 facies of Mutti, 1992), which changes laterally and upward into gravelly,
787 high-to low-density turbidity currents (F4-F5 and F7 facies of Mutti, 1992). This is similar
788 to the examples interpreted for the Monviso ophiolite.

789 Our documented sedimentological features of part of the Garten Formation and of
790 the upper ophiolitic metabreccias of the Lake Miserin in the Zermatt-Saas ophiolites confirm
791 that they represent the products of submarine mass transport processes, as suggested by
792 Bearth (1963) and Dal Piaz (1965), and by Tartarotti et al (2017a, 2019), respectively. We
793 have observed that the sedimentary fabric elements of these metabreccias are consistent with
794 the deposition from either hyperconcentrated flows (F2 of Mutti et al.,1992) or generally
795 high–density turbidity currents (F4-F5 of Mutti et al., 1992) that resulted from downslope
796 transformation of closure flows through progressive mixing with ambient fluids.

797 The sedimentological features of the syn-contractional MTD of the Lago Nero Unit
798 (i.e., the Rocher Renard Complex) in the Western Alps (i.e., prevailing shaly matrix and the
799 occurrence of angular blocks of ophiolitic material and sedimentary rocks) and its
800 stratigraphic position correlate well with the Bocco Shale in the Northern Apennines (Table
801 1; Burroni et al., 2003). Similarly, its sedimentological features fit well with those of the
802 product of multiple submarine cohesive debris flows evolving down-current to
803 hyperconcentrated turbidity deposits that were emplaced on an accretionary wedge slope.
804

Comparison between chaotic deposits and MTDs in the Northern Apennines and the Western Alps

The documented similarities of the sedimentological features and internal organization of the syn-extensional chaotic deposits in both the orogenic belts is consistent with their formation through deposition of small volumes of poorly consolidated material accumulated in the hanging walls of submarine normal faults and fault escarpments. These deposits formed above detachment faults and oceanic core complexes (Fig. 7A) during the Jurassic seafloor spreading (e.g., Tricart and Lemoine, 1983, 1991; Caby et al., 1987; Lemoine and Tricart, 1986; Dilek and Eddy, 1992; Tartarotti et al., 1998, 2017a; Dilek and Thy, 1998; Principi et al., 2004; Lagabrielle, 2009; Balestro et al., 2015a, 2019 and reference therein). The occurrence of these deposits in two different specific tectonostratigraphic positions (below or above the basaltic pillow lava flows; Figs. 3, 5, 6) in both the Northern Apennines and the Western Alps, suggests that their formation occurred in two distinct events of extensional tectonics during a continuum of syn-spreading deformation. Moreover, the chaotic deposits in the different sectors of the Jurassic LPOB (i.e., Western Alps and Northern Apennine) show the same features and the same lithological composition of clasts (Table 1), strongly indicating that the oceanic basin developed with the same features and in a similar basin floor architecture during its entire history and along its entire length (Fig. 7a). It is, however, necessary to use caution in the attempt to correlate the chaotic deposits related to syn-spreading extensional tectonics, and to discriminate between the lower and upper ophiolitic metabreccias in the metamorphosed Western Alps. This is because their correlation is hampered where the oceanic crust stratigraphy is incomplete such that extrusive rocks are missing, or when a diagnostic clast composition is not recognizable within gravitationally induced chaotic deposits.

829 Independent of the type of breccia (lower or upper), the composition of clasts depends
830 on the nature of the source area and its location with respect to the site of deposition. In these
831 cases, our findings show that the diagnostic sedimentological features of the non- to poorly
832 metamorphosed syn-extensional ophiolitic breccias of the Northern Apennines may
833 represent a proxy of comparison, providing useful constraints for the interpretation of the
834 metamorphosed Alpine breccias. For example, although basalt flows are not observed and
835 basalt clasts are lacking, the upper ophiolitic metabreccias of the Lake Miserin (i.e., the
836 "Sedimentary mélange" of Tartatotti et al., 2017a) are comparable with the syn-extensional
837 upper ophiolitic Monte Bianco breccias of the Northern Apennines, whose stratigraphic
838 position is well defined. They show the same sedimentological features and composition of
839 both clasts and the matrix (see Table 1). This correlation is further supported by field-
840 evidence, showing that the Lake Miserin upper breccia is deposited above the lower
841 ophiolitic metabreccia of the same sequence and it is covered by mixed siliciclastic-
842 carbonaceous sediments, corresponding to the Lower Cretaceous post-spreading deposits in
843 the Northern Apennines (see Tartarotti et al., 2017a for details). Therefore, although caution
844 is necessary in interpreting chaotic deposits in the highly deformed and metamorphosed
845 Western Alpine units, the use of the Northern Apennines examples may represent a useful
846 proxy for better interpretation of their metamorphosed counterparts, which were deposited
847 during the Jurassic syn-spreading tectonics of the LPOB.

848 The syn-contractional MTDs with ophiolitic material that are widespread in the
849 Internal Ligurian Units of the Northern Apennines have been also identified in the Western
850 Alps, as detected in the Lago Nero Unit of the Queyras ophiolite. In both orogenic belts, the
851 sedimentological features and internal organization of these deposits suggest they originated
852 by several events of tectonic erosion at the front of the accretionary wedge (Fig. 7b), which

853 developed in the Late Cretaceous in response to the development of an east-dipping
854 subduction of the LPOB lithosphere close to or within the thinned Adria margin (Marroni et
855 al., 2017 and reference therein). These events of frontal tectonic erosion were induced by
856 underthrusting of the seafloor morphological relief inherited from the previous Jurassic syn-
857 spreading tectonics (Fig. 7b; Marroni and Pandolfi, 2001; Burroni et al., 2003; Meneghini et
858 al., 2020). The subduction of morphological relief commonly produces the uplift of the lower
859 slope of the frontal wedge, its collapse and the subsequent downslope mobility of wide
860 MTDs and their emplacement in the lower plate and/or in the trench (Fig. 7b; e.g., von Huene
861 and Lallemand, 1990; von Huene et al., 2004; Kawamura et al., 2009; Remitti et al., 2011;
862 Festa et al., 2018; Geersen et al., 2020; Meneghini et al., 2020; Ogata et al., 2020).

863 During the Late Cretaceous – Early Paleocene convergent stage of the LPOB, these
864 ophiolitic MTDs, mainly consisting of pebbly mudstones and slides (Lamarche et al. 2008;
865 Festa et al. 2016), interfingered with thin bedded, siliciclastic turbidites supplied by the
866 European continental margin, as was the case in the Rocher Renard Complex in the Lago
867 Nero Unit (Queyras ophiolite; see also Burroni et al., 2003) and the Bocco Shale in the
868 Northern Apennines (see also Marroni and Pandolfi, 2001; Meneghini et al., 2020).
869 Therefore, syn-contractional MTDs in both transects of the convergence system can be
870 regarded as formed by similar processes widespread along the entire width of the oceanic
871 basin. In the Western Alps, however, the occurrence of syn-contractional MTDs are
872 restricted to the units subducted at moderate depths (i.e., those affected by blueschist-facies
873 P-T metamorphic peak), and they are not observed in the deeper eclogite-facies units. It is
874 hard to discriminate whether the absence of these deposits in higher grade units is simply
875 due to failure to recognize them in the field, if these deposits were not preserved, or they did
876 not form at all. An explanation for the occurrence of syn-contractional MTDs only in the

units accreted at shallow to moderate depths could be that frontal tectonic erosion was active in a restricted time span, probably in the Late Maastrichtian-Early Paleocene, when most of the eclogite facies units were already underthrust at depth in the subduction zone. On the other hand, underplating at shallow to moderate depths, especially in sediment-dominated systems, generally involves preferential removal of the sedimentary cover from the upper part of an oceanic lithosphere (Meneghini et al., 2009 and reference therein). This phenomenon occurs when the downgoing plate reaches a depth consistent with the development of eclogite-facies metamorphism (Moore and Sample, 1986). In this framework, the lack of syn-contractional ophiolitic MTDs in the eclogite-facies units of the Western Alps could be also explained by selective removal of these deposits during progressive subduction underthrusting.

CONCLUDING REMARKS

In this comparative analysis, we have examined the occurrence and the internal structure of different types of chaotic rock units with ophiolitic material in the Internal Ligurian Units of the Northern Apennines and in the Piedmont Zone of the Western Alps. Our findings document that the internal structure-stratigraphy and sedimentological characteristics of the chaotic deposits and MTDs in the Northern Apennines can be used as a proxy to identify the nature and processes of formation of their highly deformed and metamorphosed counterparts in the Western Alps. The chaotic deposits and MTDs in the Western Alps are commonly confused with tectonically produced rocks asemblages and tectonic mélanges. We have shown in this study that the MTDs in the Western Alps consist of two different types of chaotic deposits of gravitational origin, formed by different

submarine mechanisms, and that they occur in different tectonostratigraphic positions within the epi-ophiolitic sedimentary cover. The oldest chaotic deposits occur both below and above the extrusive sequences in the ophiolites, representing syn-extensional, hyper-concentrated deposits associated with the seafloor spreading evolution of the LPOB lithosphere during the Middle-Late Jurassic. The youngest chaotic deposits consist of MTDs, which occur as intercalations within turbiditic sequences above the ophiolites, representing syn–contractional submarine slides. The slides occurred on frontal accretionary prism slopes during the Late Cretaceous–Paleocene closure of the LPOB.

This comparative study provides important clues for the contextual framework of the definition of magmatic, tectonic, and sedimentary processes, which occurred throughout the formation of the Jurassic oceanic lithosphere and its sedimentary cover in the LPOB (Western Tethys), and during the subsequent Late Cretaceous–Paleocene convergent margin tectonics. These processes were remarkably uniform and synchronous as shown by the occurrence of comparable chaotic deposits and MTDs characterized by the same features and the same lithological compositions of clasts. Our data and observations indicate that the LPOB developed with the same features and in a similar basin floor architecture during its entire history and along its entire length.

The results and the geological implications of this comparative study are not limited only to the Western Alpine orogenic belt. The diagnostic features of the different types of chaotic rock units described in this study can also help in distinguishing among those similar units that extensively occur in many Precambrian to Cenozoic orogenic belts, where the overprint of tectonic and metamorphic processes obscured their primary features and the modes of formation. Their detailed lithological, structural and chronological correlations along and across the orogenic belts should provide additional constraints for reconstruction

925 of the magmatic, tectonic and sedimentary evolution of ocean basins, and for the subsequent
926 convergent margin evolution. Therefore, detailed, multidisciplinary studies of chaotic rock
927 units are an integral part of systematic investigations of the temporal evolution of different
928 stages of orogenic buildup, from continental rifting and seafloor spreading to subduction,
929 and crustal exhumation. Such studies and their results have contributed significantly to
930 further refining the plate tectonics paradigm since the mid-1960s.
931

932 **ACKNOWLEDGEMENTS**

933 We extend our sincere thanks to the two anonymous reviewers for their constructive and thorough
934 reviews, from which we have benefited greatly in revising our manuscript. The project was
935 supported by the University of Pisa (PRA project and ATENEO grant), the University of Torino
936 (Ricerca Lolcale ex 60% 2017-2020, grants to GB and AF), and by the Italian Ministry of
937 University and Research ("Finanziamento annuale individuale delle attività base di ricerca 2017",
938 grants to GB and AF). Grants to PT (PSR2018_DZANONI) were provided by the University of
939 Milan. Y Dilek acknowledges the Miami University research funds for his fieldwork in the
940 Western Alps. F. Meneghini and M. Marroni would like to dedicate this contribution to the
941 beloving memory of Casey Moore, former supervisor of F. Meneghini, for his fundamental
942 contribution to the understanding and definition of many aspects of plate tectonics concerning the
943 dynamics of convergent margins, and the processes shaping the accretionary prisms.
944

945 **REFERENCES CITED**

946

947 Abbate, E., and Sagri, M. 1982. Le unità torbiditiche cretaciche dell'Appennino
948 Settentrionale ed i margini continentali della Tetide. Mem. Soc. Geol. It. 24: 115-
949 126.

950 Abbate, E., Bortolotti, V., and Passerini, P. 1970. Olistostromes and olistoliths. Sed. Geol.
951 4: 521-557.

952 Abbate, E., Bortolotti, V., Passerini, P., Principi, G. and Treves, B. 1994. Oceanisation
953 processes and sedimentary evolution of the northern Apennine ophiolite suite: a
954 discussion. Mem. Soc. Geol. It. 48: 117-136.

955 Abbate, E., Bortolotti V., and Principi, G. (1980), Apennine ophiolites: a peculiar oceanic
956 crust. *In* G. Rocci ed. Special issue on Tethyan ophiolites, Western area. Ofioliti
957 5: 59-96.

958 Angiboust, S., Langdon, R., Agard, P., Waters, D., and Chopin, C. 2012. Eclogitization of
959 the Monviso ophiolite (W. Alps) and implications on subduction dynamics. J.
960 Metamorph. Geol. 30: 37-61.

961 Anonymous 1972. Penrose fi eld conference on ophiolites. Geotimes 17: 24-25

962 Balestro, G, Festa, A., Borghi, A., Castelli, D., Gattiglio, M. and Tartarotti, P. 2018. Role of
963 Late Jurassic intra-oceanic structural inheritance in the Alpine tectonic evolution
964 of the Monviso meta-ophiolite Complex (Western Alps). Geol. Mag. 155: 233-
965 249.

966 Balestro, G., Festa, A., and Tartarotti, P. 2015a. Tectonic significance of different block-in
967 matrix structures in exhumed converget plate margins: examples from oceanic

968 and continental HP rocks in Inner Western Alps (northwest Italy). Int. Geol. Rev.
969 57: 581-605.
970 Balestro, G., Festa, A., Dilek, Y. and Tartarotti, P. 2015b. Pre-Alpine extensional tectonics
971 of a peridotite-localized oceanic core complex in the late Jurassic, high-pressure
972 Monviso ophiolite (Western Alps). Episodes 38: 266-282.
973 Balestro, G., Festa, A., and Dilek, Y. 2019. Structural architecture of the Western Alpine
974 Ophiolites, and the Jurassic seafloor spreading tectonics of the Alpine Tethys. J.
975 Geol. Soc. 176: 913-930.
976 Balestro, G., Fioraso, G. and Lombardo, B. 2011. Geological map of the upper Pellice Valley
977 (Italian Western Alps). J. Maps 2011: 634-654.
978 Balestro, G., Lombardo, B., Vaggelli, G., Borghi, A., Festa, A. and Gattiglio, M. 2014.
979 Tectonostratigraphy of the northern Monviso meta-ophiolite complex (Western
980 Alps). It. J. Geosci. 133: 409-426.
981 Balestro, G., Nosenzo, F., Cadoppi, P., Fioraso, G., Groppo, C. and Festa, A. 2020. Geology
982 of the southern Dora-Maira Massif: insights from a sector with mixed ophiolitic
983 and continental rocks (Valmala Tectonic Unit, Western Alps). J. Maps 16 (2):
984 736-744.
985 Barbero, E., Festa, A., Saccani, E., Catanzariti, R., and D'Onofrio, R. 2020. Redefinition of
986 the Ligurian Units at the Alps-Apennines junction (NW Italy) and their role in
987 the evolution of the Ligurian accretionary wedge: constraints from mélanges and
988 broken formations. J. Geol. Soc. 177: 562-574.
989 Barbero, E., Pandolfi, L., Morteza, D., Dolati, A., Saccani, E., Catanzariti, R., Luciani, V.,
990 Chiari, M. and Marroni, M. 2021. The western Durkan Complex (Makran
991 Accretionary Prism): A Late Cretaceous tectonically disrupted seamounts chain

and its role in controlling deformation style. Geosci. Front. 12 (3): 101106. https://doi.org/10.1016/j.gsf.2020.12.001

Barféty, J.C., Lemoine, M., De Graciansky, P.C., Tricart, P. and Mercier, D., 1995. Carte géologique de la France a 1/50000, Feuille 823 Briançon.

Bearth, P. 1963. Contribution à la subdivision tectonique et stratigraphique du cristallin de la nappe du Grand Saint-Bernard dans le Valais. Geol. Soc. Fr. Mem. H. 2: 407-418.

Bearth, P. 1967. Die Ophiolithe der Zone von Zermatt-Saas Fee. Beiträge zur Geologischen Karte der Schweiz, Neue Folge, 132: 1-130.

Bearth, P. and Schwander, H. 1981. The post-Triassic sediments of the ophiolite zone Zermatt-Saas Fee and the associated manganese mineralizations. Eclogae Geol. Helv. 74: 198-205.

Beltrando, M., Manatschal, G., Mohn, G., Dal Piaz, G.V., Vitale Brovarone, A. and Masini, E. 2014. Recognizing remnants of magma-poor rifted margins in high-pressure orogenic belts: The Alpine case study. Earth Sci. Rev. 131: 88–115.

Berkland, J.O., Raymond, L.A., Kramer, J.C., Moores, E.M., and O'Day, M. 1972. What is Franciscan? AAPG Bulletin 56: 2295–2302.

Berra, F. and L. Angiolini, 2014, The evolution of the Tethys region throughout the Phanerozoic: A brief tectonic reconstruction, In Marlow L., Kendall C. and Yose L. eds. Petroleum systems of the Tethyan region. Mem. Am. Assoc. Pet. Geol. 106: 1-27.

Bettelli, G. and Panini, F. 1985. Il mélange sedimentario della Val Tiepido (Appennino modenese) — composizione litologica, distribuzione areale e posizione stratigrafica. Atti Soc. Nat. Mat. Modena 115: 91–106.

1016 Bettelli, G., Conti, S., Panini, F., Vannucchi, P., Fioroni, C., Fregni, P., Bonacci, M.,
1017 Gibellini, R. and Mondani, C. 2004. The mapping of chaotic rocks in Abruzzo
1018 (Central Italy): comparison with selected examples from Northern Apennines, In
1019 Pasquarè, G., Venturini, C. and Groppelli, G., eds., Mapping Geology in Italy.
1020 APAT – SELCA, Firenze: 199–206.
1021 Bill, M., L. O'Dogherty, J. Guex, P.O. Baumgartner, and Masson, H. 2001. Radiolarite ages
1022 in Alpine-Mediterranean ophiolites: Constraints on the oceanic spreading and
1023 the Tethys-Atlantic connection. Geol. Soc. Am. Bull. 113: 129-143.
1024 Bortolotti, V., and Principi, G. 2003. The Bargonasco-Upper Val Graveglia ophiolitic
1025 succession, Northern Apennines, Italy. Ofioliti 28: 137-140.
1026 Bucher, K., Fazis, Y., De Capitani, C. and Grapes, R. 2005. Blueschists, eclogites, and
1027 decompression assemblages of the Zermatt-Saas ophiolite: high-pressure
1028 metamorphism of subducted Tethys lithosphere. Am. Mineral. 90: 821-835.
1029 Burroni, A., Levi, N., Marroni, M. and Pandolfi, L. 2003. Lithostratigraphy and structure of
1030 the Lago nero Unit (Chenaillet Massif, Western Alps): comparison with Internal
1031 Liguride Units of Northern Apennines. Ofioliti 28: 1-11.
1032 Butler, J. P., Beaumont, C., and Jamieson, R. A. 2013. The Alps 1: A working geodynamic
1033 model for burial and exhumation of (ultra) high-pressure rocks in Alpine-type
1034 orogens. Earth Planet. Sci. Lett. 377: 114-131.
1035 Caby, R., Dupuy, C., and Dostal, J. 1987. The very beginning of the Ligurian Tethys:
1036 Petrological and geochemical evidence from the oldest ultramafite-derived
1037 sediments in Queyras, Western Alps (France). Eclogae geol. Helv. 80: 223 240.

1038 Caby, R., Michard, A. and Tricart, P. 1971. Découverte d'une brèche polygénique à éléments
1039 de granitoïdes dans les ophiolites métamorphiques piemontaises (schistes lustrés
1040 du Queyras, Alpes françaises). C.R. Acad. Sci. Paris 273: 999-1002.
1041 Campari, E., Portera, F., Tartarotti, P., and Spalla, M.I. 2004. The Rifelberg-Garten unit in
1042 the eclogitic ophiolites of the Upper Valtournanche (Piedmont Zone,
1043 Northwestern Italian Alps). 32nd IGC, Florence, Italy, August 20-28, 2004, p.
1044 294.
1045 Cannat, M. 1996. How thick is the magmatic crust at slow spreading oceanic ridges? J.
1046 Geophys. Res. Solid Earth 101(B2): 2847-2857.
1047 Cannat, M., Lagabrielle, Y., Bougault, H., Casey, J., de Coutures, N., Dmitriev, L., and
1048 Fouquet, Y. 1997. Ultramafic and gabbroic exposures at the Mid-Atlantic Ridge:
1049 Geological mapping in the 15 N region. Tectonophysics 279: 193-213.
1050 Capitanio, F. A., and Goes, S. 2006. Mesozoic spreading kinematics: consequences for
1051 Cenozoic Central and Western Mediterranean subduction. Geophys. J. Int. 165:
1052 804-816.
1053 Chiari, M., Marcucci, M., and Principi, G. 2000. The age of the radiolarian cherts associated
1054 with the ophiolites in the Apennines (Italy) and Corsica (France): a revision.
1055 Ofioliti, 25: 141-146.
1056 Cliff, R.A., Barnicoat, A.C. and Inger, S. 1998. Early Tertiary eclogite facies metamorphism
1057 in the Monviso Ophiolite. J. Metamorph. Geol. 16: 447-455.
1058 Cordey, F., Tricart, P., Guillot, S., and Schwartz, S. 2012. Dating the Tethyan Ocean in the
1059 Western Alps with radiolarite pebbles from synorogenic Oligocene molasse
1060 basins (southeast France). Swiss J. Geosci. 105: 39-48.

1061 Corno, A., Mosca, P., Borghi, S., and Gattiglio, M. 2021. Geology of the Monte Banchetta
1062 – Punta Rognosa area (Troncea valley, Western Alps). J. Maps. 17 (2): 150-160.
1063 Cortesogno, L., Galbiati, B., and Principi, G. 1987. Note alla "Carta geologica delle ofioliti
1064 del Bracco" e ricostruzione della paleogeografia Giurassico-Cretacica. Ofioliti,
1065 12: 261-342.
1066 Costa, J.E., 1988. Rheologic, geomorphic, and sedimentologic differentiation of water
1067 floods, hyperconcentrated flows, and debris flows, *In* Baker, V. R., Kochel, R.C.,
1068 and Patton, P.C. eds. Flood Geomorphology. Wiley, New York, pp. 113-122.
1069 Cowan, D.S. 1985. Structural styles in Mesozoic and Cenozoic mélanges in the western
1070 Cordillera of North America. Geol.l Soc. Am. Bull. 96: 451–462.
1071 Crispini, L., and Capponi, G. 2001, Tectonic evolution of the Voltri Group and Sestri
1072 Voltaggio Zone (southern limit of the NW Alps): a review. Ofioliti 26: 161-164.
1073 Dal Piaz, G.V. 1965. La formazione mesozoica dei calcescisti con pietre verdi fra la Valsesia
1074 e la Valtournanche ed i suoi rapporti con il ricoprimento Monte Rosa e con la
1075 Zona Sesia-Lanzo. Boll. Soc. Geol. It. 84: 67-104.
1076 Dal Piaz, G.V., 1992, Guida geologica: Le Alpi dal Monte Bianco al Lago Maggiore, Vol.
1077 3: BeMa Editrice, Milano, 311 pp.
1078 Dal Piaz, G.V. 1999. The Austroalpine–Piedmont nappe stack and the puzzle of Alpine
1079 Tethys. Mem. Sci. Geol. Padova 51: 155–176.
1080 Dal Piaz, G.V., 2004. From the European continental margin to the Mesozoic Tethyan ocean:
1081 a geological map of the upper Ayas valley (Western Alps). *In* Pasquarè, G. and
1082 Venturini, C. Eds. Mapping Geology in Italy. Mapping Geology in Italy. APAT
1083 – SELCA, Florence, pp. 265-272.

1084 Dal Piaz, G., Bistacchi, A., Gianotti, F., Monopoli, B., Passeri, L., Schiavo, A., et al. 2015.
1085 Carta Geologica d'Italia - Foglio 070 Monte Cervino. Servizio Geologico
1086 d'Italia, 219 pp.
1087 Dal Piaz, G.V., Bistacchi, A. and Massironi, M. 2003. Geological outline of the Alps.
1088 Episodes 26: 175-180.
1089 Dal Piaz, G.V., and Ernst, W.G. 1978. Areal geology and petrology of eclogites and
1090 associated metabasites of the Piemonte Ophiolite Nappe, Breuil-St. Jacques area,
1091 Italian Western Alps. Tectonophysics 51: 99-126.
1092 Decandia, F.A. and Elter, P. 1972. La zona ofiolitifera del Bracco nel settore compreso tra
1093 Levanto e la Val Graveglia (Appennino Ligure). Mem. Soc. Geol. It. 11: 503-
1094 530.
1095 Dercourt, J., Gaetani, M., Vrielynck, B., Barrier, E., Biju-Duval, B., Brunet, M.F., Cadet,
1096 J.P., Crasquin, S., and Sandulescu, M. 2000. Atlas PeriTethys,
1097 Palaeogeographical maps, 24 maps and explanatory notes I-XX.
1098 CCGM/CGMW, Paris, 1-269.
1099 Dilek, Y. 2006. Collision tectonics of the Eastern Mediterranean region: Causes and consequences.
1100 Geological Society of America Special Paper 409, 1-13. doi:
1101 10.1130/2006.2409(1).
1102 Dilek, Y., and Eddy, C.A. 1992. The Troodos (Cyprus) and Kizildag (S. Turkey) ophiolites
1103 as structural models for slow-spreading ridge segments. Journal of Geology, 100,
1104 p. 305-322.
1105 Dilek, Y., Thy, P., Moores, E.M., and Ramsden, T.W. 1990. Tectonic evolution of the
1106 Troodos ophiolite within the Tethyan framework. Tectonics, 9, 811-823.

1107 Dilek, Y., and Thy, P. 1998. Structure, petrology, and seafloor spreading tectonics of the Kizildag
1108 ophiolite (Turkey). In: Modern Ocean Floor Processes and the Geological Record,
1109 edited by R. Mills and K. Harrison, Geological Society of London Special
1110 Publication 148, 43-69.
1111 Dilek, Y., Moores, E.M., and Furnes, H. 1998. Structure of modern oceanic crust and ophiolites
1112 and implications for faulting and magmatism at oceanic spreading centers. In, R.
1113 Buck, J. Karson, P. Delaney and Y. Lagabrielle (editors), Faulting and Magmatism
1114 at Mid-Ocean Ridges, American Geophysical Union Monograph 106, 219-266.
1115 Dilek, Y., Thy, P., Hacker, B. and Grundvig, S. 1999. Structure and petrology of Tauride
1116 ophiolites and mafic dike intrusions (Turkey): Implications for the Neo-Tethyan
1117 ocean. Bulletin of the Geological Society of America, 111(8), 1192-1216.
1118 Dilek, Y and Furnes, H., 2011. Ophiolite genesis and global tectonics: geochemical and
1119 tectonic fingerprinting of ancient oceanic lithosphere. Geological Society of
1120 America Bulletin, 123, 387-411, doi: 10.1130/B30446.1.
1121 Dilek, Y., Festa, A., Ogawa, Y., and Pini, G.A. 2012. Chaos and geodynamics: mélanges,
1122 mélange-forming processes and their significance in the geological record.
1123 Tectonophysics 568-569: 1-6.
1124 Dilek, Y., and Furnes, Y. 2014. Origins of ophiolites. Elements, 10, 93-100. doi:
1125 10.2013/gselements.10.2.93.
1126 Dilek, Y., and Furnes, H. 2019. Tethyan ophiolites and Tethyan seaways. J. Geol. Soc. 176:
1127 899-912.
1128 Driesner, T. 1993. Aspects of petrographical, structural and stable isotope geochemical
1129 evolution of ophicarbonate breccias from ocean floor to subduction and uplift;

1130 an example from Chatillon, Middle Aosta Valley, Italian Alps. Schweiz.
1131 Mineral. Petrogr. Mitt. 73: 69-84.
1132 Ellero, A., Leoni, L., Marroni, M., and Sartori, F. 2001. Internal Liguride Units from Central
1133 Liguria, Italy: new constraints to the tectonic setting from white mica and
1134 chlorite studies. Swiss Bull. Miner. Petrol. 81: 39-54.
1135 Elter, G. 1971. Schistes lustrés et ophiolites de la zone piémontaise entre Orco et Doire
1136 Baltée (Alpes Graies). Hypothèses sur l'origine des ophiolites. Géol, Alpine 47:
1137 147–169.
1138 Elter, P. 1975. L'ensemble ligure. Bull. Soc. Géol. Fr. 7: 984-997.
1139 Elter, P., Trevisan, L., 1973. Olistostromes in the tectonic evolution of the Northern
1140 Apennines, In De Jong, K.A. and Scholten, R., eds., Gravity and Tectonics. John
1141 Willey and Sons, New York: 175–188.
1142 Ernst, W.G. 1970. Tectonic contact between the Franciscan mélange and the Great Valley
1143 Sequence — crustal expression of a Late Mesozoic Benioff zone. J. Geophys.
1144 Res. 75: 886–901.
1145 Ernst, W.G. 1971. Metamorphic zonations on presumably subducted lithospheric plates from
1146 Japan, California and the Alps. Contrib. Mineral. Petrol. 34(1): 43-59.
1147 Ernst, W.G. 2015. Franciscan geologic history constrained by tectonic/olistostromal
1148 highgrademetamafic blocks in the iconic California Mesozoic-Cenozoic
1149 accretionary complex. Am. Mineral. 100: 6–13.
1150 Ernst, W.G. 2016. Franciscan mélanges: coherent blocks in a low-density, ductile matrix.
1151 Int. Geol. Rev. 58: 626-642.

1152 Federico, L., Crispini, L., Malatesta, C., Torchio, S., and Capponi, G. 2015. Geology of the
1153 Pontinvrea area (Ligurian Alps, Italy): structural setting of the contact between
1154 Montenotte and Voltri units. J. of Maps 11: 101 113.
1155 Federico, L., Crispini, L., Scambelluri, M., and Capponi, G. 2007. Ophiolite mélange zone
1156 records exhumation in a fossil subduction channel. Geology 35: 499-502.
1157 Festa, A., Balestro, G., Borghi, A., De Caroli, S., and Succo, A. 2020a. The role of structural
1158 inheritance in continental break-up and exhumation of Alpine Tethyan mantle
1159 (Canavese Zone, Western Alps). Geosci. Front. 11: 167-188.
1160 Festa, A., Balestro, G., Dilek, Y. and Tartarotti, P. 2015. A Jurassic oceanic core complex in
1161 the high-pressure Monviso ophiolite (western Alps, NW Italy). Lithosphere 7:
1162 646-652.
1163 Festa, A., Cavagna, S., Barbero, E., Catanzariti, R., and Pini, G.A. 2020b. Mid-Eocene giant
1164 slope failure (sedimentary mélanges) in the Ligurian accretionary wedge (NW
1165 Italy) and relationships with tectonics, global climate changes and the
1166 dissociation of gas hydrates. J. Geol. Soc., 177: 575-586.
1167 Festa, A., Dilek, Y., Codegone, G., Cavagna, S., Pini, G.A., 2013. Structural anatomy of the
1168 Ligurian accretionary wedge (Monferrato, NW Italy), and evolution of
1169 superposed mélanges. Geol. Soc. Am. Bull. 125:1580-1598.
1170 Festa, A., Dilek, Y., Mittempergher, S., Ogata, K., Pini, G.A. and Remitti, F. 2018. Does
1171 subduction of mass transport deposits (MTDs) control seismic behavior of
1172 shallow-level megathrusts at convergent margins? Gondwana Res. 60: 186-193.
1173 Festa, A., Ogata, K., Pini, G. A., Dilek, Y., and Alonso, J. L. 2016. Origin and significance
1174 of olistostromes in the evolution of orogenic belts: A global synthesis.
1175 Gondwana Res., 39: 180-203.

1176 Festa, A., Ogata, K., and Pini, G.A. 2019a. Mélanges: 100th anniversary of the inception of
1177 the term and concept. Gondwana Res. 39: 1-6.
1178 Festa, A., Ogata, K., Pini, G.A. 2020c. Polygenetic mélanges: a glimpse on tectonic,
1179 sedimentary and diapiric recycling in convergent margins. J. Geol. Soc. 177:
1180 551-561.
1181 Festa, A., Ogata, K., Pini, G. A., Dilek, Y., and Alonso, J. L. 2016. Origin and significance
1182 of olistostromes in the evolution of orogenic belts: A global synthesis.
1183 Gondwana Res. 39: 180-203.
1184 Festa, A., Pini, G. A., Ogata, K., and Dilek, Y. 2019b. Diagnostic features and field-criteria
1185 in recognition of tectonic, sedimentary and diapiric mélanges in orogenic belts
1186 and exhumed subduction-accretion complexes. Gondwana Res. 74: 7-30.
1187 Festa, A., Pini, G.A., Dilek, Y., and Codegone, G. 2010. Mélanges and mélange-forming
1188 processes: a historical overview and new concepts. Int. Geol. Rev. 52: 1040-
1189 1105.
1190 Fierro, G., and Terranova, R. 1963. Microfacies fossilifere e sequenze litologiche nelle
1191 “Arenarie superiori” dei monti Ramaceto e Zatta. Att. Ist. Geol., Univ. Genova:
1192 1: 473-510.
1193 Fitzherbert, J. A., Clarke, G. L., and Powell, R. 2005. Preferential retrogression of high-P
1194 metasediments and the preservation of blueschist to eclogite facies metabasite
1195 during exhumation, Diahot terrane, NE New Caledonia. Lithos 83: 67-96.
1196 Flores, G. 1955. Les résultats des études pour les recherches pétroliféres en Sicile:
1197 Discussion. Proceedings of the 4th World Petroleum Congress. Casa Editrice
1198 Carlo Colombo, Rome: 121–122 (Section 1/A/2).

1199 Fonnesu, M., and Felletti, F. 2019. Facies and architecture of a sand-rich turbidite system in
1200 an evolving collisional-trench basin: a case history from the upper Cretaceous-
1201 Palaeocene Gottero system (NW Apennines). Riv. It. Pal. Strat. 125(2): 449-487.
1202 Fontana, E., Panseri, M., and Tartarotti, P. 2008. Oceanic relict textures in the Mount Avic
1203 serpentinites, Western Alps. Ofioliti 33: 105-118.
1204 Fontana, E., Tartarotti, P., Panseri, M., and Buscemi, S. 2015. Geological map of the Mount
1205 Avic massif (Western Alps Ophiolites). J. Maps 11(1): 126-135.
1206 Frezzotti, M.L., Selverstone, J., Sharp, Z.D., and Compagnoni, R. 2011. Carbonate
1207 dissolution during subduction revealed by diamond-bearing rocks from the Alps.
1208 Nature Geoscience 4: 703-706.
1209 Gao, P., and Santosh, M. 2020. Mesoarchean accretionary mélange and tectonic erosion in
1210 the Archean Dharwar Craton, southern India: Plate tectonics in the early Earth.
1211 Gonwana Res. 85: 291-305.
1212 Geersen, J., Festa, A., and Remitti, F. 2020. Structural constraints on the subduction of mass
1213 transport deposits in convergent margins. *In* Subaqueous mass movements and
1214 their consequences: advances in process understanding monitoring and hazard
1215 assesments (Georgiopoulou, A. et al., eds). Geol. Soc. London Spec. Publ. 500:
1216 115-128. https://doi.org/10.1144/SP500-2019-174
1217 Goffé, B., Bousquet, R., Henry, P., and Le Pichon, X. 2003. Effect of the chemical
1218 composition of the crust on the metamorphic evolution of orogenic wedges. J.
1219 Metamorph. Geol. 21:123-141.
1220 Golonka, J. 2007. Late Triassic and Early Jurassic palaeogeography of the world. Palaeog.,
1221 Palaeoclimatol., Palaeoecol. 244: 297-307.

1222 Groppo, C. and Castelli, D. 2010. Prograde P-T evolution of a lawsonite eclogite from the
1223 Monviso Meta-ophiolite (Western Alps): Dehydration and redox reactions
1224 during subduction of oceanic Fe-Ti-oxide gabbro. J. Petrol. 51, 2489-2514.
1225 Groppo, C., Beltrando, M., and Compagnoni, R. 2009. The P-Tpath of the ultra-high pressure
1226 Lago Di Cignana and adjoining high-pressure meta-ophiolitic units: insights into
1227 the evolution of the subducting Tethyan slab. J. Metamorph. Geol. 27: 207-231.
1228 Groppo, C., Ferrando, S., Gilio, M., Botta, S., Nosenzo, F., Balestro, G., Festa, A., and Rolfo,
1229 F. 2019. What's in the sandwich? New P-T constraints for the (U)HP nappe stack
1230 of southern Dora-Maira Massif (Western Alps). Eur. J. Mineral. 31(4): 665–683.
1231 Gusmeo, T., Spalla, M.I., Tartarotti, P., Zanoni, D., and Gosso, G. 2018. Structural-
1232 geological survey of an eclogitized chaotic complex: the Riffelberg-Garten Unit
1233 in the Breuil dell (Zermatt-Saas Zone, Italian Wester Alps). SGI-SIMP Meeting,
1234 12-14 September 2018, Catania (Italy), Abstract book: 219.
1235 Hajná J., Žák, J., Ackerman, L., Svojtka, M., and Pašava, J., 2019. A giant late Precambrian
1236 chert-bearing olistostrome discovered in the Bohemian Massif: A record of
1237 Ocean Plate Stratigraphy (OPS) disrupted by mass-wasting along an outer trench
1238 slope. Gondwana Res. 74: 173-188.
1239 Handy, M., Schmid, S., Bousquet, R., Kissling E., and Bernoulli, D. 2010. Reconciling plate-
1240 tectonic reconstructions of Alpine Tethys with the geological-geophysical record
1241 of spreading and subduction in the Alps. Earth Sci. Rev. 102: 121-158.
1242 Hosseinpour, M., Williams, S., Seton, M., Barnett-Moore, N., and Müller, R. D. 2016.
1243 Tectonic evolution of Western Tethys from Jurassic to present day: coupling
1244 geological and geophysical data with seismic tomography models. Int. Geol.
1245 Rev. 58: 1616-1645.

1246 Hsü, K.J. 1968. Principles of mélanges and their bearing on the Franciscan-Knoxville
1247 Paradox. Geol. Soc. Am. Bull. 79: 1063-1074.
1248 Kawamura, K., Ogawa, Y., Anma, R., Yokoyama, S., Kawakami, S., Dilek, Y., Moore, G.F.,
1249 Hirano, S., Yamaguchi, A., Sasaki, T., YK05-08-Leg 2, YK06-02 Shipboard
1250 Scientific Parties. Geol. Soc. Am. Bull. 121 (11-12), 1629-1646,
1251 https://doi.org/10.1130/B26219.1.
1252 Lafay, R., Baumgartner, L., Schwartz, S., Picazo, S., Montes-Hernandez, G. and
1253 Vennemann, T. 2017. Petrologic and stable isotopic studies of a fossil
1254 hydrothermal system in ultramafic environment (Chenaillet ophicalcites,
1255 Western Alps, France): processes of carbonate cementation. Lithos 294-295:
1256 319-338.
1257 Lagabrielle, Y. 1994. Ophiolites of the Western Alps and the nature of the Tethyan oceanic
1258 lithosphere. Ofioliti 19: 413-434.
1259 Lagabrielle, Y. 2009. Mantle exhumation and lithospheric spreading: An historical
1260 perspective from investigations in the oceans and in the Alps-Apennines
1261 ophiolites. Ital. J. Geosci. 128: 279-293.
1262 Lagabrielle, Y., Vitale Brovarone, A. and Ildefonse, B. 2015. Fossil oceanic core complexes
1263 recognized in the blueschist metaophiolites of Western Alps and Corsica. Earth
1264 Sci. Rev. 141: 1-26.
1265 Lagabrielle, Y. and Polino, R. 1985. Origine volcano-détritique de certaines prasinites des
1266 Schistes lustrés du Queyras (France): arguments texturaux et géochimiques.
1267 Bull. Soc. Geol. Fr. 4: 461-471.

1268 Lagabrielle, Y. and Polino, R. 1988. Un schéma structural du domaine des Schistes lustrés
1269 ophiolitifères au nord-ouest du massif du Mont Viso (Alpes sud-occidentales) et
1270 ses implications. C. R. Acad. Sci. 306: 921-928.
1271 Lagabrielle, Y., and Cannat, M. 1990. Alpine Jurassic ophiolites resemble the modern central
1272 Atlantic basement. Geology 18: 319-322.
1273 Lahondère, D., and Guerrot, C. 1997. Datation Sm-Nd du métamorphisme éclogitique en
1274 Corse alpine: un argument pour l'existence au Crétacé supérieur d'une zone de
1275 subduction active localisée sous le bloc corso-sarde. Géol. France 3: 3-11.
1276 Lamarche, G., Joanne, C. and Collot, J.-Y. 2008. Successive, large mass transport deposits
1277 in the south Kermadec fore-arc basin, New Zealand: The Matakaoa Submarine
1278 Instability Complex. Geochem., Geophys., Geosyst. 9: Q04001,
1279 https://doi.org/10.1029/2007GC001843.
1280 Lavier, L. L., and Manatschal, G. 2006. A mechanism to thin the continental lithosphere at
1281 magma-poor margins. Nature 440: 324-328.
1282 Le Mer, O., Lagabrielle, Y., and Polino, R. 1986. Une série sédimentaire détritique liée aux
1283 Ophiolites piémontaises: analyses lithostratigraphiques, texturales et
1284 géochimiques dans le massif de la Crête de Mouloun (Haut-Queyras, Alpes sud-
1285 occidentales, France). Géol. Alpine 62: 63-86.
1286 Lemoine, M. 1971. Données nouvelles sur la série du Gondran près Briançon (Alpes
1287 Cottiennes). Réflexions sur les problèmes stratigraphique et paléogéographique
1288 de la zone piémontaise. Géol. Alp. 47: 181-201.
1289 Lemoine, M., Steen, D., and Vuagnat, M., 1970. Sur le probléme stratigraphique des
1290 ophiolites piémontaises et des róches sédimentaires associées: Observations dans

1291 le massif de Chabrière en Haute-Ubaye (Basses-Alpes, France). C. R. des
1292 Séances, S.P.H.N., Genevé, 5: 44-59.
1293 Lemoine, M. and Tricart, P. 1986. Les Schistes lustrés piémontais des Alpes Occidentales:
1294 Approche stratigraphique, structural et sédimentologique. Eclogae Geol. Helv.
1295 79: 271-294.
1296 Lemoine, M., Tricart, P., and Boillot, G. 1987. Ultramafic and gabbroic ocean floor of the
1297 Ligurian Tethys (Alps, Corsica, Apennines): In search of a genetic model.
1298 Geology 15: 622-625.
1299 Leoni, L., Marroni, M., Sartori, F., and Tamponi, M. 1996, The grade of metamorphism in
1300 the metapelites of the Internal Ligurid Units Northern Apennines, Italy. Eur. J.
1301 Min. 8: 35-50.
1302 Li, X. H., Faure, M., Lin, W. and Manatschal, G. 2013. New isotopic constraints on age and
1303 magma genesis of an embryonic oceanic crust: The Chenaillet Ophiolite in the
1304 Western Alps. Lithos 160: 283-291.
1305 Li, X.P., Rahn, M. and Bucher, K., 2004. Serpentinites of the Zermatt-Saas ophiolite
1306 complex and their texture evolution. J. Metamorph. Geol. 22: 159-177.
1307 Lombardo, B., Nervo, R., Compagnoni, R., Messiga, B., Kienast, J., Mevel, C., Fiora, L.,
1308 Piccardo, G. and Lanza, R. 1978. Osservazioni preliminari sulle ofioliti
1309 metamorfiche del Monviso (Alpi Occidentali). Rend. Soc. It. Min. Petr. 34: 253-
1310 305.
1311 Lombardo, B., Rubatto, D. and Castelli, D. 2002. Ion microprobe U-Pb dating of zircon from
1312 a Monviso metaplagiogranite: Implications for the evolution of the Piedmont-
1313 Liguria Tethys in the Western Alps. Ofioliti 27: 109-117.

1314 Lucente, C. C., and Pini, G. A. 2008. Basin- wide mass- wasting complexes as markers of
1315 the Oligo- Miocene foredeep- accretionary wedge evolution in the Northern
1316 Apennines, Italy. Basin Res. 20: 49–71.
1317 Luoni, P., Rebay, G., Roda, M., Zanoni, D., and Spalla, M.I. 2020. Tectono-metamorphic
1318 evolution of UHP Zermatt-Saas serpentinites: a tool for vertical
1319 palaeogeographic restoration. Int. Geol. Rev. (first online). Doi:
1320 10.1080/00206814.2020.1758967.
1321 Luoni, P., Rebay, G., Spalla, M.I., and Zanoni, D. 2018. UHP Ti-chondrodite in the Zermatt-
1322 Saas serpentinite: Constraints on a new tectonic scenario. Am. Mineral 103(6):
1323 1002-1005.
1324 Magde, L. S., Barclay, A. H., Toomey, D. R., Detrick, R. S., and Collins, J. A. 2000. Crustal
1325 magma plumbing within a segment of the Mid-Atlantic Ridge, 35 N. Earth
1326 Planet. Sci. Lett. 175: 55-67.
1327 Malatesta, C., Crispini, L., Federico, L., Capponi, G., and Scambelluri, M. 2012. The
1328 exhumation of high pressure ophiolites (Voltri Massif, Western Alps): insights
1329 fromstructural and petrologic data on metagabbro bodies. Tectonophysics 568-
1330 569: 102-123.
1331 Manatschal, G., Sauter, D., Karpoff, A.M., Masini, E., Mohn, G. and Lagabrielle, Y. 2011.
1332 The Chenaillet Ophiolite in the French/Italian Alps: an ancient analogue for an
1333 Oceanic Core Complex? Lithos 124, 169-184.
1334 Manzotti, P., Ballevre, M., Zucali, M., Robyr, M., and Engi, M. 2014. The
1335 tectonometamorphic evolution of the Sesia-Dent Blanche nappes (internal
1336 Western Alps): review and synthesis. Swiss J. Geosci. 107: 309-336.

1337 Marroni, M., Meneghini, F., and Pandolfi, L. 2004. From accretion to exhumation in a fossil
1338 accretionary wedge: a case history from Gottero Unit (Northern Apennines,
1339 Italy). Geod. Acta 17: 41-53.
1340 Marroni M., Meneghini F., and Pandolfi, L. 2017. A revised subduction inception model to
1341 explain the Late Cretaceous, double vergent orogen in the pre-collisional
1342 Western Tethys: evidence from the Northern Apennines. Tectonics 36: 2227–
1343 2249.
1344 Marroni, M., and Pandolfi, L. 2001. Debris flow and slide deposits at the top of the Internal
1345 Liguride ophiolitic sequence, Northern Apennines, Italy: A record of frontal
1346 tectonic erosion in a fossil accretionary wedge. Isl. Arc 10: 9-21.
1347 Marroni, M., and Pandolfi, L. 2007. The architecture of the Jurassic Ligure-Piemontese
1348 oceanic basin: tentative reconstruction along the Northern Apennines - Alpine
1349 Corsica transect. Int. J. Earth Sci. 96: 1059-1078.
1350 Marroni, M. and Perilli, N. 1990. The age of the ophiolite sedimentary cover from the Mt.
1351 Gottero Unit (Internal Liguride Units, Northern Apennines): new data from
1352 calcareous nannofossils. Ofioliti 15: 232-251.
1353 Marroni, M., Molli, G., Montanini, A., and Tribuzio, R. 1998. The association of continental
1354 crust rocks with ophiolites (northern Apennines, Italy): Implications for the
1355 continent-ocean transition. Tectonophysics 292: 43-66.
1356 Marroni, M., Monechi, S., Perilli, N., Principi, G., and Treves, B. 1992. Late Cretaceous
1357 flysch deposits in the Northern Apennines, Italy: age of inception of orogenesis-
1358 controlled sedimentation. Cretaceous Res. 13: 487-504.
1359 Meneghini, F., Marroni, M., Moore, J.C., Pandolfi, L., and Rowe, C.D. 2009, The process
1360 of underplating in the geologic record: structural diversity between the

1361 Franciscan Complex California, the Kodiak Complex Alaska and the Internal
1362 Ligurian Units Italy. Geol. J. 44: 126-152.
1363 Meneghini, F., Pandolfi, L., and Marroni, M. 2020. Recycling of heterogeneous material in
1364 the subduction factory: evidence from the sedimentary mélange of the Internal
1365 Ligurian Units, Italy. J. Geol. Soc. 177: 587-599.
1366 Michard, A., Chalouan, A., Feinberg, H., Goffé, B., and Montigny, R. 2002. How does the
1367 Alpine belt end between Spain and Morocco? Bull. Soc. Geol. Fr. 173(1): 3–15.
1368 Michard, A., Goffe, B., Chopin, C. and Henry, C. 1996. Did the Western Alps develop
1369 through an Oman-type stage? The geotectonic setting of high-pressure
1370 metamorphism in two contrasting Tethyan transects. Eclogae Geol. Helv. 89: 43-
1371 80.
1372 Miyashiro, A., 1973, Metamorphism and Metamorphic Belts: Halsted Press, JohnWiley &
1373 Sons, New York: 492p.
1374 Mohn, G., Manatschal, G., Beltrando, M., Masini, E., and Kusznir, N. 2012. Necking of
1375 continental crust in magma-poor rifted margins: Evidence from the fossil Alpine
1376 Tethys margins. Tectonics 31: doi:10.1029/2011TC002961
1377 Montanini, A., Tribuzio, R., and Anczkiewicz, R. 2006. Exhumation history of a garnet
1378 pyroxenite-bearing mantle section from a continent-ocean transition (Northern
1379 Apennine ophiolites, Italy). J. Petrol. 47: 1943-1971.
1380 Moore, J.C. and Sample, J. 1986. Mechanism of accretion at sediment-dominated subduction
1381 zones: consequences for the stratigraphic record and accretionary prism
1382 hydrogeology. Mem. Soc. Geol. It. 31: 107–118.

1383 Müntener, O., and Hermann, J. 2001. The role of lower crust and continental upper mantle
1384 during formation of non-volcanic passive margins: evidence from the Alps, *In*
1385 Al Hosani, K., Roure, F., Ellison, R., Stephen Lokier, S., eds. Lithosphere
1386 Dynamics and Sedimentary Basins: The Arabian Plate and Analogues. Geol.
1387 Soc. London Spec. Publ. 187(1): 267 288.
1388 Mutti, E. 1992. Turbidite sandstones. AGIP-Istituto di Geologia, Università di Parma, San
1389 Donato Milanese, 275 pp.
1390 Nielsen, T. H., and Abbate, E. 1983. Submarine-fan facies associations of the Upper
1391 Cretaceous and Paleocene Gottero sandstone, Ligurian Apennines Italy. Geo-
1392 Mar. Lett. 3: 193-197.
1393 Ogata, K., Festa, A., Pini, G. A., Pogačnik, Ž., and Lucente, C. C. 2019. Substrate
1394 deformation and incorporation in sedimentary mélanges (olistostromes):
1395 Examples from the northern Apennines (Italy) and northwestern Dinarides
1396 (Slovenia). Gondwana Res. 74: 101-125
1397 Ogata, K., Festa, A., Pini, G.A., and Alonso, J.L., 2020. Submarine landslide deposits in
1398 orogenic belts: olistostromes and sedimentary mélanges. *In* Ogata, K., Festa, A.,
1399 and Pini, G.A. Eds. Submarine Landslides: subaqueous mass transport deposits
1400 from outcrop to seismic profiles. Geophysical Monograph 247, First Edition,
1401 American Geophysical Union, John Wiley and Sons Inc., USA, p. 3-26.
1402 Ogata, K., Tinterri, R., Pini, G. A., and Mutti, E. 2012. Mass transport- related stratal
1403 disruption within sedimentary melanges: Examples from the northern Apennines
1404 (Italy) and south- central Pyrenees (Spain). Tectonophysics 568–569: 185–199.

1405 Ogawa, Y., Mori, R., Tsunogae, T., Dilek, Y., and Harris, R. 2015. New interpretation of the
1406 Franciscan mélange at San Simeon coast, California: tectonic intrusion into an
1407 accretionary prism. Int. Geol. Rev. 57: 824-842.
1408 Orange, D.L. 1990. Criteria helpful in recognizing shear-zone and diapiric mélanges:
1409 examplesfrom the Hoh accretionary complex, Olympic Peninsula, Washington.
1410 Geol. Soc. Am. Bull. 102: 935-951.
1411 Palin, R.M., Santosh, M., Cao, W., Li, S-S., Hernandez-Uribe, D., and Parsons, A. 2020.
1412 Secular change and the onset of plate tectonics on Earth. Eart-Science Rev. 207:
1413 103172.
1414 Pandolfi, L. 1997. Stratigrafia ed evoluzione strutturale delle successioni torbiditiche
1415 cretacee della Liguria orientale (Appennino Settentrionale). PhD Thesis,
1416 Università di Pisa.
1417 Panseri, M., Fontana, E., and Taratrotti, P., 2008. Evolution of rodingitic dykes:
1418 metasomatism and metamorphism in the Mount Avic serpentinites (Alpine
1419 ophiolites, southern Aosta Valley). Ofioliti 33(2): 165-185.
1420 Péron-Pinvidic, G., and Manatschal, G. 2009. The final rifting evolution at deep magma-
1421 poor passive margins from Iberia-Newfoundland: a new point of view. Int. J.
1422 Earth Sci. 98: 1581-1597.
1423 Piccardo, G.B., Padovano, M., and Guarnieri, L. 2014. The Ligurian Tethys: mantle
1424 processes and geodynamics. Earth Sci. Rev. 138: 409–434.
1425 Pinet, N., Lagabrielle, Y. and Whitechurch, H. 1989. Le complexe du Pic des Lauzes (Haut
1426 Queyras, Alpes Occidentales, France): structures alpines et océaniques dans un
1427 massif ophiolitique de type liguro-piémontais. Bull. Soc. Geol. Fr. 2: 317-326.

1428 Pini, G. A. (1999). Tectonosomes and olistostromes in the Argille Scagliose of the Northern
1429 Apennines, Italy (Vol. 335). Geol. Soc. Am. Spec. Pap. 338: 73 pp.
1430 Pini, G.A., Ogata, K., Camerlenghi, A., Festa, A., Lucente, C.C., and Codegone, G. 2012.
1431 Sedimentary mélanges and fossil mass-transport complexes: a key for better
1432 understanding submarine mass movements? In Yamada, Y. et al., eds.,
1433 Submarine Mass Movements and Their ConsequencesAdvances in Natural and
1434 Technological Hazards Research 31. Springer Science+Business Media B.V.:
1435 585–594
1436 Pini, G. A., Venturi, S., Lucente, C. C., and Ogata, K. 2020. Mass transport complexes of
1437 the Marnoso- arenacea foredeep turbidites system, Northern Apennine of Italy:
1438 A twenty- year after reappraisal, In Ogata K., Festa A., and Pini G.A., eds.,
1439 Submarine landslides: Subaqueous mass transport deposits from outcrops to
1440 seismic profiles: 117–137. Hoboken, NJ/Washington, WC: Wiley/American
1441 Geophysical Union.
1442 Plunder, A., Agard, P., Chopin, C., Pourteau, A., and Okay, A. I. 2015. Accretion,
1443 underplating and exhumation along a subduction interface: from subduction
1444 initiation to continental subduction (Tavşanlı zone, W. Turkey). Lithos 226: 233-
1445 254.
1446 Pognante, U., Perotto, A., Salino, C., and Toscani, L. 1986. The ophiolitic peridotites of the
1447 Western Alps: record of the evolution of a small oceanic type basin in the
1448 Mesozoic Tethys. Tsch. Min. Petr. Mitt. 35: 47-65.

1449 Polat, A., and Kerrich, R. 1999. Formation of an Archean tectonic mélange in the Schreiber-
1450 Hemlo greenstone belt, Superior Province, Canada: Implications for Archean
1451 subduction-accretion process. Tectonics 18 (5): 733-755.
1452 Polino, R., 1984. Les series oceaniques du haut val de Suse (Alpes Cottiennes): analyse des
1453 couvertures sedimentaires. Ofioliti, 9: 547-554.
1454 Polino, R., Dal Piaz, G.V., Gosso, G. 1990. Tectonic erosion at the Adria margin and
1455 accretionaryprocesses for the Cretaceous orogeny of the Alps. Mém. Soc. Géol.
1456 Fr. 156: 345-367.
1457 Principi, G., Bortolotti, V., Chiari, M., Cortesogno, L., Gaggero, L., Marcucci, M., Saccani,
1458 E. and Treves, B. 2004. The pre-orogenic volcano-sedimentary covers of the
1459 western Tethys oceanic basin: a review. Ofioliti 29:177-212.
1460 Rabain, A., Cannat, M., Escartín, J., Pouliquen, G., Deplus, C., and Rommevaux Jestin, C.
1461 2001. Focused volcanism and growth of a slow spreading segment (Mid-Atlantic
1462 Ridge, 35 N). Earth Planet. Sci. Lett. 185: 211-224.
1463 Rampone, E., Borghini, G., and Basch, V. 2020. Melt migration and melt-rock reaction in
1464 the Alpine-Apennine peridotites: Insights on mantle dynamics in extending
1465 lithosphere. Geosci. Front. 11: 151-166.
1466 Raymond, L.A., 1973, Tesla-Ortigalita fault, Coast Range thrust fault, and Franciscan
1467 metamorphism, northeastern Diablo Range, California. Geol. Soc. Am. Bull. 84:
1468 3547–3562.
1469 Raymond, L.A. 1984. Classification of melanges, In Raymond, L.A., ed., Melanges: Their
1470 Nature, Origin and Significance. Boulder, Colorado Geological Society of
1471 America Special Papers 198: 7–20.

1472 Raymond, L.A. 2019, Perspectives on the roles of melanges in subduction accretionary
1473 complexes: A review. Gondwana Res. 74: 68-89.
1474 Rebay, G., Zanoni, D., Langone, A., Luoni, P., Tiepolo, M., and Spalla, M. I. 2018. Dating
1475 of ultramafic rocks from the Western Alps ophiolites discloses Late Cretaceous
1476 subduction ages in the Zermatt-Saas Zone. Geol. Mag. 155: 298-315.
1477 Rebay, G.; Spalla, M.I.; and Zanoni, D. 2012. Interaction of deformation and metamorphism
1478 during subduction and exhumation of hydrated oceanic mantle: Insights from the
1479 Western Alps. J. Metamorph. Geol. 30: 687-702.
1480 Remitti, F., Vannucchi, P., Bettelli, G., Fantoni, L., Panini, F., and Vescovi, P. 2011.
1481 Tectonic and sedimentary evolution of the frontal part of an ancient subduction
1482 complex at the transition from accretion to erosion: the case of the Ligurian
1483 wedge of the northern Apennines, Italy. Geol. Soc. Am. Bull, 123: 51–70.
1484 Renna, M.R., Tribuzio, R., Sanfilippo, A. and Thirlwall, M. 2018. Role of melting process
1485 and melt-rock reaction in the formation of Jurassic MORB-type basalts (Alpine
1486 ophiolites). Contr. Min. Petr. 173: 31.
1487 Ribes, C., Ghienne, J. F., Manatschal, G., Decarlis, A., Karner, G. D., Figueredo, P. H., and
1488 Johnson, C. A. 2019. Long-lived mega fault-scarps and related breccias at distal
1489 rifted margins: Insights from present-day and fossil analogues. J. Geol. Soc. 176:
1490 801-816.
1491 Roda, M., Regorda, A., Spalla, M.I., and Marotta, A.M. 2019, What drives Alpine Tethys
1492 opening? Clues from the review of geological data and model predictions: Geol.
1493 J. 54: 2646-2664.

1494 Roda, M., Zucali, M., Regorda, A., and Spalla, M. I. 2020. Formation and evolution of a
1495 subduction-related mélange: The example of the Rocca Canavese Thrust Sheets
1496 (Western Alps). Geol. Soc. Am. Bull. 132: 884-896.
1497 Rosenbaum G., and Lister, G. S. 2005. The Western Alps from the Jurassic to Oligocene:
1498 spatio-temporal constraints and evolutionary reconstructions. Earth Sci. Rev.,
1499 69(3-4): 281-306.
1500 Rubatto, D., Gebauer, D. and Fanning, M. 1998. Jurassic formation and Eocene subduction
1501 of the Zermatt-Saas-Fee ophiolites: Implications for the geodynamic evolution
1502 of the Central and Western Alps. Contr. Min. Petr. 132: 269-287.
1503 Rubatto, D. and Hermann, J. 2003. Zircon formation during fluid circulation in eclogites
1504 (Monviso, Western Alps): implications for Zr and Hf budget in subduction
1505 zones. Geochim. Cosmochim. Acta 67 (12): 2173-2187.
1506 Saby, P. 1986. La lithosphère océanique de la Tethys ligure: etude du magmatisme et des
1507 mineralisations associées dans les ophiolites du Queyras (zone piémontaise des
1508 Alpes occidentales). PHD Thesis. Universite Scientique et Medicale de
1509 Grenoble, 222 pp.
1510 Saccani, E., Dilek, Y., Marroni, M., and Pandolfi, L. 2015. Continental margin ophiolites of
1511 Neotethys: remnants of ancient Ocean-Continent Transition Zone (OCTZ)
1512 Lithosphere and their geochemistry, mantle sources and melt evolution patterns.
1513 Episodes 38: 230-249.
1514 Sample, J.C., and Moore, J.C. 1987. Structural style and kinematics of an uderplated slate
1515 belt, Kodiak and adjacent islands, Alaska. Geol. Soc. Am. Bull. 99: 7-20.

1516 Scarsi, M., Malatesta, C. and Fornasero, S. 2018. Lawsonite-bering eclogite from a tectonic
1517 mélange in the Ligurian Alps: new constraints for the subduction plate-interface
1518 evolution. Geol. Mag. 155: 280-297.
1519 Schettino, A., and Turco, E. 2011. Tectonic history of the western Tethys since the Late
1520 Triassic. Geol. Soc. Am. Bull. 123: 89-105.
1521 Schwartz, S., Lardeaux, J., Guillot, S. and Tricart, P. 2000. Diversité du métamorphisme
1522 éclogitique dans le massif ophiolitique du Monviso (Alpes occidentales, Italie).
1523 Geod. Acta 13: 169-88.
1524 Silver, E.A. and Beutner, E.C. 1980. Melanges. Geology 8: 32–34.
1525 Skora, S., Mahlen, N.J., Johnson, C.M., Baumgartner, L.P., Lapen, T.J., Beard, B.L., and
1526 Szilvagyi, E.T. 2015. Evidence for protracted prograde metamorphism followed
1527 by rapid exhumation of the Zermatt-Saas Fee ophiolite. J. Metamorph. Geol. 33:
1528 711-734
1529 Stampfli, G. M., and Borel, G. D. 2002. A plate tectonic model for the Paleozoic and
1530 Mesozoic constrained by dynamic plate boundaries and restored synthetic
1531 oceanic isochrons. Earth Planet. Sci. Lett. 196: 17-33.
1532 Stampfli, G. M., Borel, G. D., Marchant, R., and Mosar, J. 2002. Western Alps geological
1533 constraints on western Tethyan reconstructions. J. Virt. Expl. 8: 77.
1534 Stampfli, G. M., and Kozur, H. W. 2006. Europe from the Variscan to the Alpine cycles.
1535 Geol. Soc. London Mem. 32: 57-82.
1536 Tartarotti, P., Festa, A., Benciolini, L. and Balestro, G. 2017a. Record of Jurassic mass
1537 transport processes through the orogenic cycle: Understanding chaotic rock units
1538 in the high pressure Zermatt-Saas ophiolite (Western Alps). Lithosphere 9: 399-
1539 407.

1540 Tartarotti, P., Guerini, S., Rotondo, F., Festa, A., Balestro, G., Bebout, G.E., Cannaò, E.,
1541 Epstein, S., and Scambelluri, M. 2019. Superposed Sedimentary and Tectonic
1542 Block-In-Matrix Fabrics in a Subducted Serpentinite Mélange (High-Pressure
1543 Zermatt Saas Ophiolite, Western Alps). Geosciences 9: 358.
1544 Tartarotti, P., Benciolini, L., and Monopoli, B. 1998. Brecce serpentinitiche nel massiccio
1545 ultrabasico del Monte Avic (Falda Ofiolitica Piemontese): possibili evidenze di
1546 erosione sottomarina. Atti Tic. Sc. Terra 7: 73-86.
1547 Tartarotti, P., Martin, S., Festa, A., and Balestro, G. 2021. Metasediments covering
1548 ophiolites in the HP internal belt of the Western Alps: Review of tectono-
1549 stratigraphic successions and constraints for the Alpine evolution. Minerals 11:
1550 411, http://doi.org/10.3390/min11040411.
1551 Tartarotti, P., Martin, S., Monopoli, B., Benciolini, L., Schiavo, A., Campana, R., and Vigni,
1552 I. 2017b. Geology of the Saint-Marcel valle metaophiolites (Northwestern Alps,
1553 Italy). J. Maps 13(2): 707-717.
1554 Treves, B. 1984. Orogenic belts as accretionary prisms: The example of the northern
1555 Apennines. Ofioliti 9: 577-618.
1556 Treves, B.A., and Harper, G.D. 1994. Exposure of serpentinites on the ocean floor: sequence
1557 of faulting and hydrofracturing in the Northern Apennines ophicalcites. Ofioliti
1558 19: 435-466.
1559 Tribuzio, R., Garzetti, F., Corfu, F., Tiepolo, M., and Renna, M. R. 2016. U-Pb zircon
1560 geochronology of the Ligurian ophiolites (Northern Apennine, Italy):
1561 Implications for continental breakup to slow seafloor spreading. Tectonophysics
1562 666: 220-243.

1563 Tricart, P. 1973. Les Schistes lustrés du Haut-Cristillan; analyse tectonique d'un secteur
1564 externe du domaine piémontais (Alpes cottiennes, France). Thesis 3 cycle,
1565 Strasbourg, 193 p.
1566 Tricart, P., and Lemoine, M. 1983. Serpentinite oceanic bottom in South Queyras ophiolites
1567 (French Western Alps): record of the incipient oceanic opening of the mesozoic
1568 ligurian Tethys. Eclogae. Geol. Helv. 76: 611-629.
1569 Tricart, P. and Lemoine, M. 1991. The Queyras ophiolite west of Monte Viso (Western
1570 Alps): indicator of a peculiar ocean floor in the Mesozoic Tethys. J. Geod. 13:
1571 163-181.
1572 Tricart, P., and Schwartz, S. 2006. A north-south section across the Queyras Schistes lustrés
1573 (Piedmont zone, western Alps): Syn-collision refolding of a subduction wedge.
1574 Eclogae Geol. Helv. 99: 429-442.
1575 Valloni, R., and Zuffa, G.G. 1984. Provenance changes for arenaceous formations of the
1576 Northern Apennines (Italy). Geol. Soc. Am. Bull. 95: 1035-1039.
1577 Van de Kamp, P.C. and Leake, B.E. 1995. Petrology and geochemistry of siliciclastic rocks
1578 of mixed feldspatic and ophiolitic provenance in the Northern Apennines, Italy.
1579 Chem. Geol. 122: 1-20.
1580 Vitale Brovarone, A., Picatto, M., Beyssac, O., Lagabrielle, Y., and Castelli, D., 2014. The
1581 blueschist-eclogite transition in the Alpine chain: P-T paths and the role of slow-
1582 spreading extensional structures in the evolution of HP-LT mountain belts.
1583 Tectonophysics 615-616: 96-121.
1584 von Huene, R., and Lallemand, S. 1990. Tectonic erosion along the Japan and Peru
1585 convergent margin. Geol. Soc. Am. Bull. 102: 704–720.

1586 von Huene, R., Ranero, C.R., and Vannucchi, P. 2004. Generic model of subduction erosion.
1587 Geology 32: 913–916.
1588 Wakabayashi, J. 2011. Mélanges of the Franciscan Complex, California: diverse structural
1589 settings, evidence for sedimentary mixing, and their connection to subduction
1590 processes: in Wakabayashi, J., and Dilek, Y. eds. Mélanges: Processes of
1591 Formation and Societal Significance, Geological Society of America Special
1592 Paper 480: 117–141.
1593 Wakita, K. 2015. OPS mélange: a new term for mélanges of convergent margins of the
1594 world. Int. Geol. Rev. 57 (5–8): 529–539.
1595 Whitmarsh, R. B., Manatschal, G., and Minshull, T. A. 2001. Evolution of magma-poor
1596 continental margins from rifting to seafloor spreading. Nature 413: 150-154.
1597 Wood, D.S. 1974. Ophiolites, mélanges, blue schists, and ignimbrites: early Caledonian
1598 subduction inWales? In Dott, R.H., and Shaver, R.H., eds., Modern and Ancient
1599 Geosynclinal Sedimentation. SEPM Special Publications 19: 334–343.
1600 Yamamoto, Y., Ogawa, Y., Uchino, T., Muraoka, S., and Chiba, T. 2007, Large-scale
1601 chaotically mixed sedimentary body within the Late Pliocene to Pleistocene
1602 Chikura Group, Central Japan. Island Arc 16: 505-507.
1603 Žák, J., Svojtka, M., Hajná J., and Ackerman, L. 2020. Detrital zircon geochronology and
1604 processes in accretionary wedges. Earth-Science Rev. 207: 103214.
1605 Zanoni, D., Rebay, G. and Spalla, M. I. 2016. Ocean floor and subduction record in the
1606 Zermatt-Saas rodingites, Valtournanche, Western Alps. Journal Metamorphic
1607 Geology 34: 941-961.

FIGURE AND TABLE CAPTIONS

Figure 1. A- Tectonic map of the Western Alps and the Northern Apennines, showing the distribution of different lithospheric plates and ocean basins that were involved in the evolution of the orogenic belts in this region (modified from Balestro et al., 2015). Locations of the major chaotic rock units and MTDs discussed in the text are also shown in red circles and numbers. B- Index map, showing the Alps and the Apennines in their Mediterranean context.

Figure 2. Paleogeographic reconstruction of the Western Tethyan realm (Ligurian-Piedmont Ocean Basin) in the (**A**) Middle Jurassic (modified from Sampfli and Kozur, 2006; Schettino and Turco, 2011) and (**B**) late Maastrichtian (modified from Michard et al., 2002; Sampfli and Kozur, 2006; Schettino and Turco, 2011; Marroni et al., 2017; Festa et al., 2020).

Figure 3. Stratigraphic columnar sections and outcrop photos showing the sedimentary and structural features of the syn-extensional, lower and upper ophiolitic breccias of the Internal Ligurian Units in the Graveglia (**A**) and Bracco (**E**) sections (Northern Apennines). (**B**) Polymictic clasts composed of Fe-gabbro, Fe-basalt, plagiogranite, and serpentinite units in a scarce sandy matrix of the Monte Capra Breccia (lower ophiolitic breccia). Hammer for scale; (**C**) Close-up view of subrounded clasts of Mg-gabbros in the Monte Zenone Breccia (upper ophiolitic breccias) and their stratigraphic relationships (**D**) with Radiolarian cherts. Hammer for scale; (**F**) close-up view of the ophicalcite texture of the Levanto Breccia; (**G**) close-up view of the Framura Breccia (lower ophiolitic breccia) showing serpentinite clasts in a serpentinite-derived matrix. Coin for scale; (**H**) Panoramic view displaying the

relationships between the lower ophiolitic breccia (Levanto Breccia) and massive basalts. The stratigraphic relationships are highlighted by ophiolitic sandstones.

Figure 4. Inferred tectonic settings for the emplacement of the syn-contractional MTDs in the Northern Apennines: (**A**) General; (**B**) In detail. (**C**) Representative stratigraphic columnar sections (with scale). (**D**) Close-up view of the cohesive debris flows in the Val Lavagna Shale Group (i.e., "Olistostroma del Passo della Forcella", showing angular to subangular clasts of calcilutites embedded in a muddy-silty matrix. Coin for scale; (**E**) stratigraphic contact (white arrows) between the Bocco Shale (BS) and the Val Lavagna Shale (VLS) in the Portello Unit. Coin for scale; (**F**) Panoramic, and (**G**) Detail view of the Bocco Shale (early Paleocene), showing angular to subangular clasts of calcilutite in muddy-silty, foliated matrix. Hammer for scale.

Figure 5. (**A**) Representative stratigraphic sections, depicting the distribution of the lower and upper syn-extensional ophiolitic metabreccias within the Zermatt-Saas ophiolites in the sector between the Lake Miserin (modified from Tartarotti et al., 2017) and Mt. Avic. (**B**) Field evidence of the superposition of two tectono-metamorphic stages (D1 and D2) of the Alpine deformation onto the eclogite-facies ophiolite metabreccias of the Lake Miserin (Zermatt-Saas ophiolites). Note that the orientation of irregularly shaped clasts, centimeter in size, marks the relict of S1 foliation (dashed yellow line) which is deformed by D2 folds (dashed white lines indicate S2 foliation and D2 fold axial plane; see Tartarotti et al., 2017a for details). (**C**) Field occurrence of lower ophiolite metabreccias (Zermatt-Saas ophiolites) in the Lake Miserin area, showing alternating layers of different sized clast-supported metabreccias, made of angular clasts of serpentinized metaperidotite and metaophicarbonate.

Field book for scale; (**D** and **E**) Different close-up views of the Lake Miserin Sedimentary mélange (syn-extensional upper ophiolitic metabreccias; Zermatt-Saas ophiolites), showing angular to sub-rounded clasts of serpentinized metaperidotite in a carbonate-rich (marble) matrix. Dashed white line indicates the S2 foliation. Pencil for scale; (**F**) Close-up view of the Mt. Avic lower ophiolitic metabreccias (Zermatt-Saas ophiolites), showing angular shaped clasts of serpentinized metaperidotite and metaophicarbonate in a mixed carbonate-ultramafic metasandstone matrix. (**G**) Close-up view of the polymictic syn-extensional upper ophiolitic metabreccias (blueschist facies) of the Queyras ophiolite, showing angular clasts of serpentinized metaperidotite and metagabbros in a calcschist matrix; (**H**) Close-up view of the syn-contractional MTDs of the Rocher Renard Complex (Lower Paleocene?), showing rounded clasts of serpentinized metaperidotite and marble in a metapelite matrix. Camera cap for scale; (**I**) Stratigraphic columnar section of the Queyras ophiolite (modified from Balestro et al., 2019), depicting the stratigraphic position of the lower and upper syn-extensional ophiolitic metabreccias, and syn-contractional MTDs.

Figure 6. (**A**) Stratigraphic columnar section of the Monviso ophiolite (modified from Balestro et al., 2019), depicting the lateral and vertical relations between the syn-extensional chaotic deposits, the exhumed upper mantle rocks and the sedimentary succession. (**B**, **C** and **D**) Various close-up views of angular to irregular – shaped clasts of gabbro in a coarse-grained matrix of mafic-metasandstone (lower syn-extensional ophiolitic metabreccias), and line drawing (**E**) of the overturned peridotite – cover succession relationship, cropping out at Colle del Baracun (Monviso ophiolite); notice the stratigraphic position of mafic metabreccias and metasandstones within the calcschist sequence (modified from Balestro et al., 2015a) (**F**) Panoramic view of the Garten Formation (syn-extensional upper ophiolitic

metabreccias) to the East of Cime Bianche (Aosta Valley), showing intercalations of hyperconcentrated deposits (dashed white lines), decimeters to one meters thick, in a calcschist matrix. Dashed black line indicates the S2 foliation. Backpack for scale. (**G** and **H**) Close-up views of the internal arrangement of the Garten Formation, showing rounded to elongated shaped clasts of metabasalt in a coarse-grained calcschist matrix. (**I**) Interpreted stratigraphic sections, depicting the distribution of the syn-extensional upper ophiolitic metabreccias of the Garten Formation in the Zermatt-Saas ophiolite sequence of the Cime Bianche sector.

Table 1. Comparison among syn-extensional lower and upper ophiolitic breccias and syn-contractional MTDs of the Internal Ligurian Units of Northern Apennines and Western Alps.

Figure 7. Interpretative block diagrams depicting the geodynamic and tectono-stratigraphic depositional setting for syn-extensional, lower and upper ophiolitic breccias and syn-contractional MTDs during: (**A**) The Middle–Late Jurassic seafloor spreading, and (**B**) Late Cretaceous – Paleocene convergence tectonic stages of the evolution of the Western Tethyan realm (Ligurian – Piemont Ocean Basin), respectively.

Figure 1

Click here to access/download;Figure;Fig 1_Festa et al_J Geol_R2.jpg

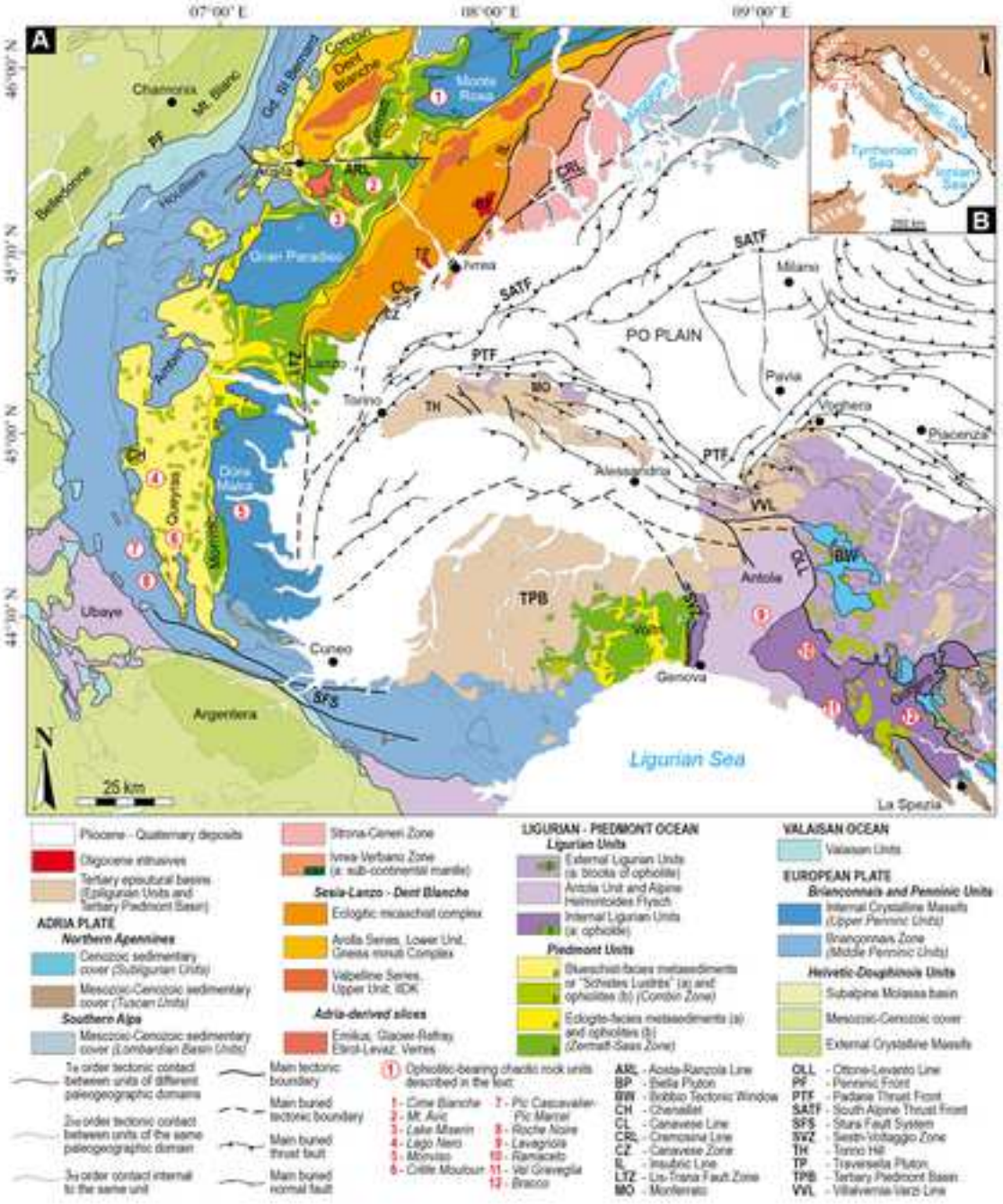

Figure 1 - *Festa et al.* (width 170 mm)

Figure 2

Click here to access/download;Figure;Fig 2_Festa et al_J Geol_R1.jpg

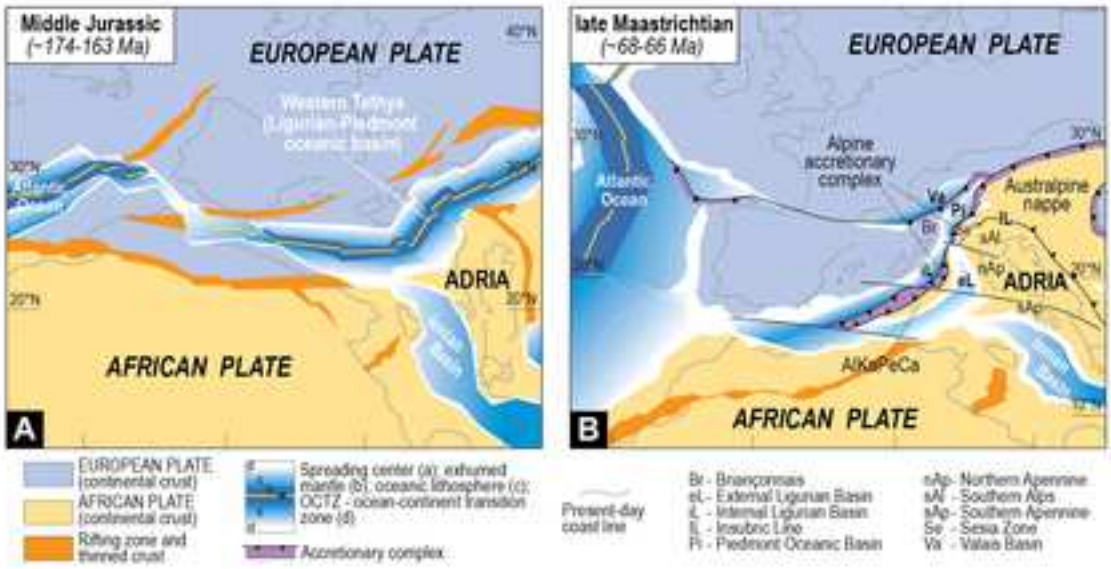

Figure 2 - *Festa et al.* (width 170 mm)

Figure 3

Click here to access/download;Figure;Fig 3_Festa et al_J Geol_R1.jpg

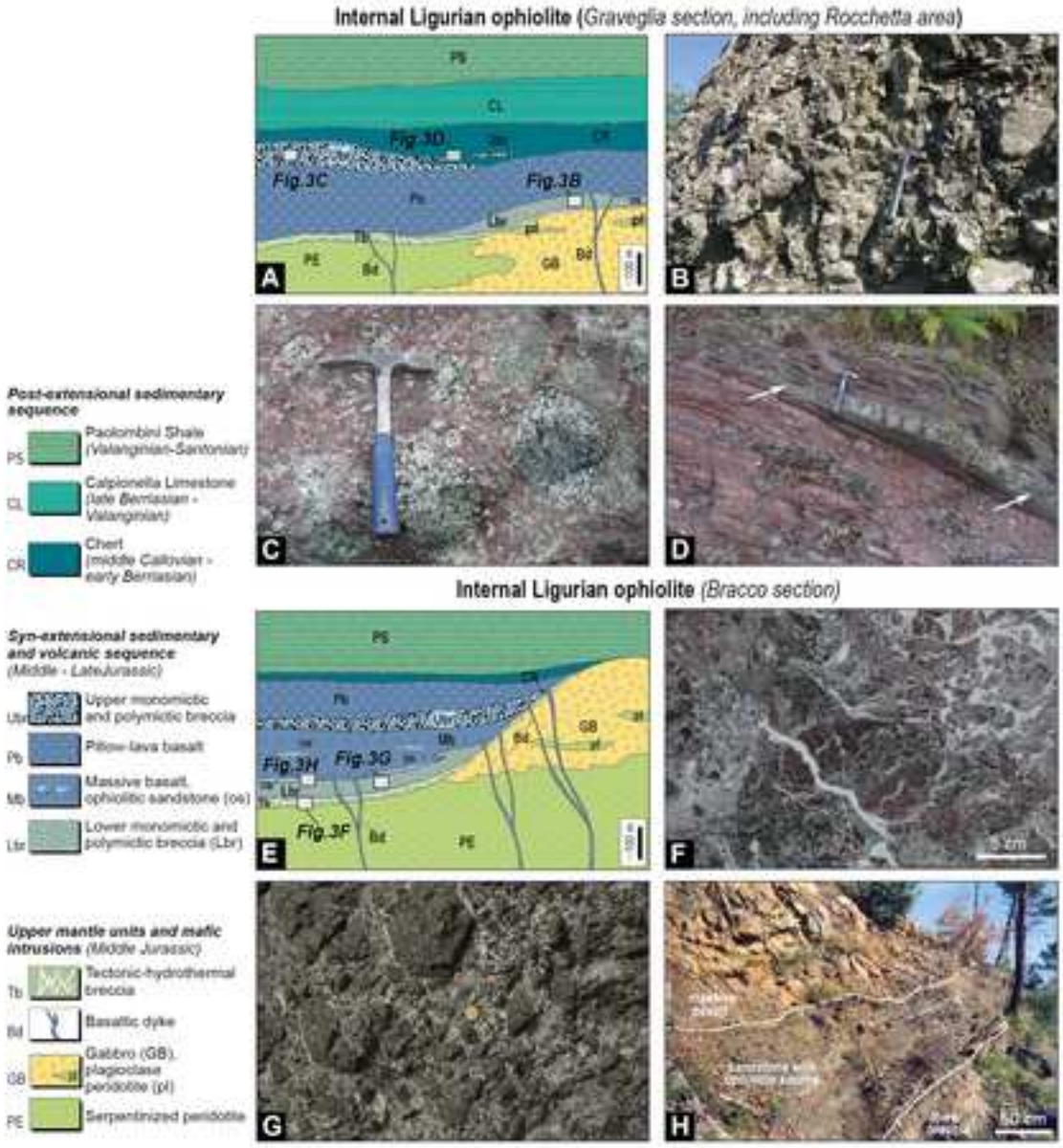

Figure 3 - *Festa et al.* (width 170 mm)

Figure 4

Click here to access/download;Figure;Fig 4_Festa et al_J Geol.jpg

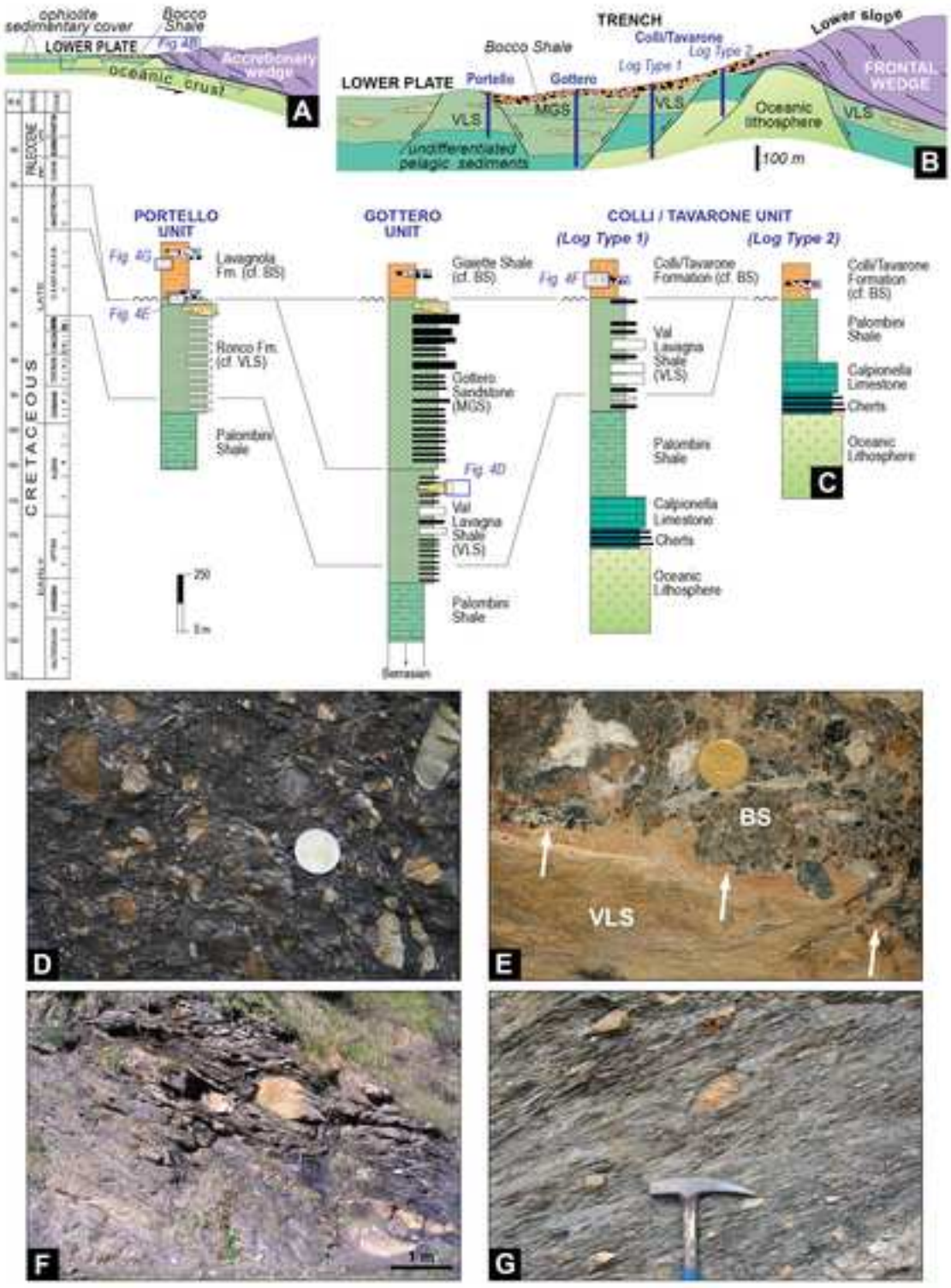

Figure 4 - *Festa et al.* (width 170 mm)

Figure 5

Click here to access/download;Figure;Fig 5_Festa et al_J Geol_R2.jpg

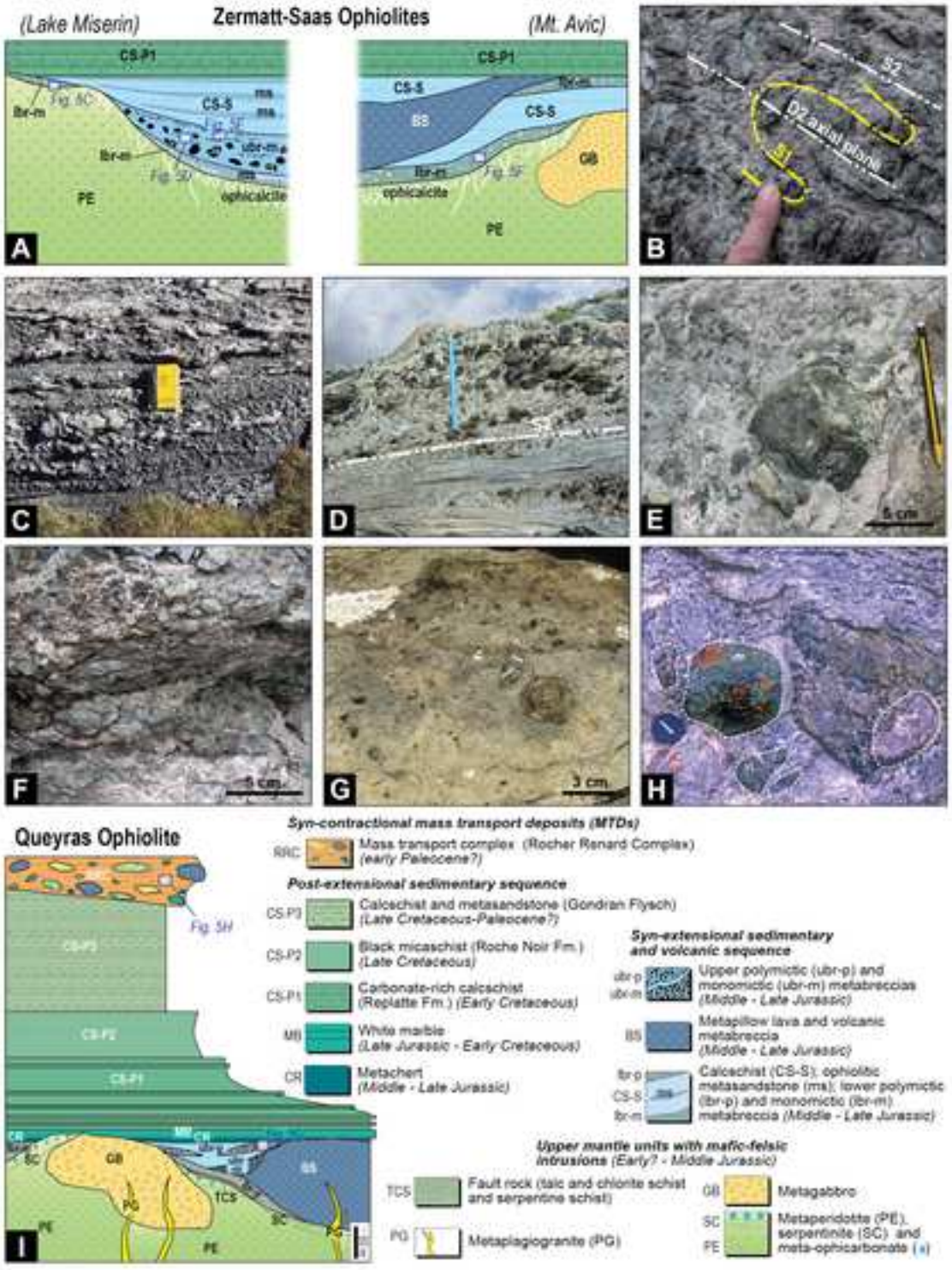

Figure 5 - *Festa et al.* (width 170 mm)

Figure 6

Click here to access/download;Figure;Fig 6_Festa et al_J Geol_R2.jpg

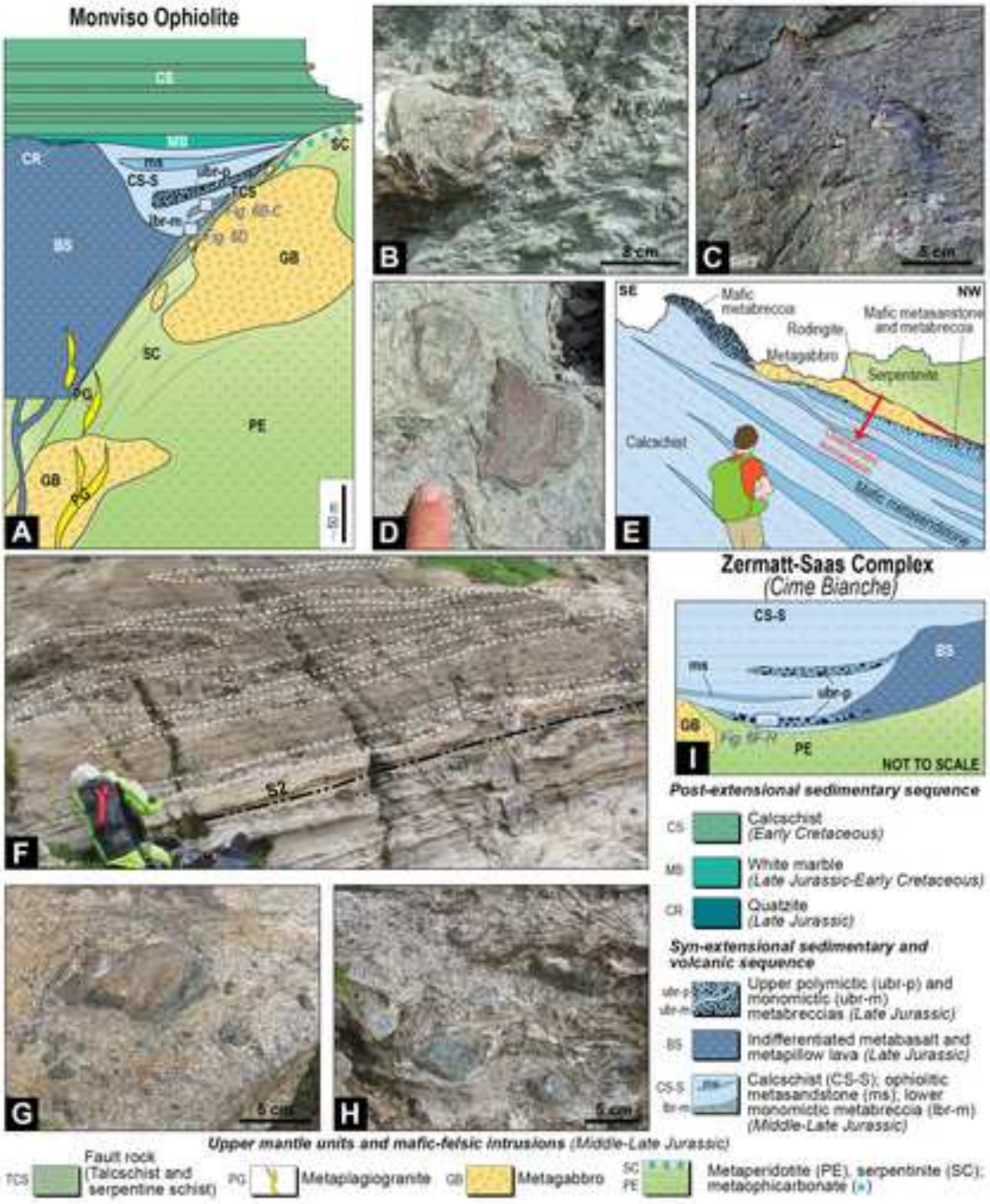

Figure 6 - *Festa et al.* (width 170 mm)

Table 1

		Name	Texture	Matrix	Clasts (in abundance order)	Clasts size	Stratigraphic position	Age
NORTHERN APENNINE	Lower breccias	Levanto Breccia (ophicalcite)	cataclastic	no-matrix	serpentinized peridotite, gabbro, foliated gabbro	cm-m	- Bottom: mantle peridotite - Top: ophiolite-bearing sandstones and basalt	Middle to Late Jurassic
		Framura Breccia	clast-supported	hematitic	ophicalcite, serpentinized peridotite, gabbro	dm-m	- Bottom: Framura Breccia - Top: Basalt flow/Cherts(?)	Middle to Late Jurassic
		Case Boeno Breccia	clast-supported	sandy	serpentinized peridotite, ophicalcite, gabbro	cm-m	- Bottom: mantle peridotite and gabbro - Top: pillow lava basalt	Middle to Late Jurassic
		Monte Capra Breccia	clast-supported	sandy	Fe-gabbro, Fe-basalt, plagiogranite, serpentinite, ophicalcite	cm-m	- Bottom: mantle peridotite and gabbro - Top: pillow lava basalt	Middle to Late Jurassic
	Upper breccias	Movea Breccia	clast-supported	sandy	Mg-gabbro, Mg-basalt, serpentinite, ophicalcite,	cm-m	- Bottom: pillow lava basalt - Top: Monte Zenone Breccia	Late Jurassic
		Monte Zenone	clast-supported	sandy	Mg-gabbro	cm-m	- Bottom: pillow lava basalt - Top: chert	Late Jurassic
		Monte Bianco	clast-supported	sparry	ophicalcite, serpentinized peridotite	cm-m	- Bottom: mantle peridotite - Top: Chert	Late Jurassic
	MTDs	Forcella Breccia	matrix-supported	shaly	limestone, marl, fine-grained arenite	cm-m	Inside the Zonati Shale and Gottero Sandstone	Maastrichtian to Early Paleocene
		Bocco Shale	matrix-supported	shaly	limestone, arenite, marl, basalt, gabbro, serpentinite, chert	cm-dam	Unconformbly on: Palombini Shale, Manganesiferous Shale, Verzi Marl, Zonati Shale and Gottero Sandstone	Early Paleocene
WESTERN ALPS	Lower breccias	Meta-ophicarbonate	cataclastic to hydrofract,	no-matrix	serpentinite	cm-m	- Bottom: mantle peridotite - Top: ophiolite-bearing metabreccia and metasandstone	Middle to Late(?) Jurassic
		Lake Miserin and Mt. Avic metabreccia	clast- to matrix-supported	mixed ultramafic-carbonate (calcschist) to carbonate (marble)	meta-ophicarbonate, serpentinite	cm-dm	- Bottom: ophicarbonate and peridotite - Top: sedimentary mélange (Lake Miserin) and basalt (Mt. Avic)	Middle to Late Jurassic
		Queyras lower mono- and polymictic-metabreccia	clast-supported	mixed mafic-carbonate (calcschist)	- Monomictic: serpentinite, meta-ophicarbonate or metagabbro - Polymictic: serpentinite and metagabbro	cm-dm (rarely m)	- Bottom: mantle peridotite or gabbro or shear zones - Top: basalt sequence or calcschist	Middle to Late Jurassic
		Monviso metabreccia and metasandstone	matrix-supported	mafic metasandstone	metagabbro	cm-dm	- Bottom: Mg-Al metagabbro in the footwall of an extensional detachment fault - Top: post-extensional carbonate-rich metasediment	Middle to Late Jurassic
	Upper breccias	Lake Miserin sedimentary mélange	matrix-supported	carbonate (marble)	massive serpentinite and veined serpentinite (meta-ophicarbonate)	dm-m	- Bottom: Lake Miserin lower metabreccia - Top: post-extensional calcschist	Middle(?) to Late Jurassic
		Queyras upper mono- and polymicitic metabreccia	clast- to matrix-supported	metasandstone (same composition of clasts)	- Monomictic: metabasalt - Polymictic: metabasalt, metagabbro, ingneous quartz-feldspatic rocks (plagiogranite?)	cm-dm	- Bottom (or inside to): metabasalt and meta-pillow lava basalt - Top: post-extensional metasediment (metaradiolarite or marble)	Late Jurassic
		Garten Formation	clast- to matrix-supported	micaschist and calcschist	Metabasalt, serpentinite and marble	cm-dm	Inside the base of metabasite or (locally) within calcschist	Late(?) Jurassic
	MTDs	Rocher Renard Complex	matrix-supported	shaly	metabasalt, meta-ophicarbonate, serpentinite, metagabbro, metalimestone, metachert)	cm-dam	- Bottom: Gondrand Flysch - Top: ?	Maastrichtian to Early Paleocene

Table 1 – Festa et al. (width 170 mm)

Figure 7

Click here to access/download;Figure;Fig 7_Festa et al_J Geol_R1.jpg

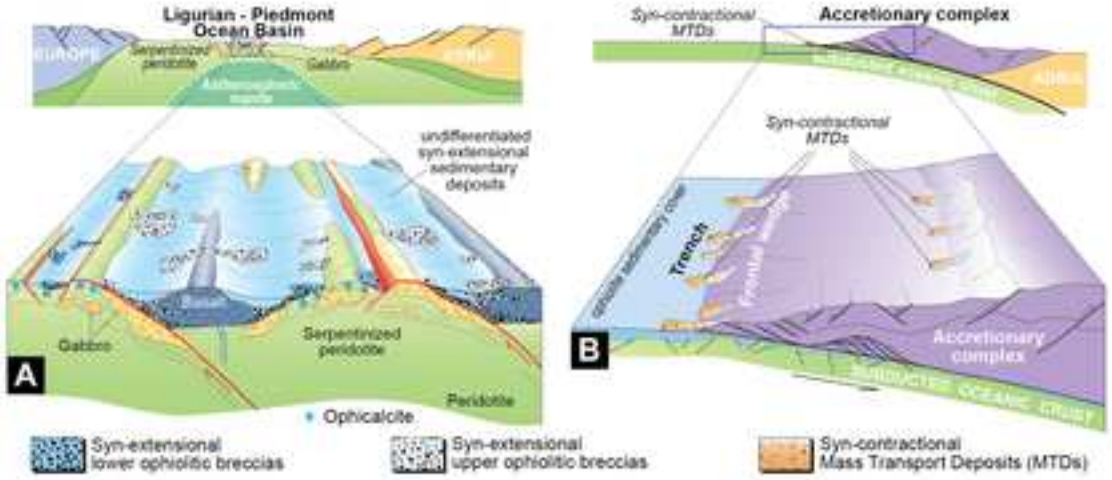

Figure 7 - *Festa et al.* (width 170 mm)